Hyperons, Hypernuclei & Neutron Stars

Isaac Vidaña

CFC, University of Coimbra

CENTRO DE FÍSICA COMPUTACIONAL

Galileo Galilei Institute for Theoretical Physics

Firenze (Italia), March 10^{th}-14^{th} 2014

Road Map for a Strange Trip

- ✧ Hypernuclei & Hypernuclear Physics
- ✧ YN & YY Interactions
- ✧ EoS of Hypernuclear Matter
- ✧ Role of Hyperons on Neutron Stars

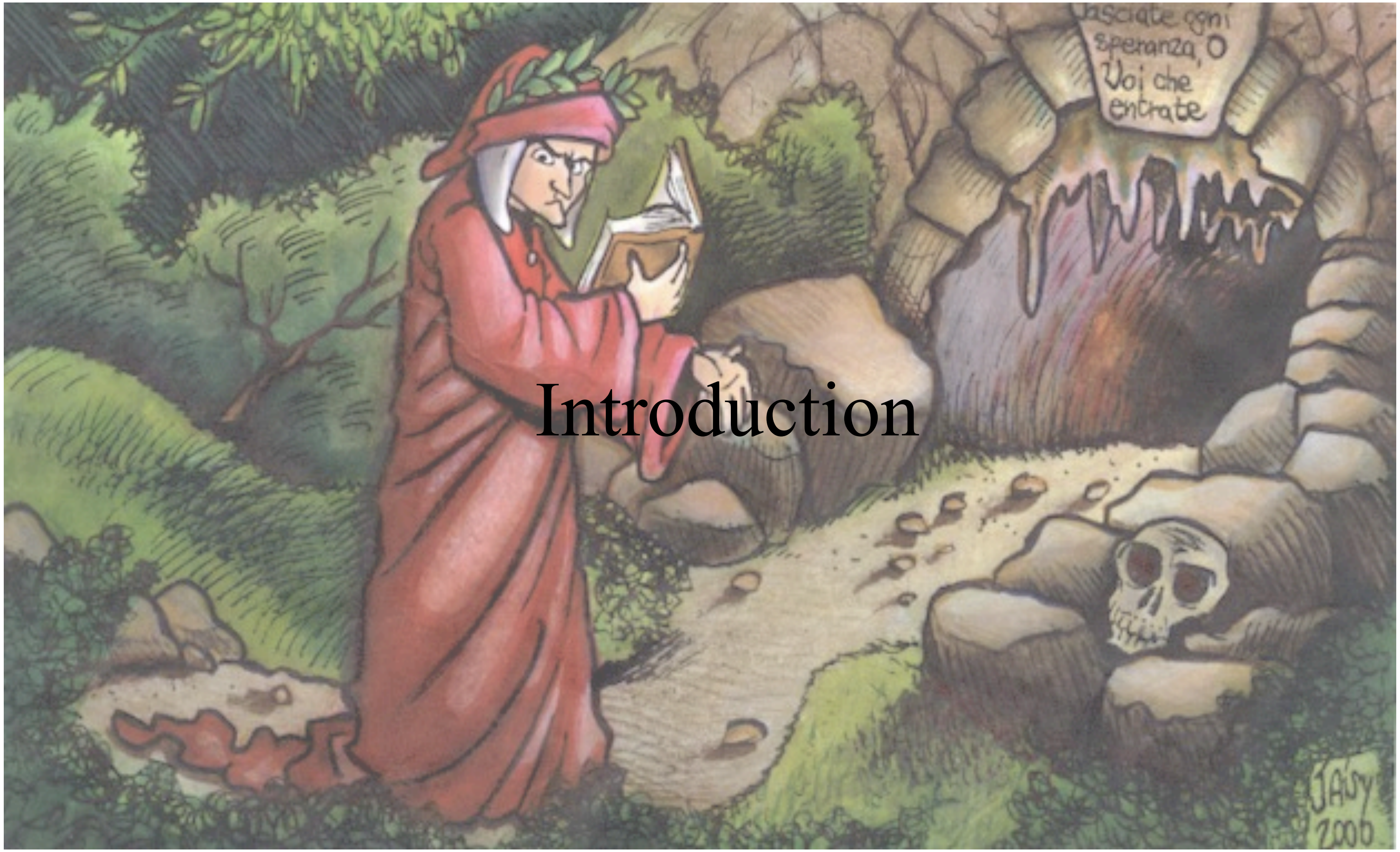

Introduction

What is a hyperon ?

- A hyperon is a baryon made of one , two or three strange quarks

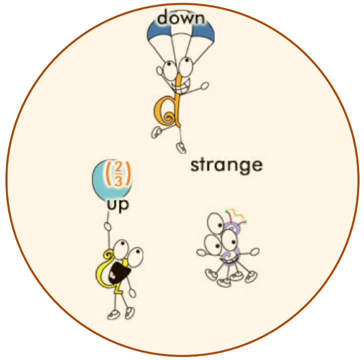

Hyperon	Quarks	I(J^P)	Mass (MeV)
Λ	uds	$0(1/2^+)$	1115
Σ^+	uus	$1(1/2^+)$	1189
Σ^0	uds	$1(1/2^+)$	1193
Σ^-	dds	$1(1/2^+)$	1197
Ξ^0	uss	$1/2(1/2^+)$	1315
Ξ^-	dss	$1/2(1/2^+)$	1321
Ω^-	sss	$0(3/2^+)$	1672

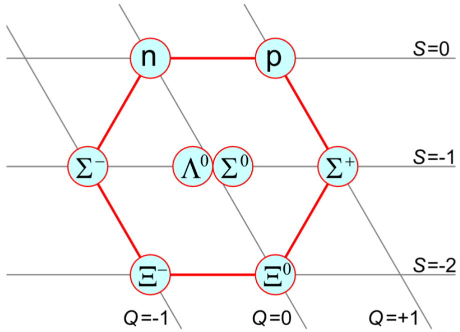

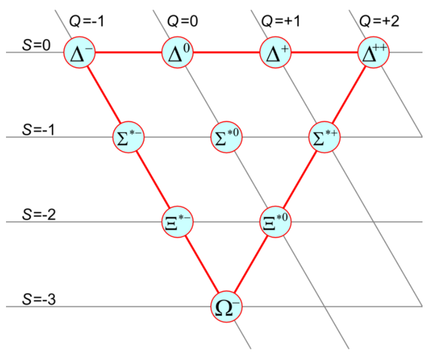

What is a hypernucleus ?

✧ A hypernucleus is a bound system of nucleons with one or more strange baryons ($\Lambda, \Sigma, \Xi, \Omega^-$ hyperons).

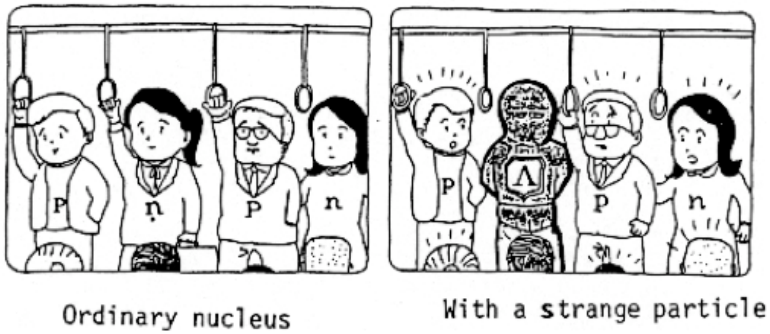

H. Bando, PARITY 1, 54 (1986)

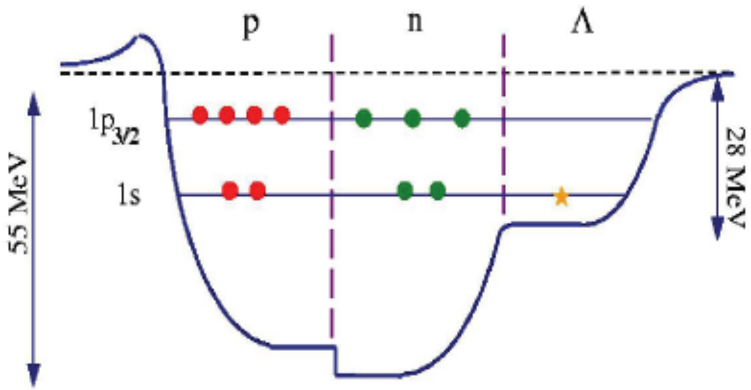

Simple s.p. model of $^{12}_{\Lambda}C$

✧ In a simple single-particle model: protons, neutrons and hyperons are considered distinguishable particles placed in independent effective potential wells in which Pauli exclusion principle is applied.

✧ Since hyperons are distinguishable from nucleons, they are privileged probes to explore states deep inside the nucleus, extending our knowledge of conventional to flavored nuclear physics.

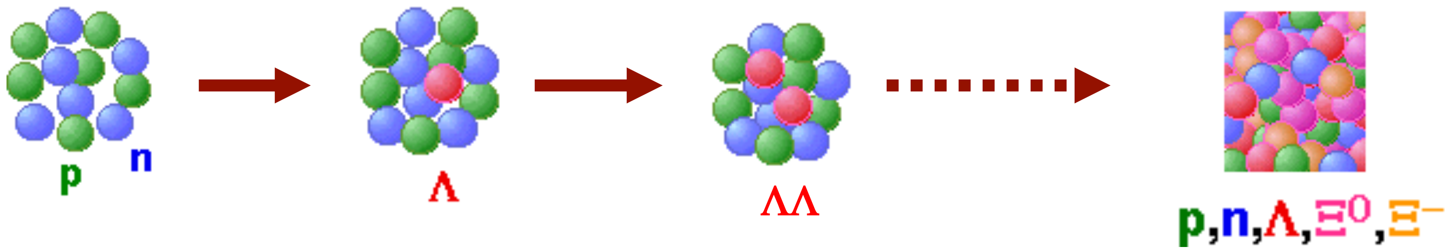

✧ Hyperons can change the nuclear nuclear structure. For instance the glue-like role of the Λ hyperon can facilitate the existance of neutron-rich hypernuclei, being a more suitable framework to study matter with extreme n/p ratios as compared to ordinary nuclei.

✧ A hypernucleus is a “laboratory” to study hyperon-nucleon (YN) and hyperon-hyperon (YY) interactions.

A simple model of hypernuclei: Hyperon-Nucleus effective potential

Hypernucleus = Ordinary Nuclear Core + Hyperon in a s.p. state of a hyperon-nucleus effective potential derived from hyperon-nucleon interaction

$$V_{\Lambda N}^{eff}(r) = \underbrace{V_0(r)}_{\text{central}} + \underbrace{V_S(r)\left(\vec{S}_N \cdot \vec{S}_\Lambda\right)}_{\text{spin-spin}} + \underbrace{V_T(r)S_{12}}_{\text{tensor}} + \underbrace{V_{ls}(r)\left(\vec{L} \times \vec{S}^+\right)}_{\text{symmetric spin-orbit}} + \underbrace{V_{als}(r)\left(\vec{L} \times \vec{S}^-\right)}_{\text{antisymmetric spin-orbit (zero in NN due to Pauli principle)}}$$

Present status of Λ Hypernuclear Spectroscopy

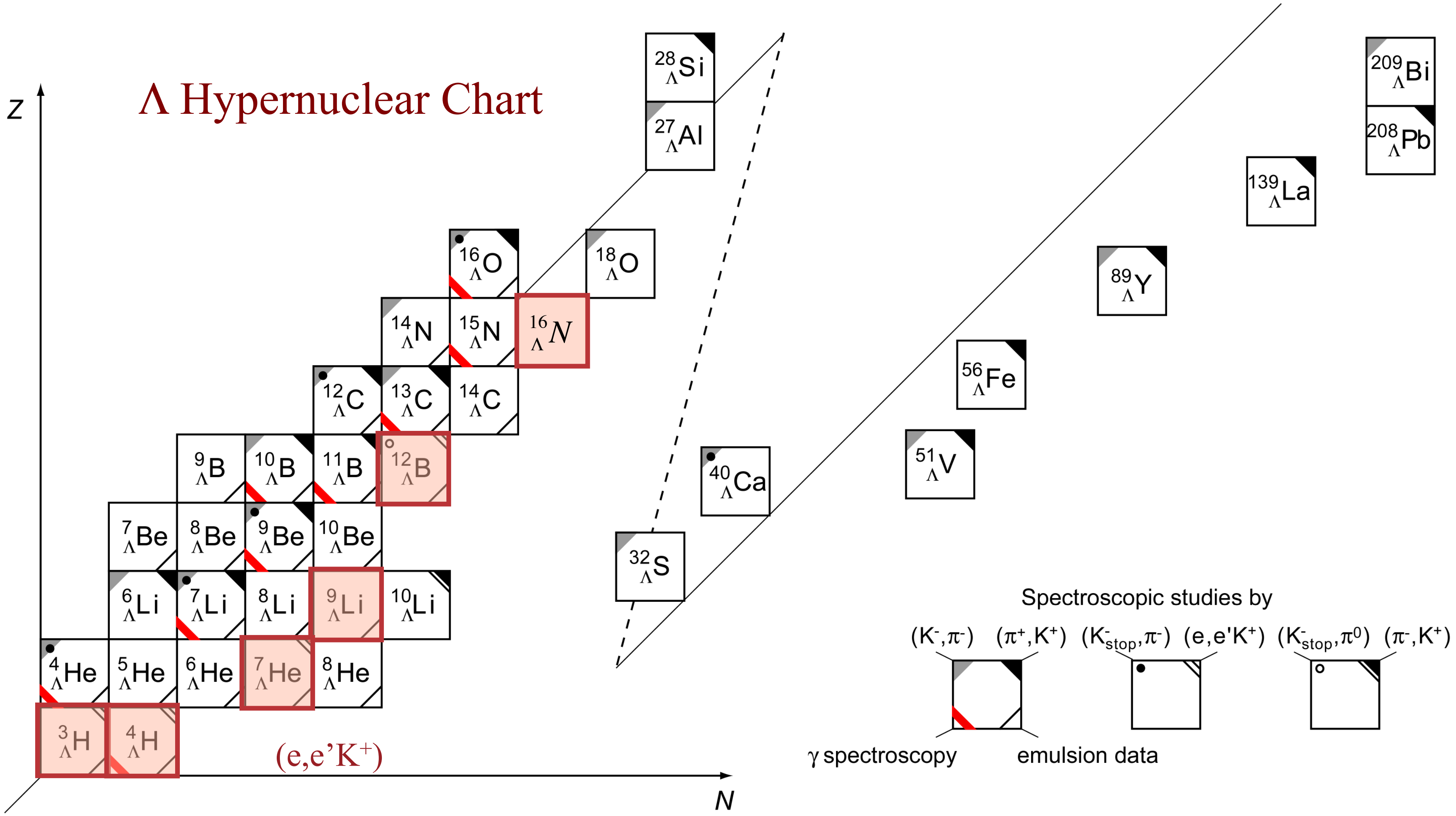

O. Hashimoto and H. Tamura, Prog. Part. Nucl. Phys. 57, 564 (2006)

The 3D Nuclear Chart

Double Λ-hypernuclei (S=-2) studied with:

$$(K^-, K^+)$$

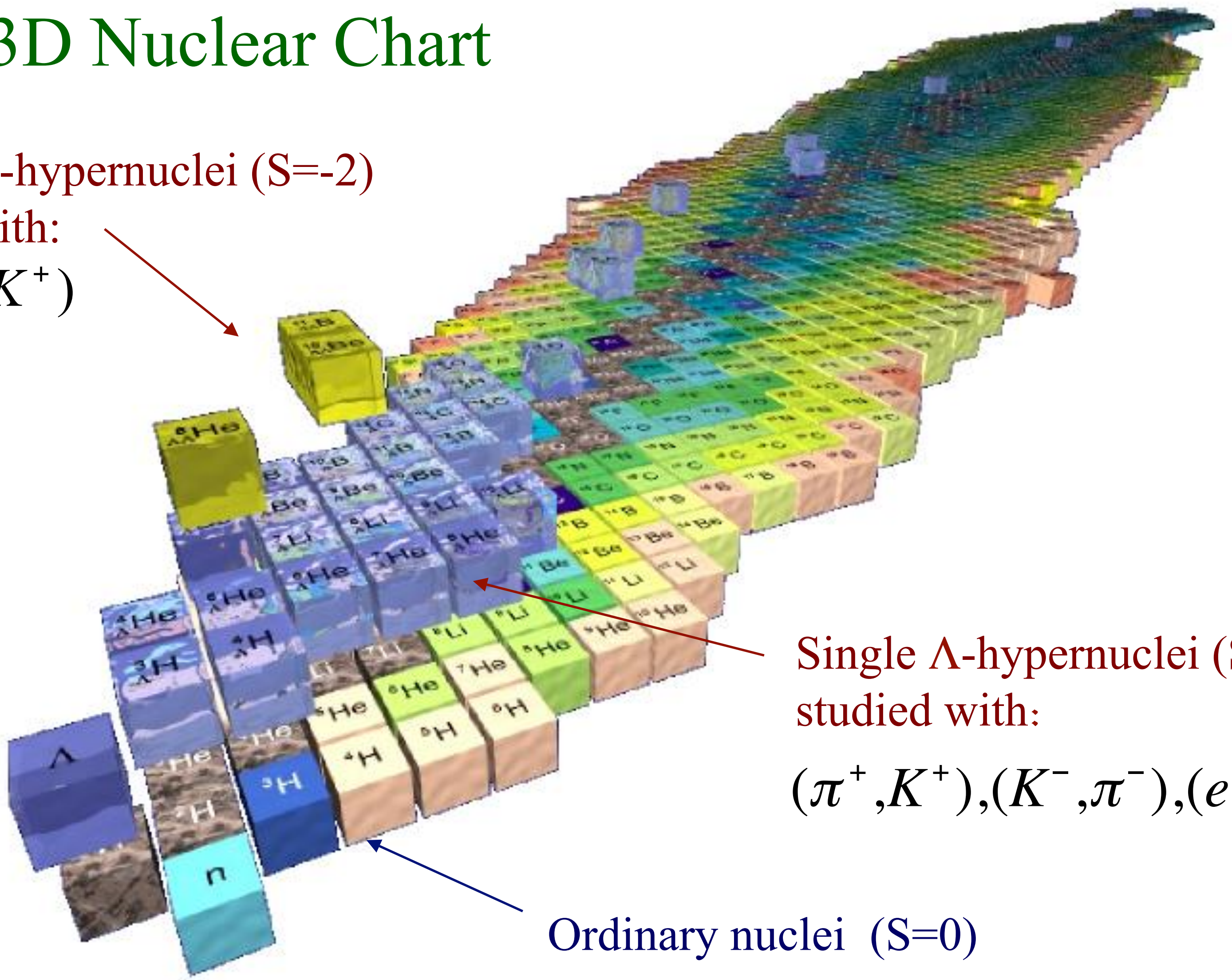

Single Λ-hypernuclei (S=-1) studied with:

$$(\pi^+, K^+), (K^-, \pi^-), (e, e' K^+)$$

Ordinary nuclei (S=0)

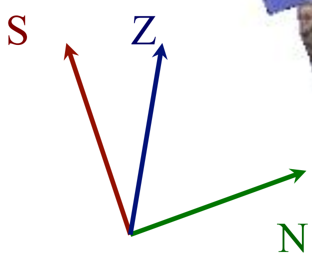

Brief History of Hypernuclear Physics

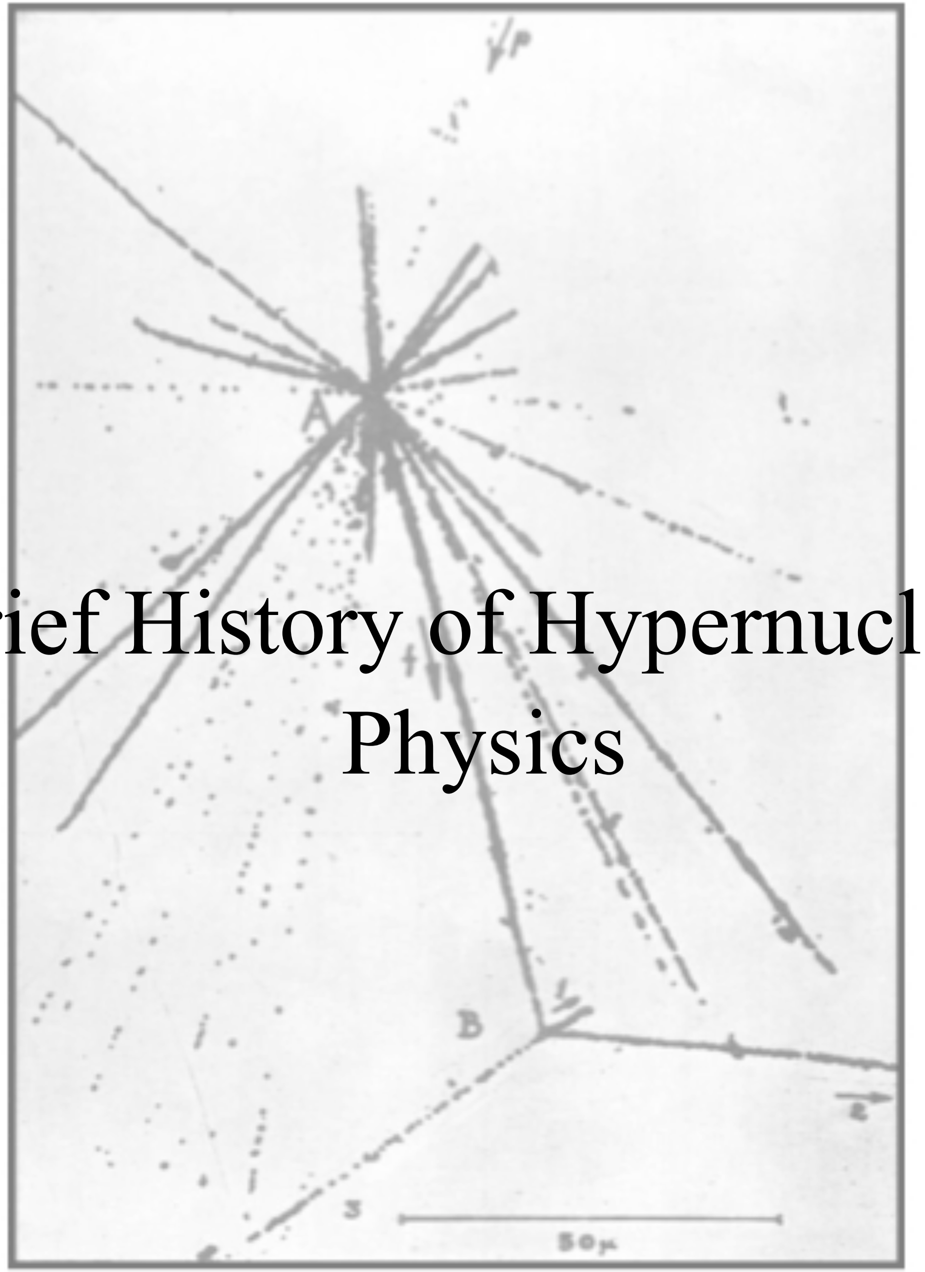

First hypernuclear event observed in a nuclear emulsion by Marian Danysz and Jerzy Pniewski in 1952

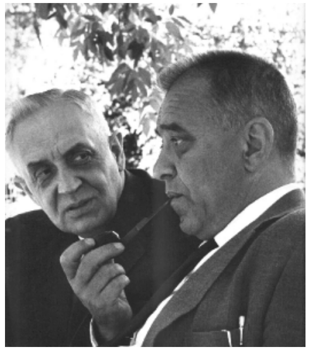

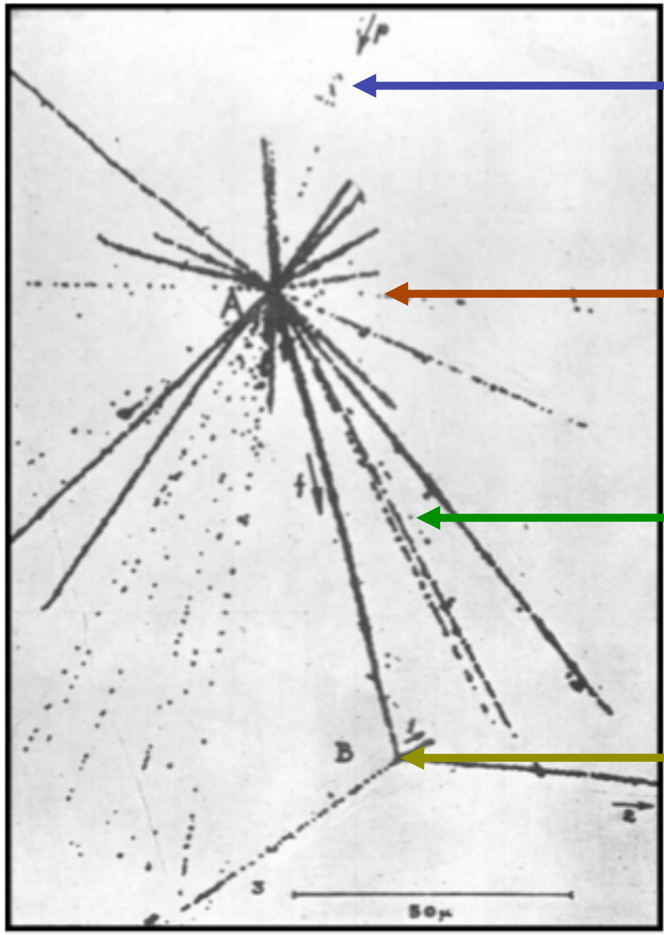

Incoming high energy cosmic ray (proton)

Collision with the nucleus

Nuclear fragments that eventually stop in the emulsion

One fragment containing a hyperon disintegrates weakly

To commemorate the discovery of Danysz and Pniewski a postcard was issued by the Polish Post in May 1993

(200.000 postcards, postcard price 2000 zl, stamp 1500 zl)

A few years earlier, in 1989, the postmark designed on the basis of the first hypernucleus observation was used for the 20th International Physics Olympiad at the Warsaw post office number 64

Historical Overview

1953 → 1970 : hypernuclear identification with visualizing techniques emulsions, bubble chambers

1962 : first double Λ hypernucleus discovered in a nuclear emulsion irradiated by a beam of K^- mesons at CERN

1970 → Now : Spectrometers at accelerators:

CERN (up to 1980)

BNL : (K^-, π^-) and (π^+, K^+) production methods

KEK : (K^-, π^-) and (π^+, K^+) production methods

After 2000 : Stopped kaons at DAΦNE (FINUDA) : (K^-_{stop}, π^-)

The new electromagnetic way :

HYPERNUCLEAR production with

ELECTRON BEAM $(e,e'K^+)$ at JLAB &MAMI-C

International Hypernuclear Network

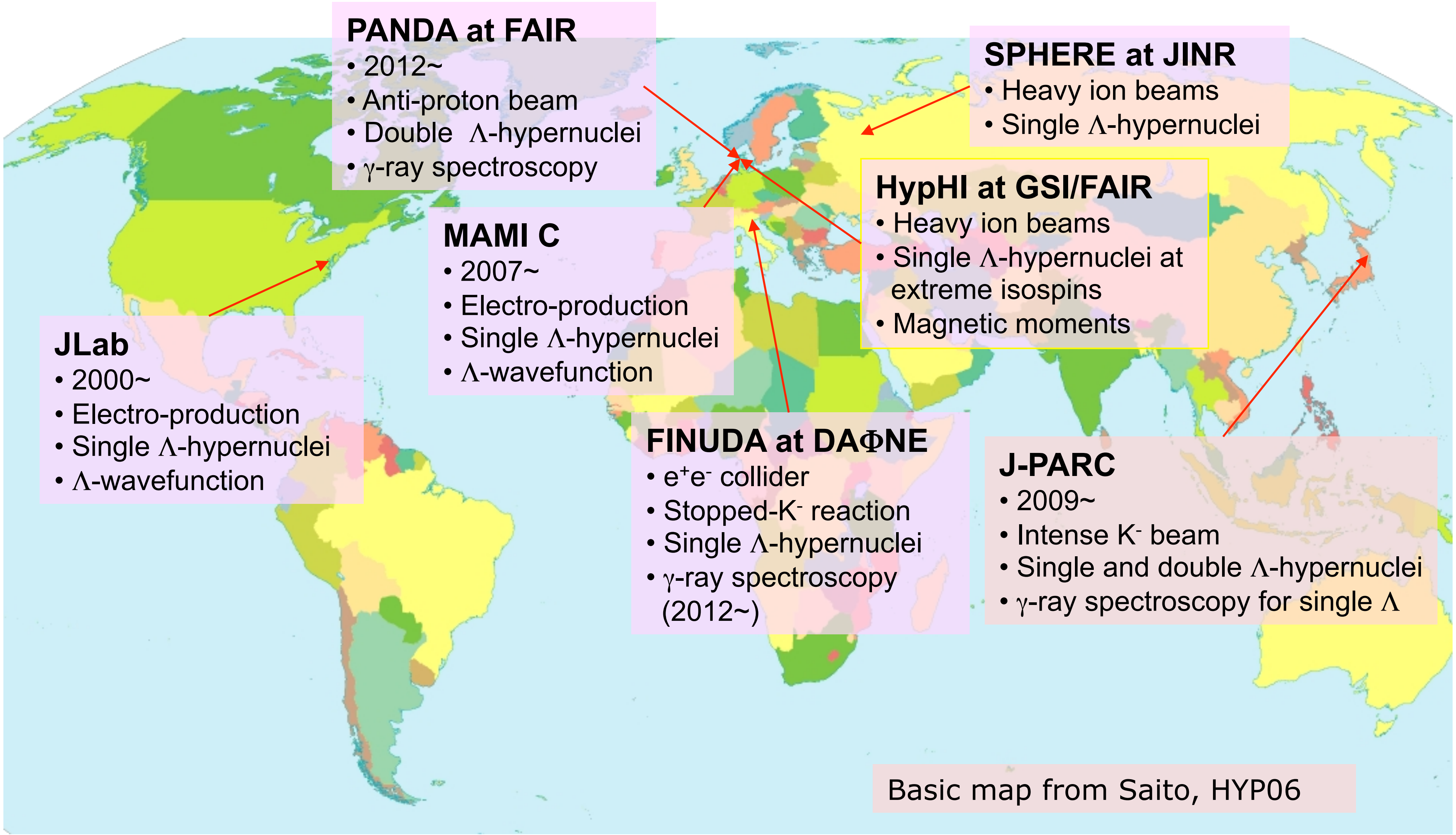

Hypernuclei: from the cradle to the grave

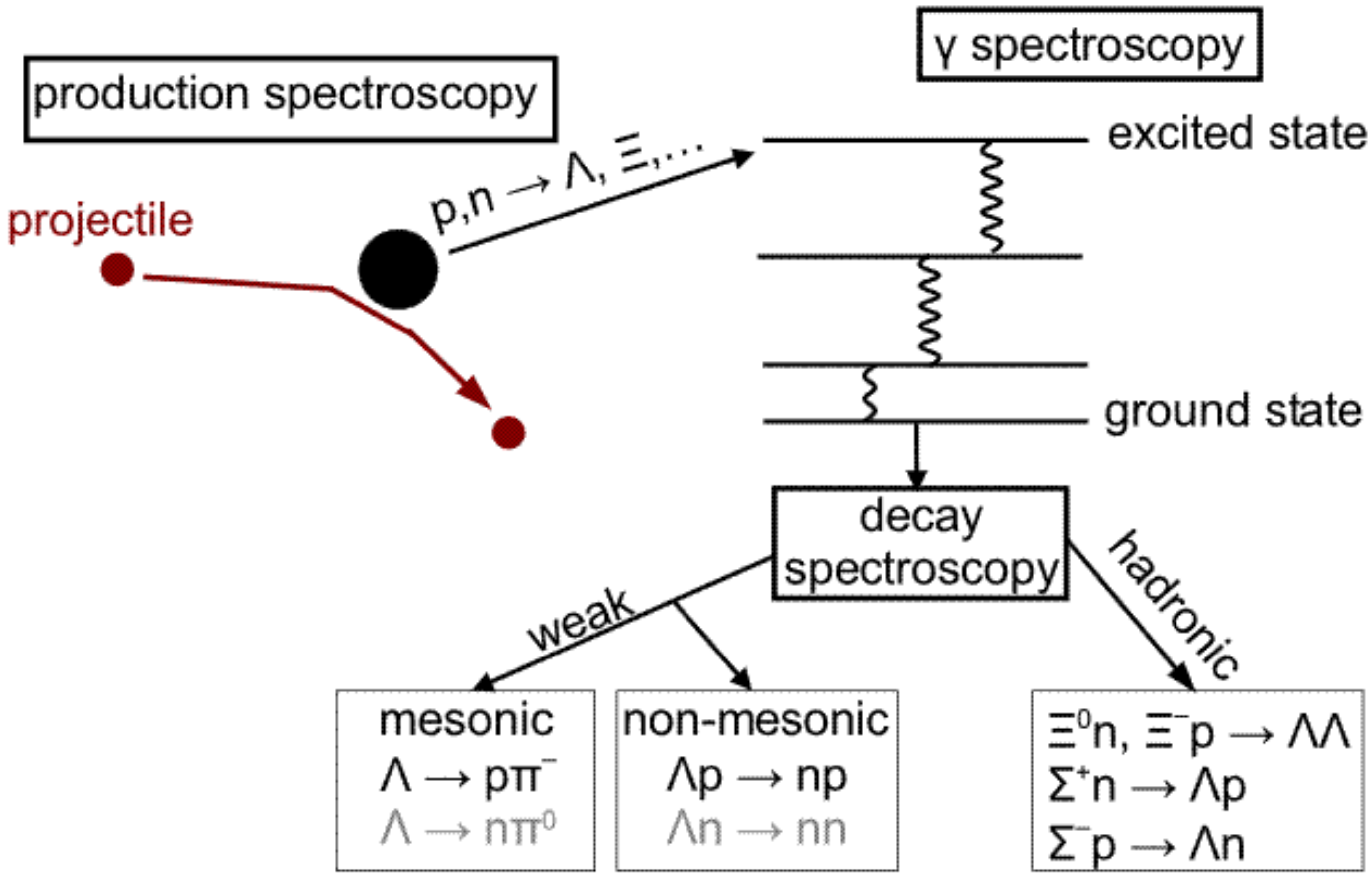

Production of Λ hypernuclei can occur by …

✧ Strangeness exchange: (BNL, KEK, JPARC)

(replace a u or d quark with an s quark)

$$K^- + {}^{A}Z \rightarrow {}^{A}_{\Lambda}Z + \pi^-$$

Where the K⁻ in-flight or stopped

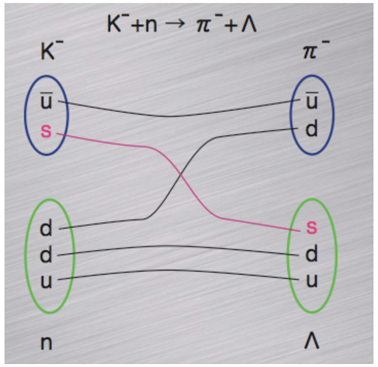

✧ Associated production: (BNL, KEK, GSI)

(produces an $s\bar{s}$ pair)

$$\pi^+ + {}^{A}Z \rightarrow {}^{A}_{\Lambda}Z + K^+$$

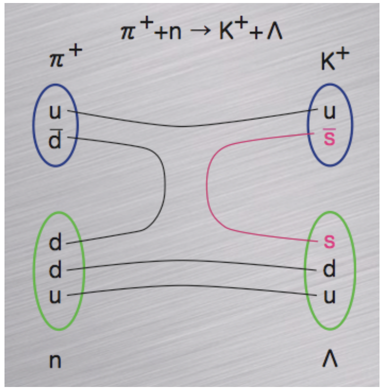

✧ Electroproduction: (JLAB, MAMI-C)

$$e^- + {}^{A}Z \rightarrow e^{-\prime} + K^+ + {}^{A}_{\Lambda}(Z-1)$$

${}^{A}Z(e,e'K){}^{A}(Z-1)_{\Lambda}$

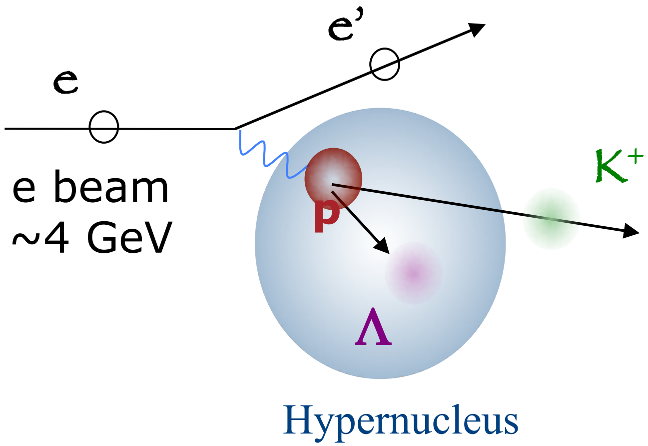

elementary process

$$\gamma + p \rightarrow \Lambda + K^+$$

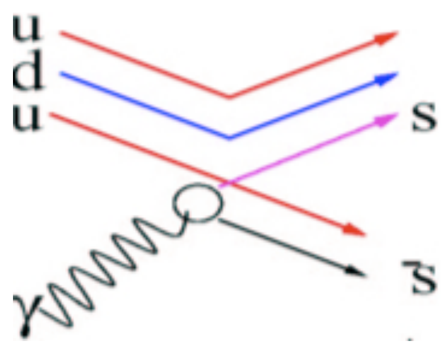

Production kinematics

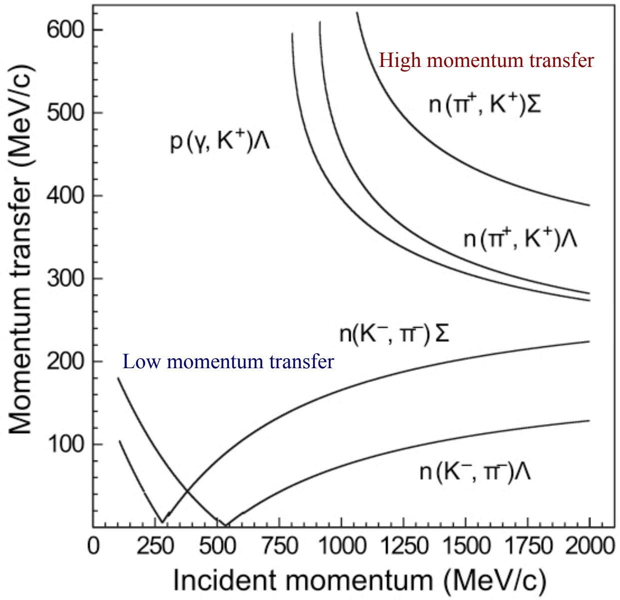

✧ $n(\pi^+,K^+)\Lambda$, $p(\gamma,K^+)\Lambda$

✓ High momentum transfer ➔ hyperon has large probability of escaping the nucleus.

✓ Longer π^+ and K^+ mean free path ➔ interaction with interior nucleons, significant angular momentum transfer.

✧ $n(K^-,\pi^-)\Lambda$

✓ Low momentum transfer ➔ hyperon has large probability of being bound.

✓ Attenuation of (K^-,π^-) reaction in matter (resonance states). Interacion with outer shell neutrons replacing it with a Λ in the same shell.

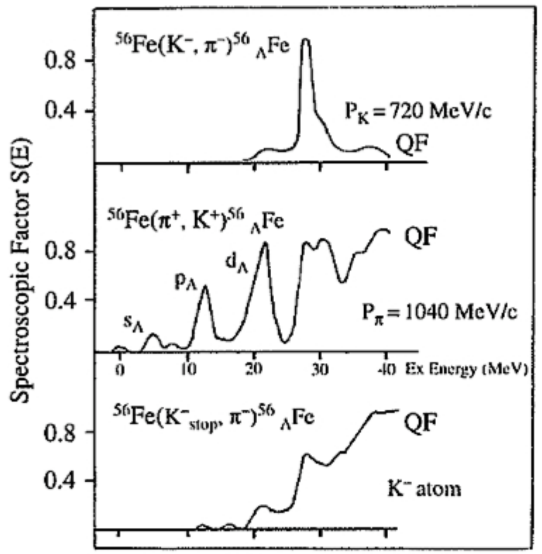

Measurement of hypernuclear masses

$$M_{{}^{A}_{\Lambda}Z} - M_{{}^{A}Z} = B_{{}^{A}Z} - B_{{}^{A}_{\Lambda}Z} + M_{\Lambda} - M_{N}$$

✧ Stopped K⁻ reaction

($K^-_{stopped}$, π^-)

$$K^-_{stopped} + {}^{A}Z \to {}^{A}_{\Lambda}Z + \pi^-$$

$$M_{{}^{A}_{\Lambda}Z} = \sqrt{\left(E_{\pi} - M_{K} - M_{{}^{A}Z}\right)^2 - p_{\pi}^2}$$

Need only π^- outgoing momentum ➔
One Spectrometer

✧ In-flight reactions

($K^-_{in-flight}$, π^-) (π^+,K^+)

$$K^-_{in-flight} + {}^{A}Z \to {}^{A}_{\Lambda}Z + \pi^-$$

$$\pi^+ + {}^{A}Z \to {}^{A}_{\Lambda}Z + K^+$$

$$M_{{}^{A}_{\Lambda}Z} = \sqrt{\left(E_{\pi} - E_{K} - M_{{}^{A}Z}\right)^2 - \left(\vec{p}_{\pi} - \vec{p}_{K}\right)^2}$$

Need incident & outgoing momenta ➔
Two Spectrometers

Example: spectrum for a (π^+,K^+) on a heavy target

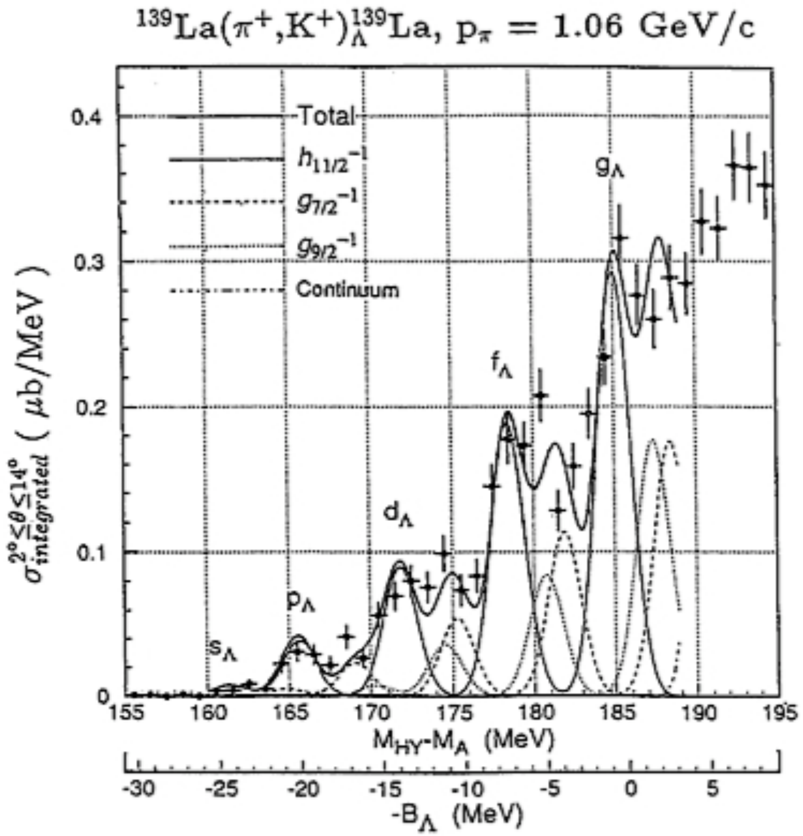

T. Hasegawa et al., Phys. Rev. C 53, 1210 (1996)

$$\pi^+ + {}^{139}La \rightarrow {}^{139}_{\Lambda}La + K^+$$

- ✓ Energy resolution: 2.5 MeV
- ✓ Clear shell structure
- ✓ Obtained with a typical magnetic spectrometer for the detection of K^+

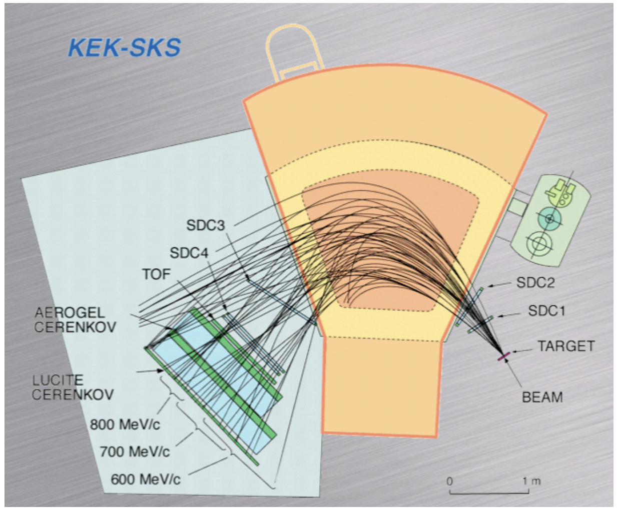

The FINUDA experiment @ DAΦNE (Frascati)

DAΦNE: Double Annular e^+e^-
Φ-factory for Nice Experiments

e^+e^- collider dedicated to the production of Φ resonance

FINUDA: FIsica NUcleare at DAΦNE

produce hypernuclei by stopping negative kaon originating from Φ decay in nuclear target

$$e^+ + e^- \rightarrow \Phi \rightarrow K^+ + K^-$$

$$K^-_{stopped} + {}^AZ \rightarrow {}^A_\Lambda Z + \pi^-$$

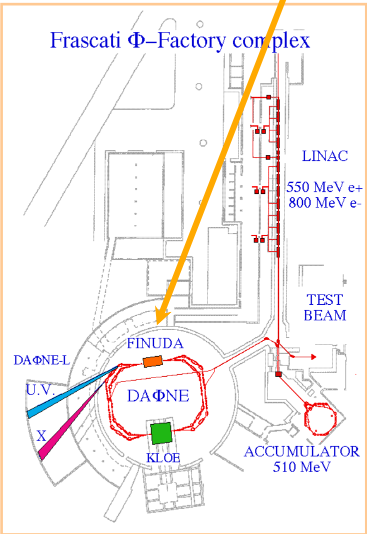

FINUDA results on $^{12}{}_{\Lambda}C$

Very good agreement between FINUDA results
& E368 @ KEK ones

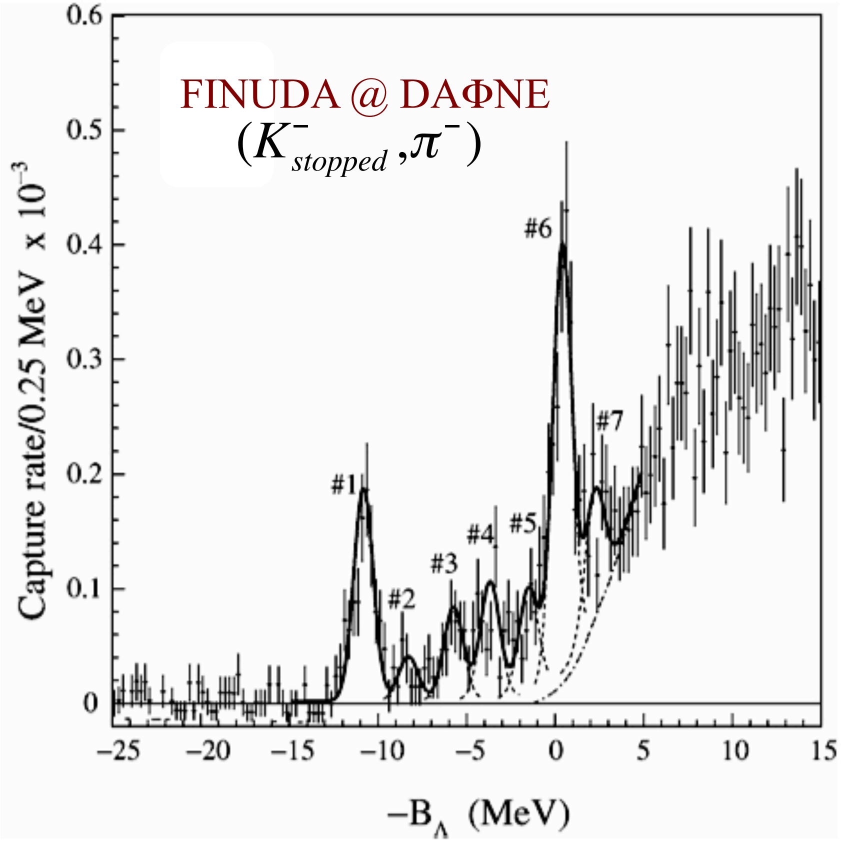

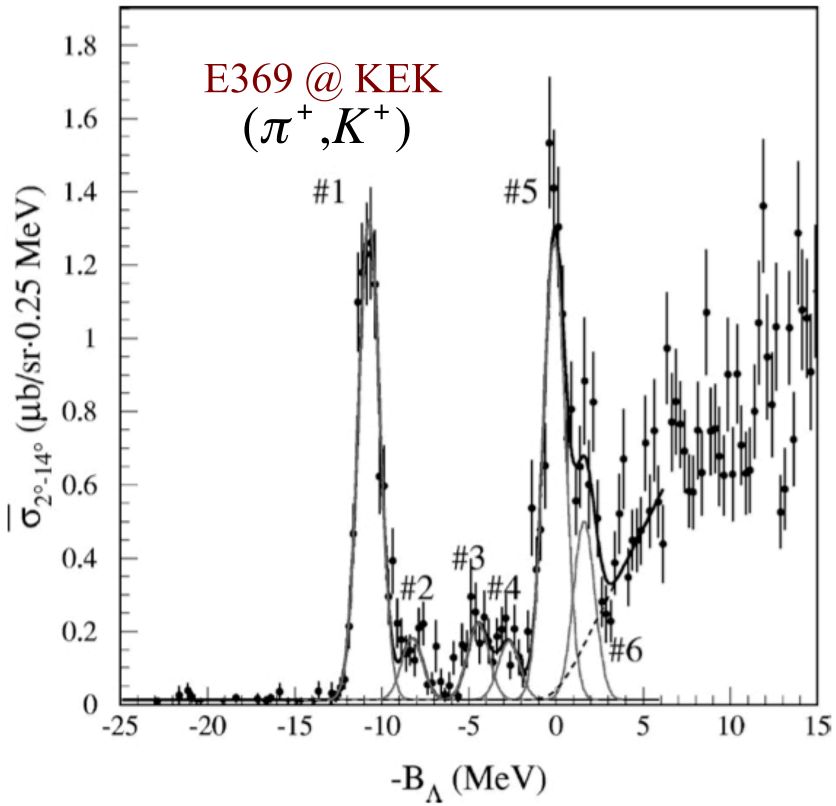

M. Agnello et al., Phys. Lett. B 622, 35 (2005)

H. Hotchi et al., Phys. Rev. C 64, 044302 (2001)

The (e,e'K$^+$) reaction

- ✧ Relatively new (JLAB, MAMI-C).
- ✧ Excellent energy resolution of energy spectrum.
- ✧ Although the cross section is 10^{-2} smaller than that of (π^+,K$^+$) this is compensated by larger beam intensity.

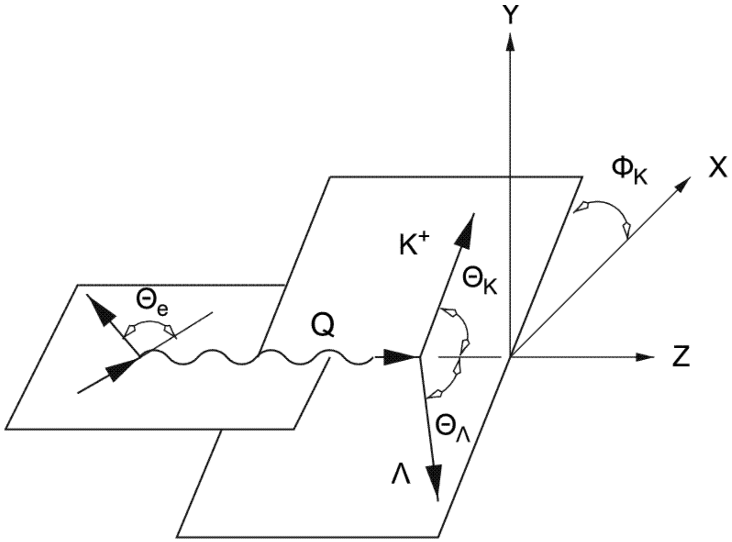

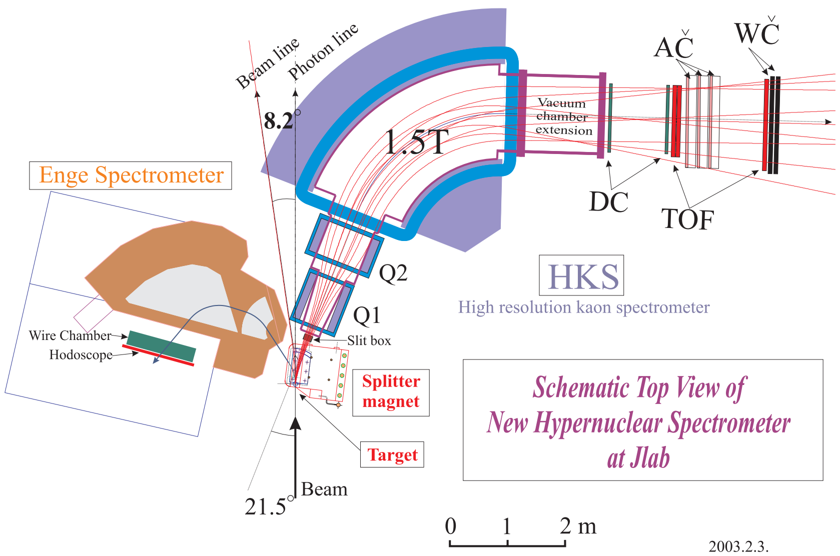

The experimental geometry requires two spectrometers to detect:

- ✓ the scattered electrons which defines the virtual photons
- ✓ the kaons

Hypernuclear spectrum from the (e,e’K$^+$) reaction

Energy left inside the nucleus
(related to the excitation energy)

$$E_x = E_e - E_{e'} - E_{K^+}$$

Incoming electron

Outgoing electron

Outgoing kaon

$^{12}C(e,e'K^+)^{12}{}_{\Lambda}B$ spectrum

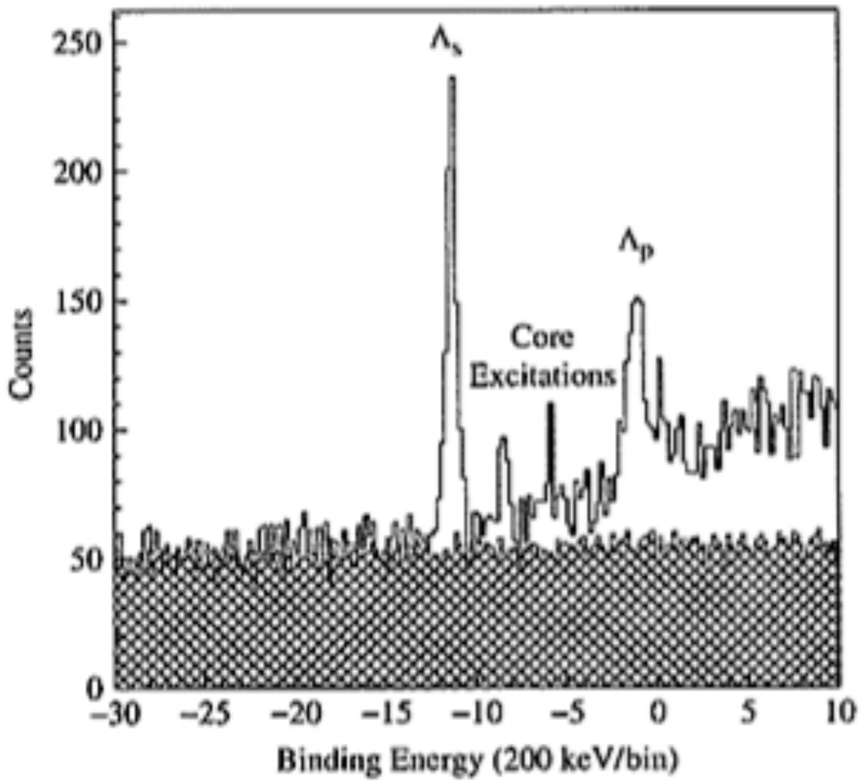

V. Rodrigues, PhD Thesis, University of Houston (2006)

In summary …

The Λ single particle states

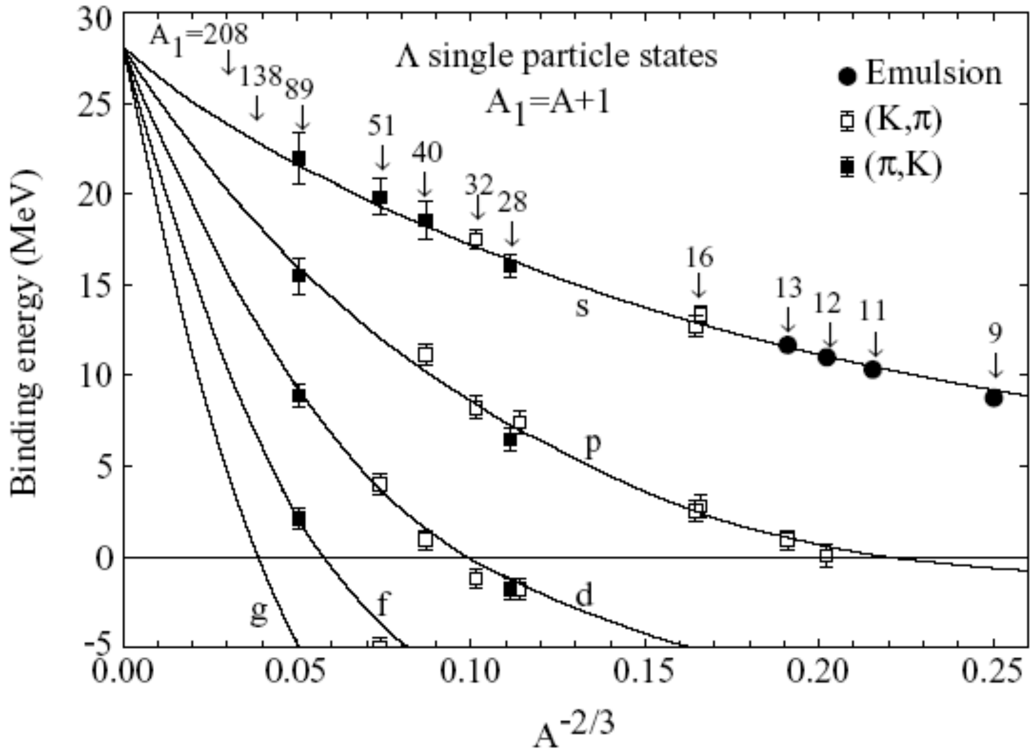

Hypernuclear binding energies

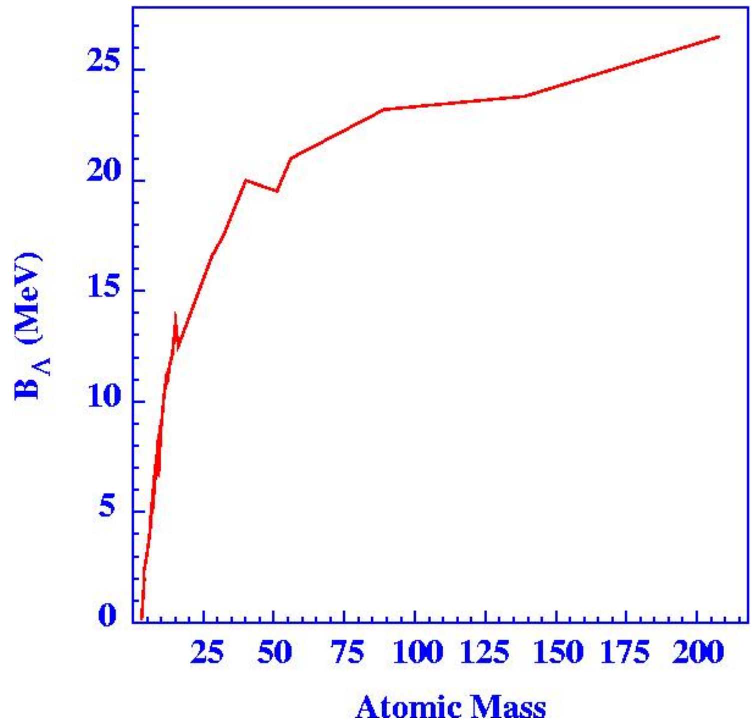

Hypernuclear binding energies show saturation as ordinary nuclei

Production of Σ hypernuclei

Production mechanisms similar to the ones considered for Λ hypernuclei like, e.g., strangeness exchange $(K^-,\pi^\pm)$

$^4_\Sigma$He bound state
E ~ 4 MeV, Γ ~ 7 MeV

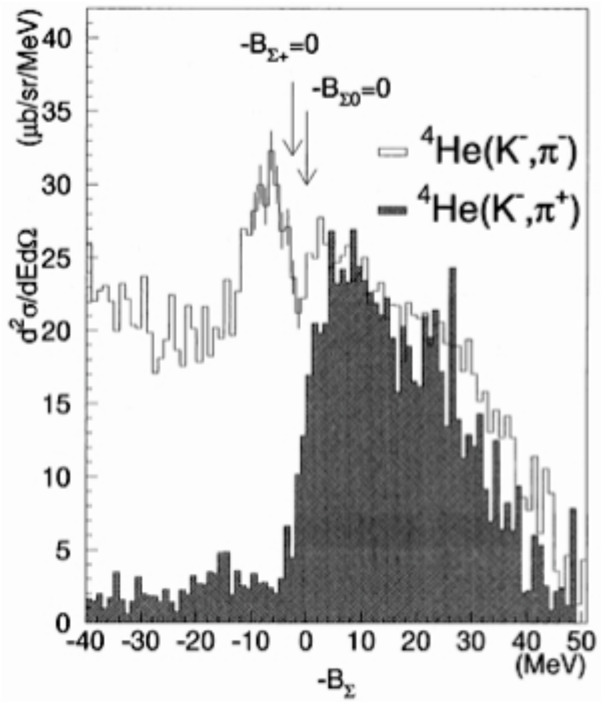

T. Nagae et al., Phys. Rev. Lett. 80, 1605 (1998)

Σ hypernuclear states in
p-shell hypernuclei

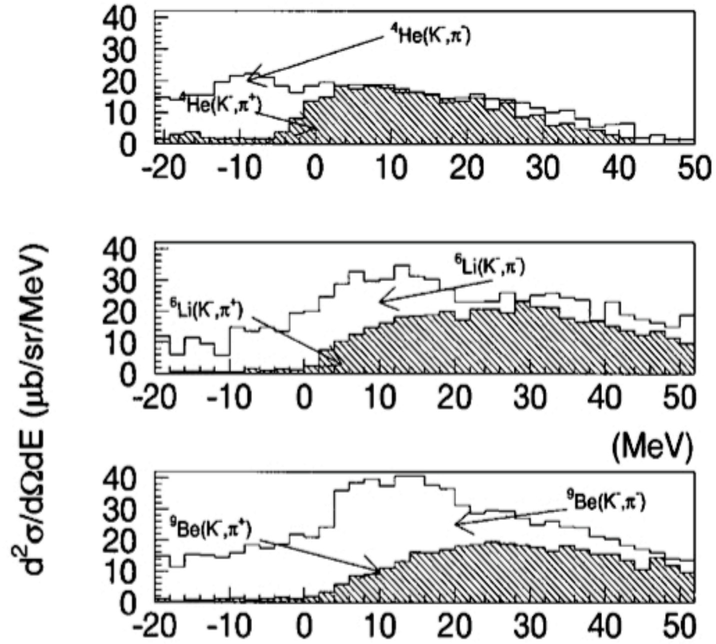

S. Bart et al., Phys. Rev. Lett. 83, 5238 (19989)

What do we know about double Λ hypernuclei ?

Not so much ….

	$B_{\Lambda\Lambda}$ (MeV)	$\Delta B_{\Lambda\Lambda}$ (MeV)		
${}^{6}_{\Lambda\Lambda}He$	10.9 ± 0.5	4.7 ± 0.6	Prowse	(1966)
${}^{6}_{\Lambda\Lambda}He$	$7.25 \pm 0.19^{+0.18}_{-0.11}$	$1.01 \pm 0.20^{+0.18}_{-0.11}$	KEK-E373	(2001)
${}^{10}_{\Lambda\Lambda}Be$	17.7 ± 0.4	4.3 ± 0.4	Danysz	(1963)
${}^{10}_{\Lambda\Lambda}Be$	8.5 ± 0.7	-4.9 ± 0.7	KEK-E176	(1991)
${}^{13}_{\Lambda\Lambda}B$	27.6 ± 0.7	4.8 ± 0.7	KEK-E176	(1991)
${}^{10}_{\Lambda\Lambda}Be$	$12.33^{+0.35}_{-0.21}$		KEK-E373	(2001, unpublished)

Nagara event

same event

$$B_{\Lambda\Lambda}({}^{A}_{\Lambda\Lambda}Z) = B_{\Lambda}({}^{A}_{\Lambda\Lambda}Z) + B_{\Lambda}({}^{A-1}_{\Lambda}Z)$$

$$\Delta B_{\Lambda\Lambda}({}^{A}_{\Lambda\Lambda}Z) = B_{\Lambda\Lambda}({}^{A}_{\Lambda\Lambda}Z) - 2B_{\Lambda}({}^{A-1}_{\Lambda}Z) = B_{\Lambda}({}^{A}_{\Lambda\Lambda}Z) - B_{\Lambda}({}^{A-1}_{\Lambda}Z)$$

The production of double Λ hypernuclei

✧ Ξ^- conversion in two Λ's:

$$\Xi^- + p \rightarrow \Lambda + \Lambda + 28.5\,MeV$$

- Ξ^- production:

✓ (K^-,K^+) reaction (BNL, KEK)

$$K^- + p \rightarrow \Xi^- + K^+$$

✓ Antiproton production (PANDA@FAIR)

$$p + \overline{p} \rightarrow \Xi^- + \overline{\Xi}^+$$

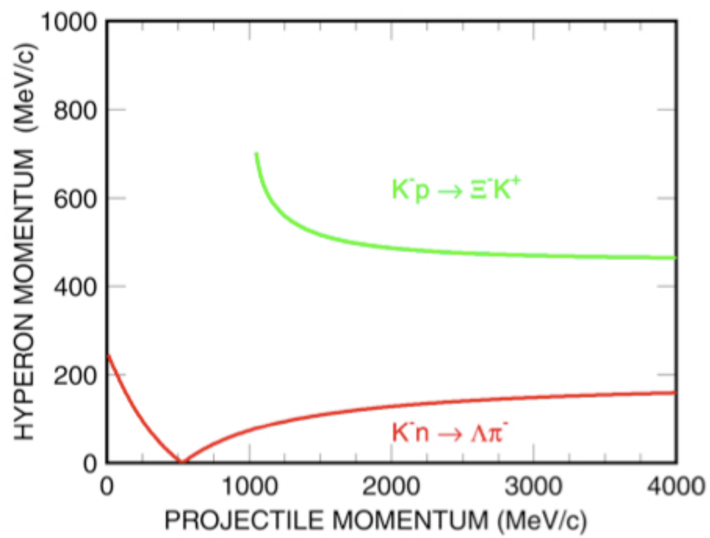

Hypernuclear γ-ray spectroscopy

- Produced hypernuclei can be in an excited state.
- Energy released by emission of neutrons or protons or γ-ray when hyperon moves to lower states.

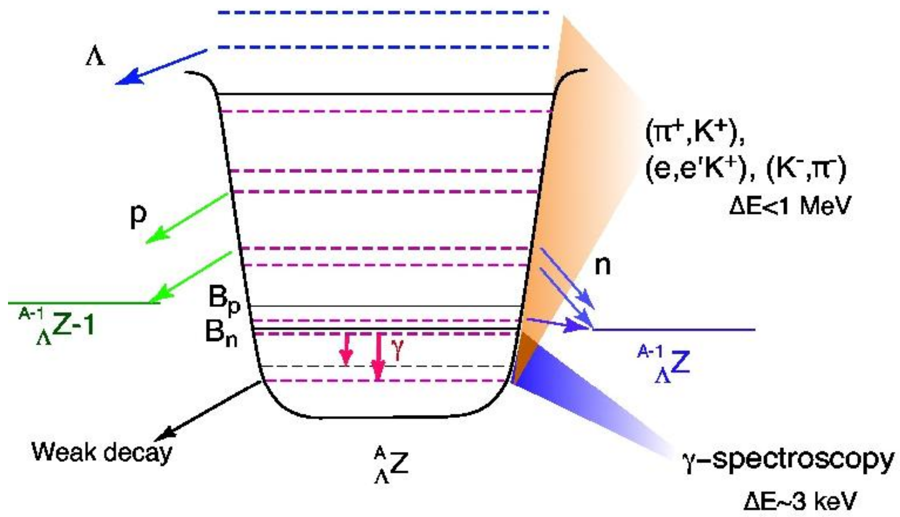

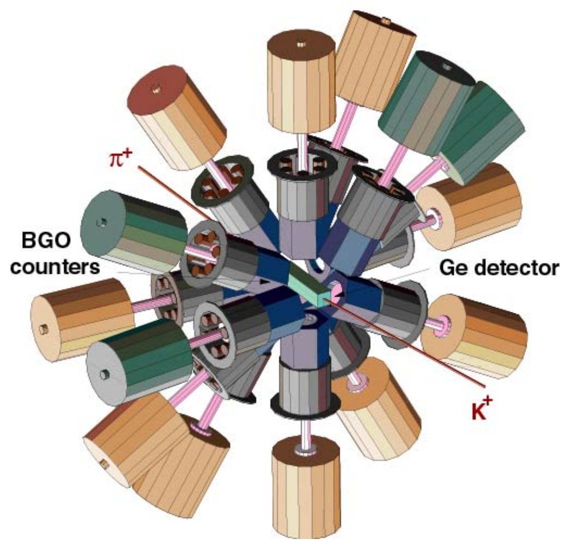

Hyperball

- Excellent resolution with Ge (NaI) detectors.
- Λ depth potential in nucleus ~ 30 MeV ➔ observation of γ-rays limited to low excitation region.
- γ-ray transition measures only energy difference between two states.

Hypernuclear fine structure & the spin-dependent ΛN interaction

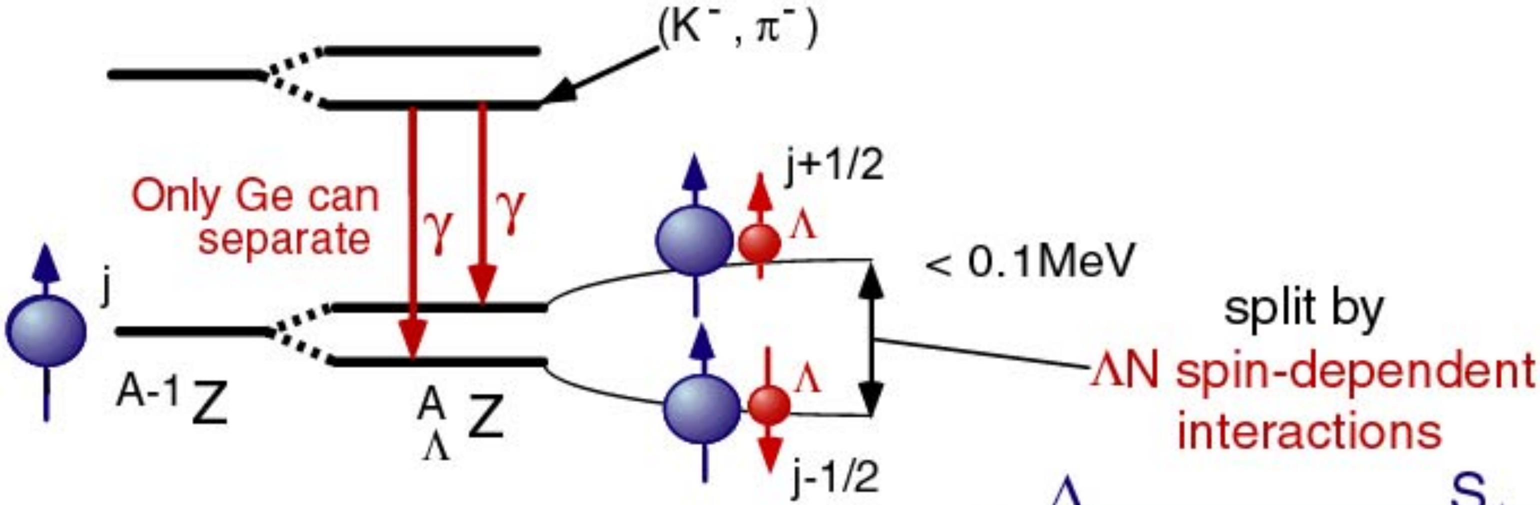

$$V^{\mathrm{eff}}_{\Lambda N} = V_0(r) + \boxed{\begin{array}{l} \overset{\Delta}{V_\sigma(r)\,\vec{s}_\Lambda\vec{s}_N} + \overset{S_\Lambda}{V_\Lambda(r)\,\vec{l}_{\Lambda N}\vec{s}_\Lambda} \\ + \underset{S_N}{V_N(r)\,\vec{l}_{\Lambda N}\vec{s}_N} + \underset{T}{V_T(r)\,S_{12}} \end{array}}$$

Integrated with shell-model w.f.
(Millener's parameterization)

γ~ray spectrum of $^{16}{}_{\Lambda}O$

- Observed twin peaks demonstrate hypernuclear fine structure for $^{16}{}_{\Lambda}O$ ($1^- \rightarrow 1^-, 0^-$) transitions.
- Small spacing in twin peaks caused by spin-dependent ΛN interaction.
- Recent analysis revealed another transition at 6758 keV corresponding to $^{16}{}_{\Lambda}O$ ($2^- \rightarrow 0^-$).

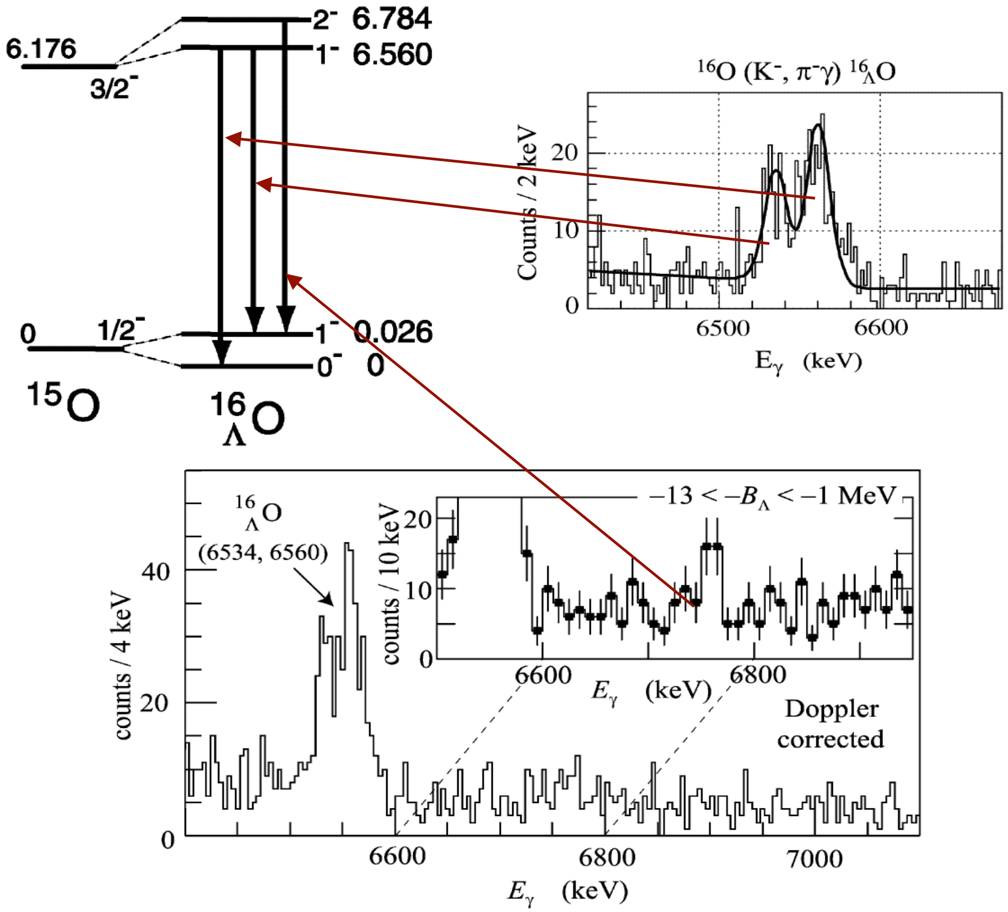

M. Ukai et al., Phys. Rev. C 77, 05315 (2008)

The Weak Decay of Λ hypernuclei

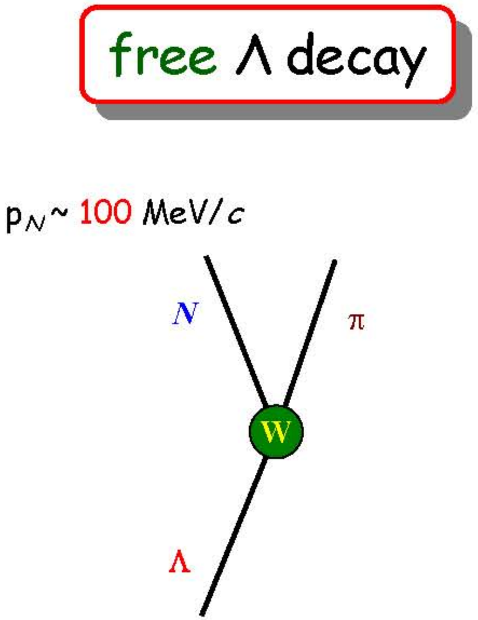

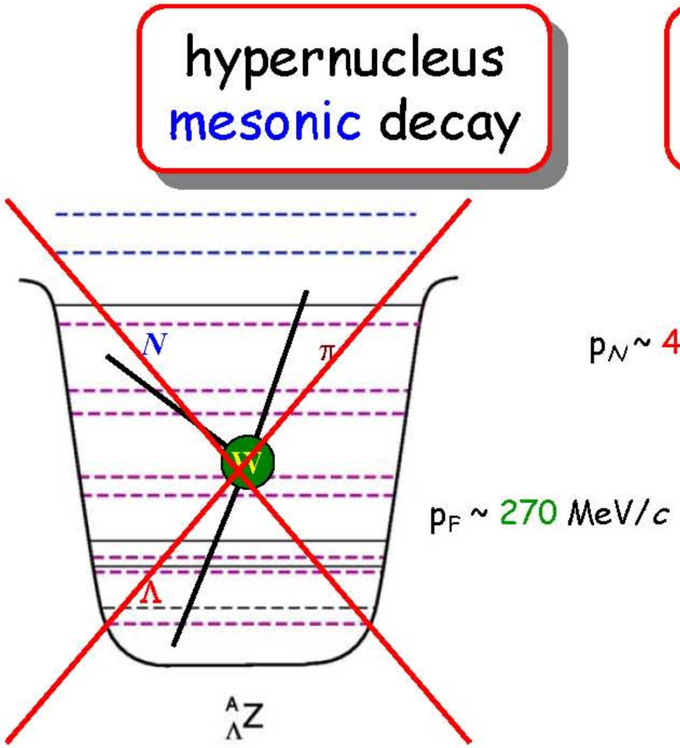

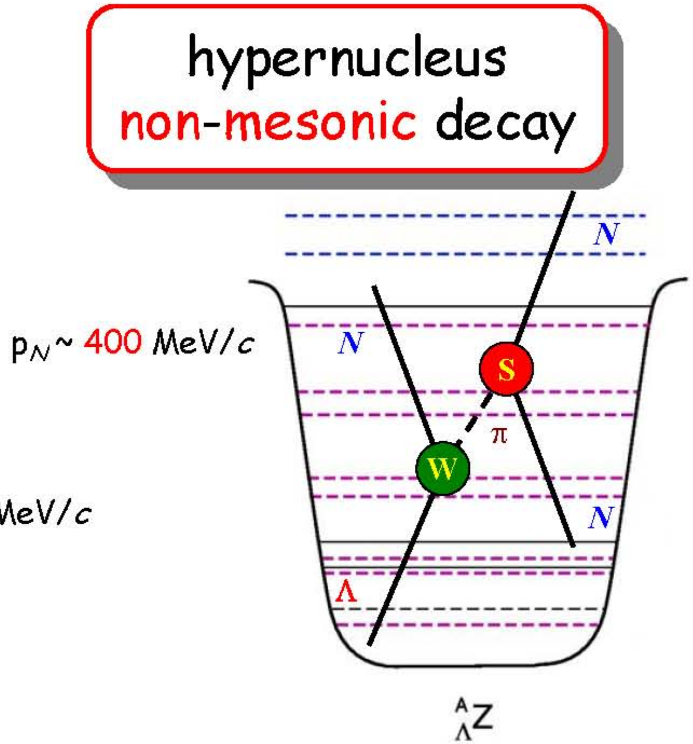

$\Lambda \to n + \pi^0 + 41$ MeV (36%)

$\Lambda \to p + \pi^- + 38$ MeV (64%)

$\tau_\Lambda = 263$ ps

suppressed by Pauli blocking

$\Lambda + n \to n + n + 176$ MeV

$\Lambda + p \to n + p + 176$ MeV

Decay observables

Hypernuclear lifetimes-Decay Rates

$$\Gamma = \Gamma_M + \Gamma_{NM} + \Gamma_{2N}$$

$$= \Gamma_{\pi^0} + \Gamma_{\pi^-} + \Gamma_n + \Gamma_p + \Gamma_{np}$$

$\Lambda \to N\pi$

$p_N \sim 100\ MeV$

$\Lambda N \to NN$

$p_N \sim 420\ MeV$

$\Lambda NN \to NNN$

$p_N \sim 340\ MeV$

$$\Gamma \sim \Gamma_\Lambda^{free} = 3.8 \times 10^9\ s^{-1}$$

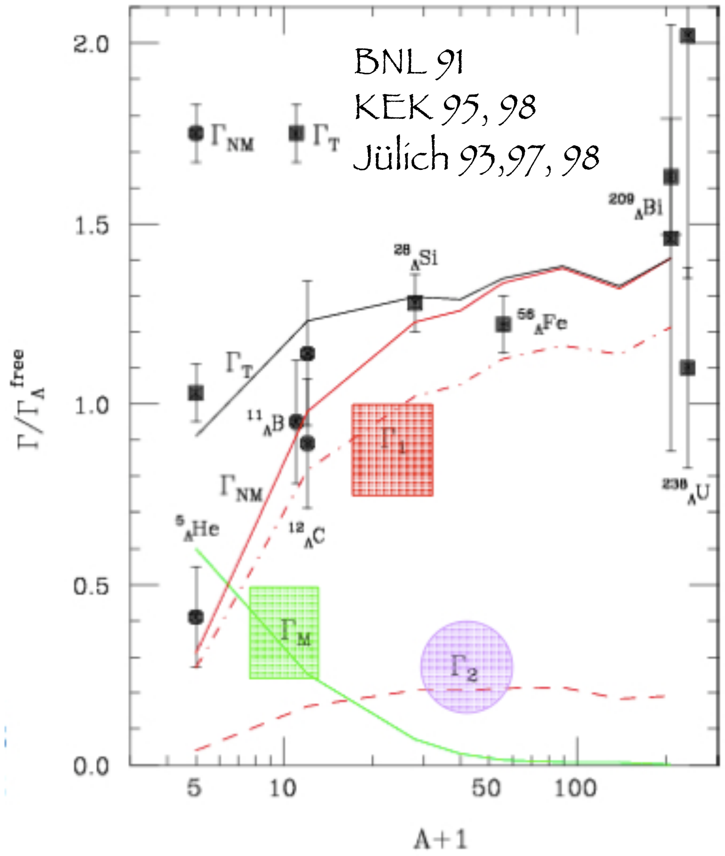

W. M. Alberico et al., Phys. Rev. C 61, 044314 (2000)

(well reproduced by theoretical models)

Building YN & YY Interactions

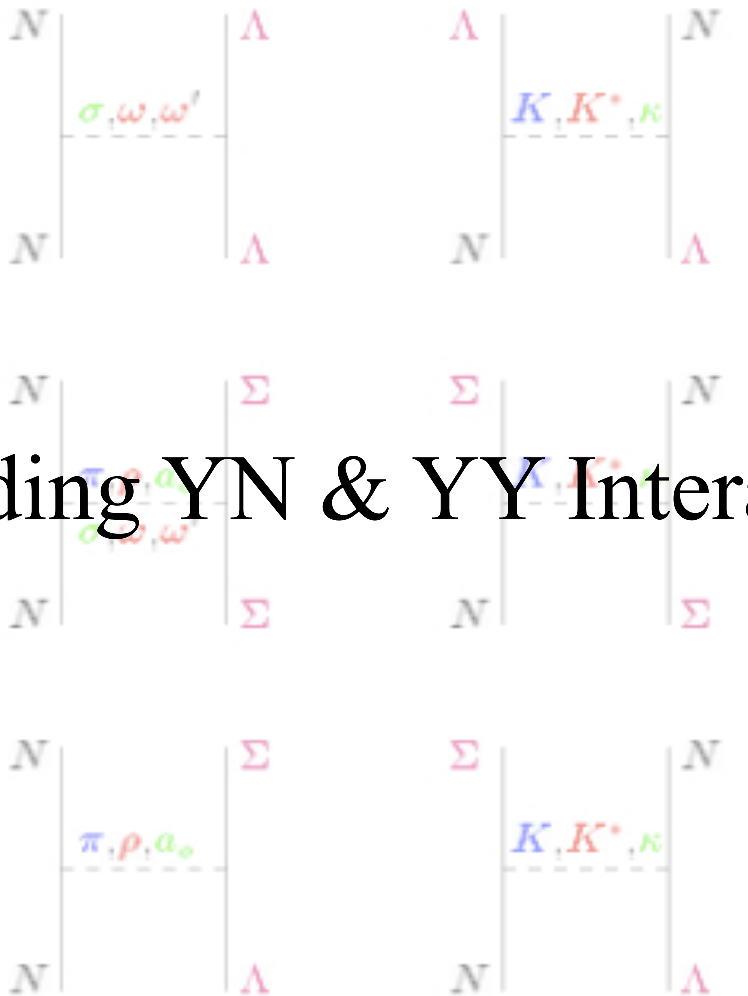

The YN & YY Interactions

✧ Study of the role of strangeness in low and medium energy nuclear physics.

✧ Test of $SU(3)_{flavor}$ symmetry.

✧ Input for Hypernuclear Physics & Astrophysics (Neutron Stars).

But due to:

✓ difficulties of preparation of hyperon beams.

✓ no hyperon targets available.

- YN: Only about 35 data points, all from the 1960´s
- 10 new data points, from KEK-PS E251 collaboration (2000)
- YY: No scattering data at all

(cf. > 4000 NN data for E_{lab} < 350 MeV)

YN meson-exchange models

Strategy: start from a NN model & impose $SU(3)_{flavor}$ constraints

$$L = g_M \Gamma_M \left(\overline{\Psi}_B \Psi_B\right)\phi_M$$

- ✧ scalar: σ,δ $\quad \Gamma_s = 1$
- ✧ pseudocalar: π,K,η $\quad \Gamma_{ps} = i\gamma^5$
- ✧ vector: ρ,K,ω, ϕ $\quad \Gamma_v = \gamma^\mu, \quad \Gamma_T = \sigma^{\mu\nu}$

$$\left\langle p_1' p_2' \middle| V_M \middle| p_1 p_2 \right\rangle = \bar{u}(p_1') g_M^{(1)} \Gamma_M^{(1)} u(p_1) \frac{P_M}{\left(p_1 - p_1'\right)^2 - m_M^2} \bar{u}(p_2') g_M^{(2)} \Gamma_M^{(2)} u(p_2)$$

$$\Downarrow$$

$$V(r) = V_0(r) + V_S(r)\left(\vec{\sigma}_1 \cdot \vec{\sigma}_2\right) + V_T(r) S_{12} + V_{ls}(r)\left(\vec{L} \times \vec{S}^+\right) + V_{als}(r)\left(\vec{L} \times \vec{S}^-\right)$$

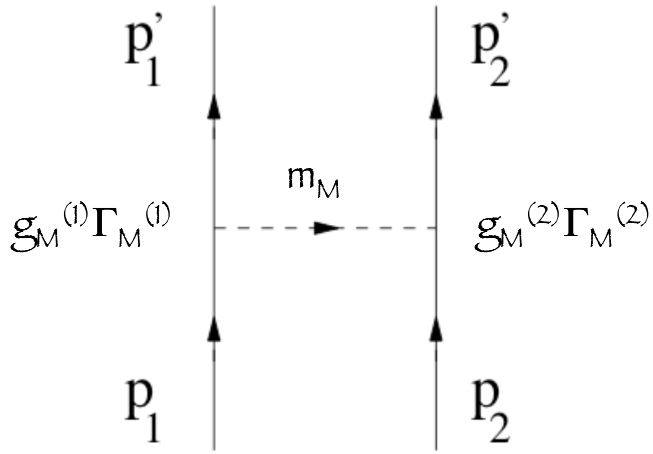

The Nijmegen & Jülich models

Nijmegen

(Nagels, Rijken, de Swart, Maessen)

- ✧ Based on Nijmegen NN potential.
- ✧ Momemtum & Configuration Space.
- ✧ Exchange of nonets of pseudo-scalar, vector and scalar.
- ✧ Strange vertices related by SU(3) symmetry with NN vertices.
- ✧ Gaussian Form Factors:

$$F_M(k^2) = e^{-\frac{k^2}{2\Lambda_M^2}}$$

Jülich

(Holzenkamp, Reube, Holinde, Speth, Haidenbauer, Meissner, Melnitchouck)

- ✧ Based on Bonn NN potential.
- ✧ Momemtum Space & Full energy-dependence & non-locality structure.
- ✧ higher-order processes involving π- and ρ-exchange (correlated 2π-exchange) besides single meson exchange.
- ✧ Strange vertices related by SU(6) $=SU(3)_{flavor} x SU(2)_{spin}$ symmetry with NN vertices.
- ✧ Dipolar Form Factors:

$$F_M(k^2) = \left(\frac{\Lambda_M^2 - m_M^2}{\Lambda_M^2 - k^2}\right)^2$$

Scattering amplitudes

Scattering amplitudes describing the hyperon-nucleon scattering are obtained by solving the Lipmann-Schwinger equation

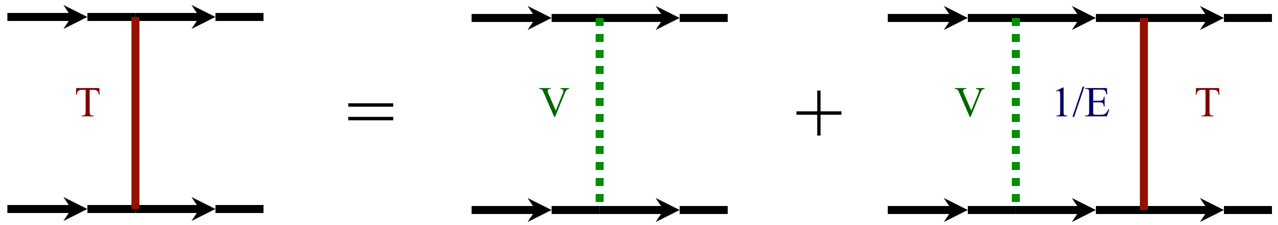

$$T = V + V \frac{1}{E} T$$

Chiral Effective Field Theory for YN

Strategy: start from a chiral effective lagrangian in a way similar to the NN case

Leading order (LO)

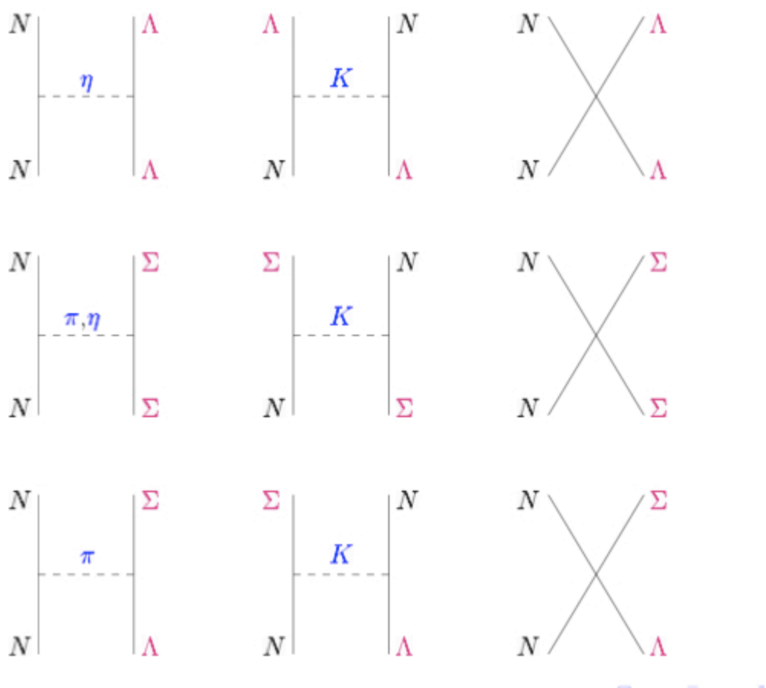

Polinder, Haidenbauer & Meissner, NPA 779, 244 (2006)

✧ Contact terms

$$L_1 = C_i^1 \langle \bar{B}_a \bar{B}_b (\Gamma_i B)_b (\Gamma_i B)_a \rangle$$

$$L_2 = C_i^2 \langle \bar{B}_a (\Gamma_i B)_a \bar{B}_b (\Gamma_i B)_b \rangle$$

$$L_3 = C_i^3 \langle \bar{B}_a (\Gamma_i B)_a \rangle \langle \bar{B}_b (\Gamma_i B)_b \rangle$$

$$\Downarrow$$

$$V^{B_1 B_2 \to B_3 B_4} = C_S^{B_1 B_2 \to B_3 B_4} + C_T^{B_1 B_2 \to B_3 B_4} \vec{\sigma}_1 \cdot \vec{\sigma}_2$$

✧ One-pseudoscalar meson exchange

$$L = \left\langle i\bar{B}\gamma^\mu D_\mu B - M_0 \bar{B}B + \frac{D}{2}\bar{B}\gamma^\mu \gamma_5 \{u_\mu, B\} + \frac{F}{2}\bar{B}\gamma^\mu \gamma_5 [u_\mu, B] \right\rangle$$

$$\Downarrow$$

$$V^{B_1 B_2 \to B_3 B_4} = -f_{B_1 B_2 M} f_{B_3 B_4 M} \frac{(\vec{\sigma}_1 \cdot \vec{k})(\vec{\sigma}_2 \cdot \vec{k})}{k^2 + m_M^2}$$

✧ Lippmann-Schwinger equation cut-off with the regularized

$$F(p,p',\Lambda) = e^{-\frac{\left(p^4+p'^4\right)}{\Lambda^4}}$$

Cutoff dependence:
Λ≈550-700 MeV

YN data rather
well described

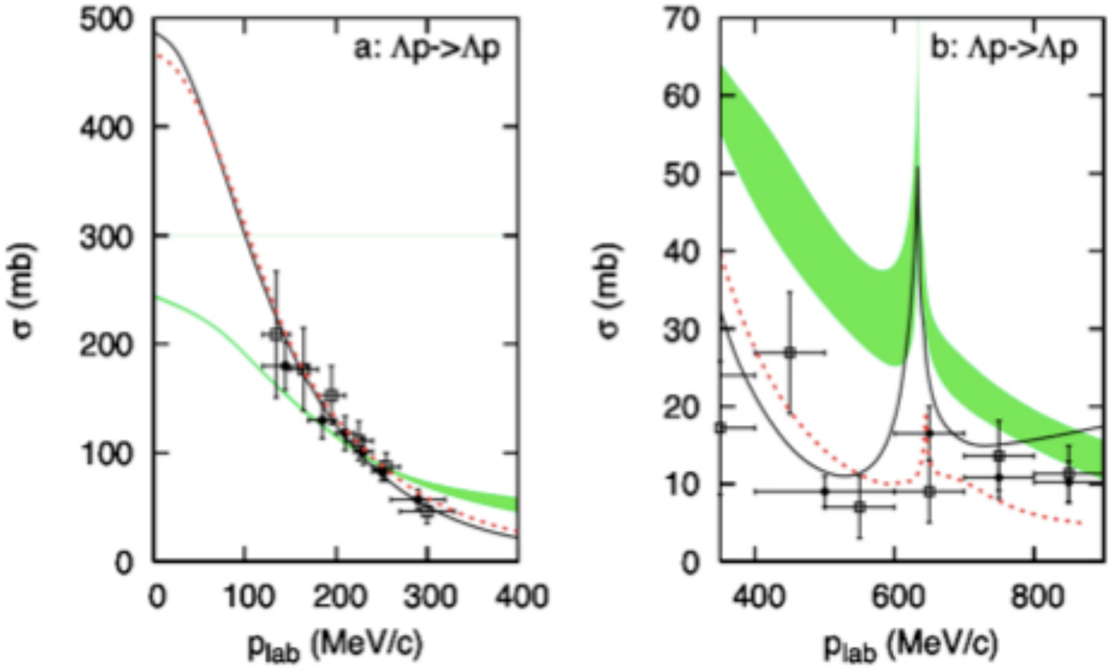

Total cross YN sections

Differential YN cross sections

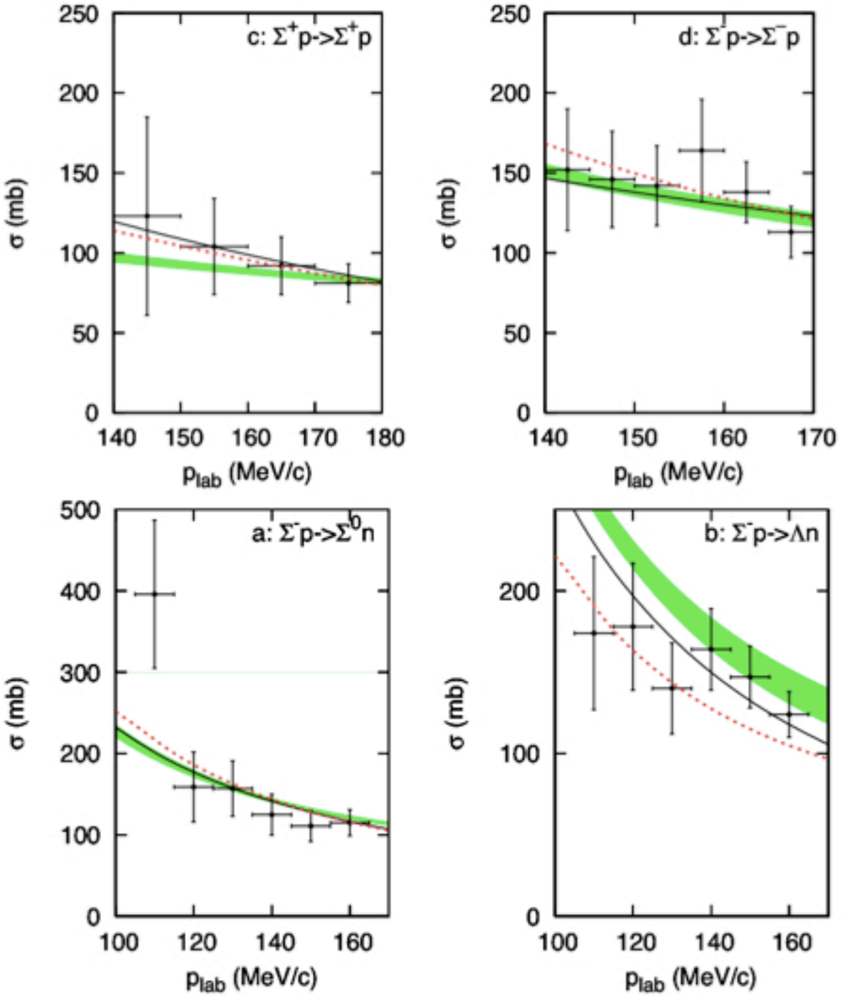

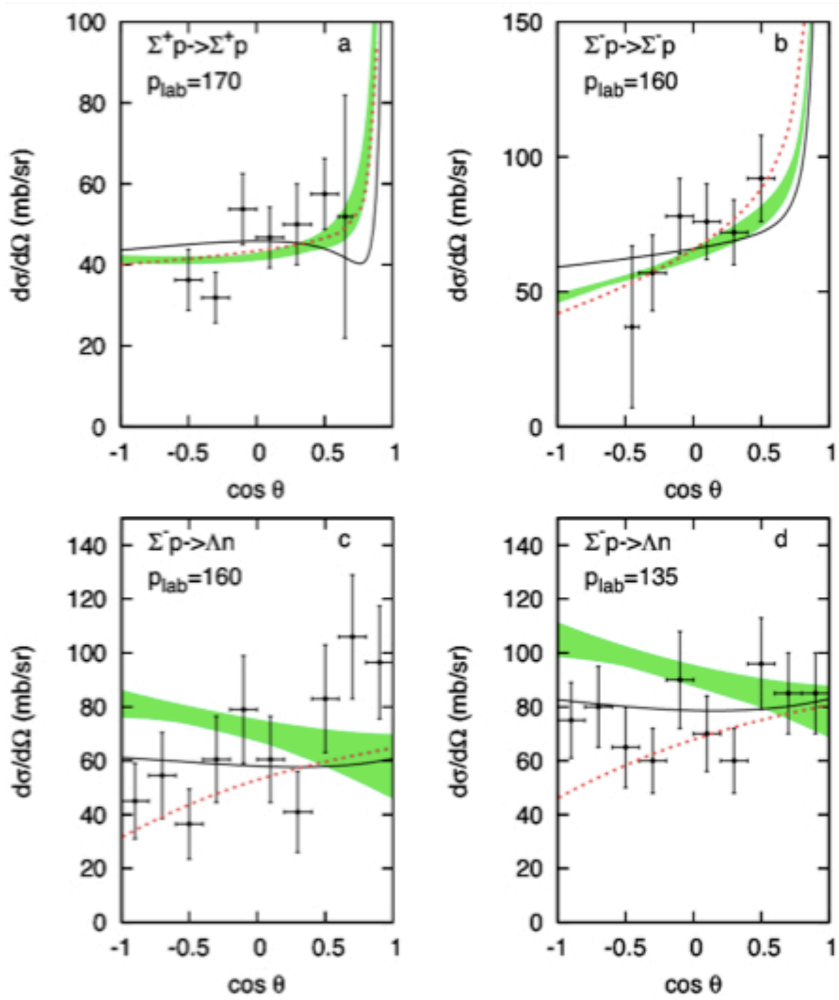

Solid: NSC97f

NPA 779, 224 (2006)

Green band: EFT

Dashed: Jülich04

Light hypernuclei properties

✧ Hypertriton ($^3H_\Lambda$) binding energy cutoff independent

Λ≈550	Λ≈600	Λ≈650	Λ≈700	Jülich04	NSC97f	Expt.
-2.35	-2.34	-2.34	-2.36	-2.27	-2.30	-2.354(50)

Deuteron B(^2H): -2.224 MeV

✧ A=4 doublet: $^4H_\Lambda$ -$^4He_\Lambda$

$^4H_\Lambda$	Λ=550	Λ≈600	Λ≈650	Λ=700	Jülich04	NSC97f	Expt.
$E_{sep}(0^+)$	2.63	2.46	2.36	2.38	1.87	1.60	2.04
$E_{sep}(1^+)$	1.85	1.51	1.23	1.04	2.34	0.54	1.00
ΔE_{sep}	0.78	0.95	1.13	1.34	-0.48	0.99	1.04

CSB-0^+	0.01	0.02	0.02	0.03	-0.01	0.10	0.35
CSB-1^+	-0.01	-0.01	-0.01	-0.01		-0.01	0.24

(All units are given in MeV)

Low-momentum YN interaction

Idea: start from a realistic YN interaction & integrate out the high-momentum components in the same way as as been done for NN.

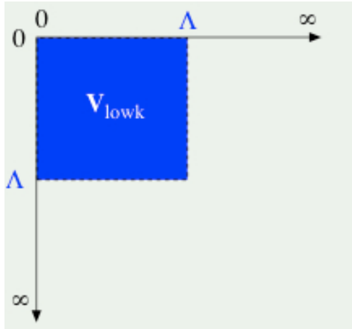

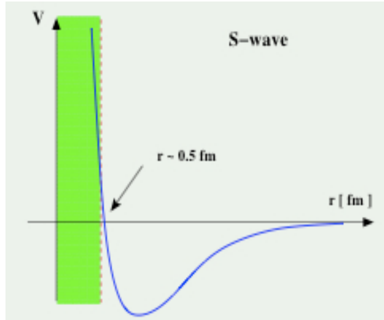

$V_{\text{low k}}$

- ✓ phase shift equivalent
- ✓ energy independent
- ✓ softer (no hard core)
- ✓ hermitian

B. -J. Schaefer et al., Phys. Rev. C 73, 011001 (2006)

Lippmann-Schwinger Equation

$$T(k',k;E_k) = V_{low\,k}(k',k) + \frac{2}{\pi} P \int_0^{\Lambda} dq\, q^2 V_{low\,k}(k',q) \frac{1}{E_k - H_0(q)} T(q,k;E_k)$$

Conditions

$$\frac{dT_\Lambda}{d\Lambda} = 0; \quad V_{low\,k} = \Lambda \qquad \Lambda \to \infty : V_{low\,k} = V_{bare}$$

Renormalization Group Flow Equation

$$\frac{d}{d\Lambda} V_{low\,k}(k',k) = -\frac{2}{\pi} \frac{V_{low\,k}(k',\Lambda) T(\Lambda,k;\Lambda^2)}{E_k - H_0(\Lambda)}$$

$^1S_0$ (I=3/2)matrix elements and phase-shift for ΣN→ΣN

Λ≈500 MeV

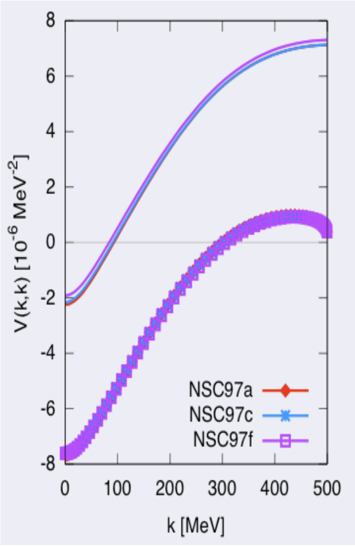

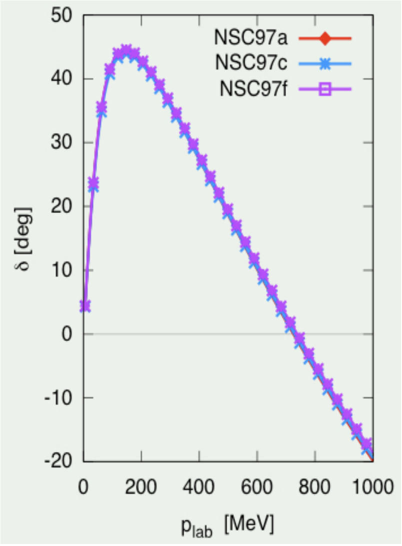

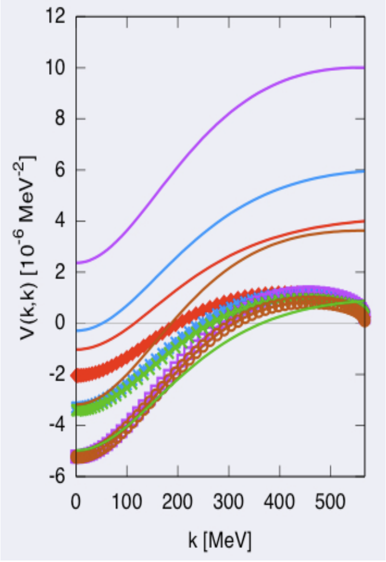

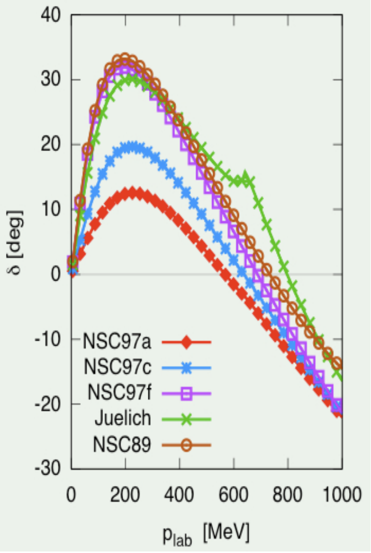

$^1S_0$ (I=1/2)matrix elements and phase-shift for ΛN→ΛN

Λ≈500 MeV

B. -J. Schaefer et al., Phys. Rev. C 73, 011001 (2006)

Cut-off dependence

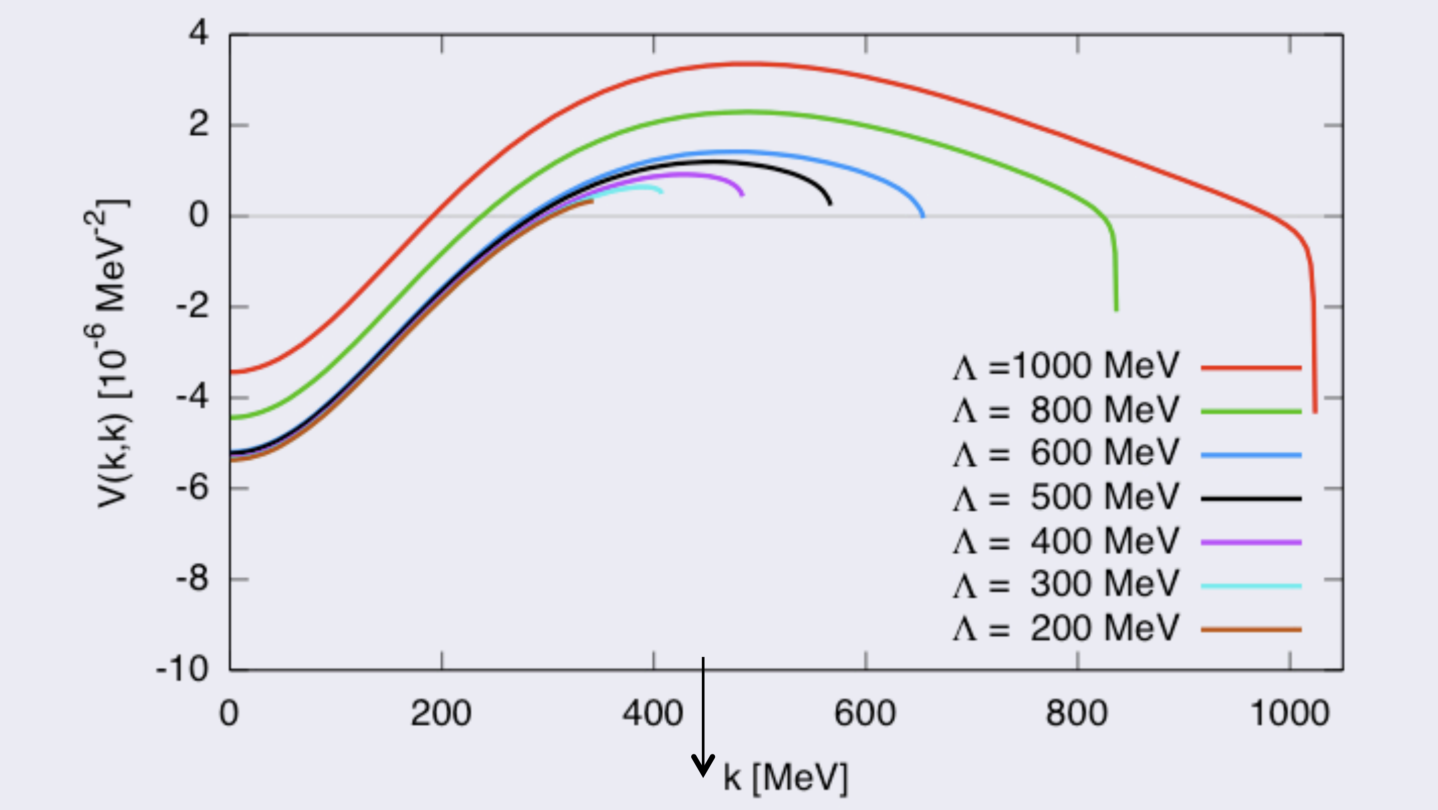

$^1S_0$ (I=1/2)matrix elements for $\Lambda N \rightarrow \Lambda N$ (NSC97f)

B. -J. Schaefer et al., Phys. Rev. C 73, 011001 (2006)

Hypernuclear Matter EoS

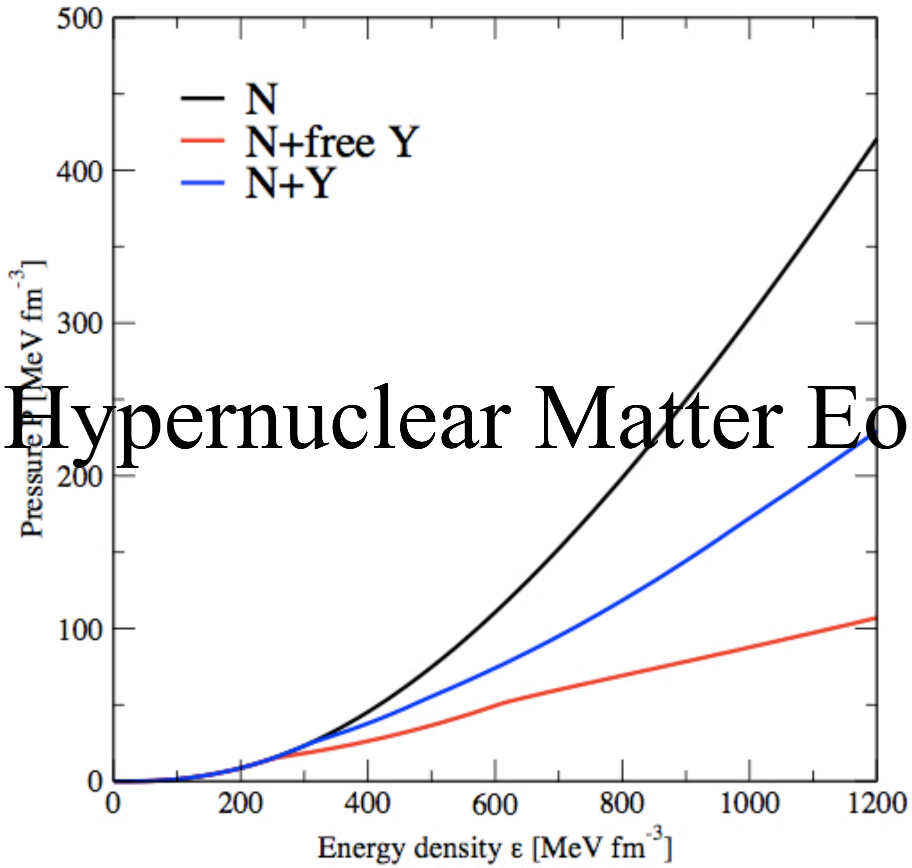

Approaches to Hypernuclear Matter EoS

The Hypernuclear Matter EoS has been considered by many authors using

- <u>Phenomenological approaches</u>

  Based on effective density-dependent interactions with parameters adjusted to reproduce nuclear and hypernuclear observables and compact star properties (e.g., Skyrme, RMF, …)

- <u>Microscopic approaches</u>

  Based on realistic two-body baryon-baryon interactions that describe scattering data in free space. To obtain the EoS one has to “solve” the complicated many-body problem (e.g., BHF, DBHF, $V_{\text{low }k}$, …)

Brueckner Theory for Hyperonic Matter

Consider a system of A fermions described by

$$H = \sum_{i=1}^{A} K_i + \sum_{i<j}^{A} V_{ij} \Longrightarrow \text{Ground State} \quad H|\psi\rangle = E|\psi\rangle$$

UNSOLVABLE !!!

✧ Idea: introduce an auxiliary s. p. potential U_i

$$H = \underbrace{\sum_{i=1}^{A}\left(K_i + U_i\right)}_{\substack{H_o \\ \text{unperturbed}}} + \underbrace{\sum_{i<j}^{A} V_{ij} - \sum_{i=1}^{A} U_i}_{\substack{H_1 \\ \text{perturbation}}}$$

$$E = E_0 + \Delta E$$

$$H_0|\phi_0\rangle = E_0|\phi_0\rangle$$

$$\Delta E \Longrightarrow \text{perturbation theory}$$

✧ Goldstone Expansion

(only linked diagrams)

$$\Delta E = \langle \phi_0 | H_1 \sum_{n=0}^{\infty} \left[\frac{1 - |\phi_0\rangle\langle\phi_0|}{E_0 - H_0} H_1 \right]^n |\phi_0\rangle_l$$

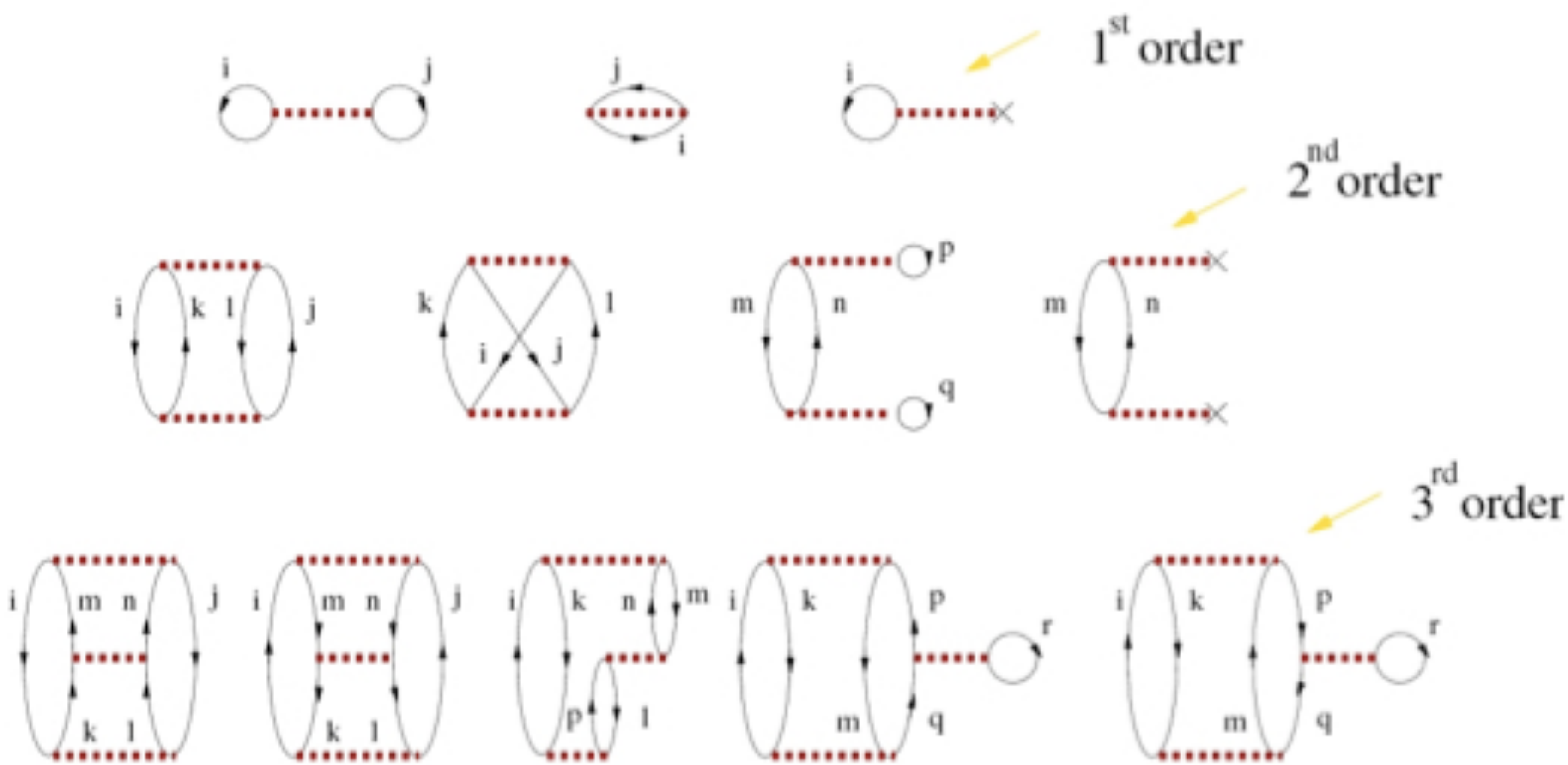

✧ Brueckner's reaction matrix (G-matrix)

✓ Partial summation of the set of pp ladder diagrams

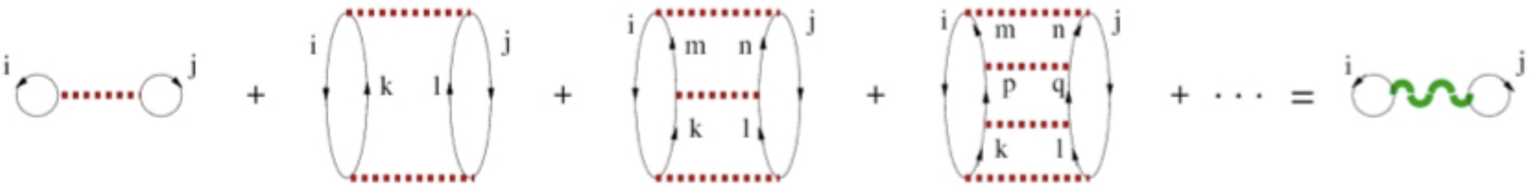

✓ G-matrix obtained by solving the Bethe-Goldstone equation

$$G = V + V\frac{Q}{\omega - H_0 + i\eta}V + V\frac{Q}{\omega - H_0 + i\eta}V\frac{Q}{\omega - H_0 + i\eta}V + \cdots$$

$$= \quad V + V\frac{Q}{\omega - H_0 + i\eta}\underbrace{\left[V + V\frac{Q}{\omega - H_0 + i\eta}V + V\frac{Q}{\omega - H_0 + i\eta}V\frac{Q}{\omega - H_0 + i\eta}V + \cdots\right]}_{G}$$

Then:

$$G = V + V \frac{Q}{\omega - H_0 + i\eta} G$$

Note that the Bethe-Goldstone equation is formally identical to the Lippmann-Schwinger equation describing the scattering of two particles in free space

$$T = V + V \frac{1}{\omega - K + i\eta} T$$

$\Rightarrow$ The G-matrix describes the scattering of two particles in the presence of a surrounding medium

✧ Medium Effects

➢ Pauli blocking of intermediate states

The Pauli operator Q prevents the scattering to any occupied state, limiting the phase space of intermediate states

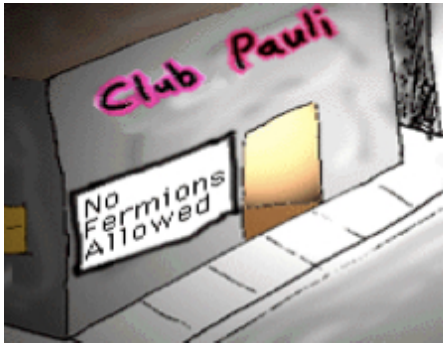

➢ Dressing of intermediate particles

The s.p. spectrum is modified by U which represents the average potential "felt" by a particle due to the presence of the medium

✧ Hole-line expansion & the BHF approximation

Goldstone expansion in terms of G

➡ Brueckner-Goldstone expansion

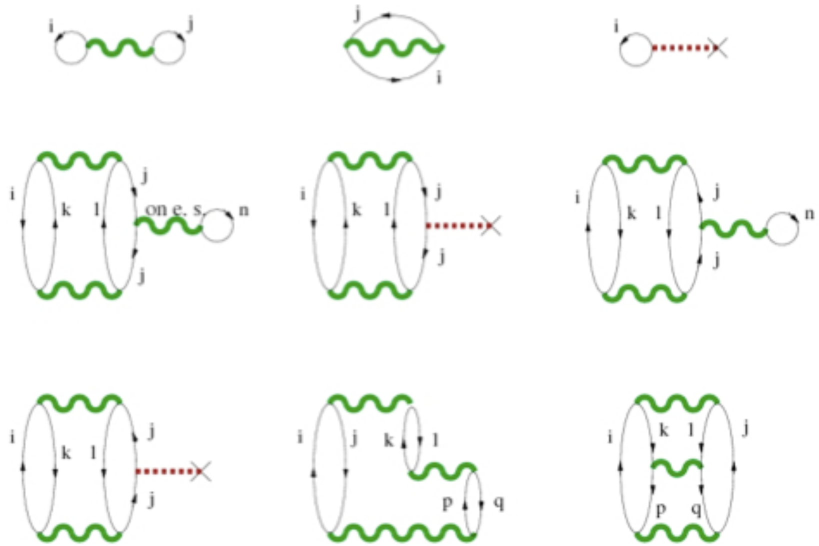

Grouping by number of hole lines ($c/r_0<1$) ➡ hole-line or Brueckner-Bethe-Goldstone expansion. Leading term: BHF approximation

$$E_{BHF} = \sum_{i \le A} \langle \alpha_i | K | \alpha_i \rangle + \frac{1}{2} \mathrm{Re}\left[\sum_{i,j \le A} \langle \alpha_i \alpha_j | G(\omega) | \alpha_i \alpha_j \rangle \right]$$

Convergence of the hole-line expansion

Depends on the choice of the auxiliary potential

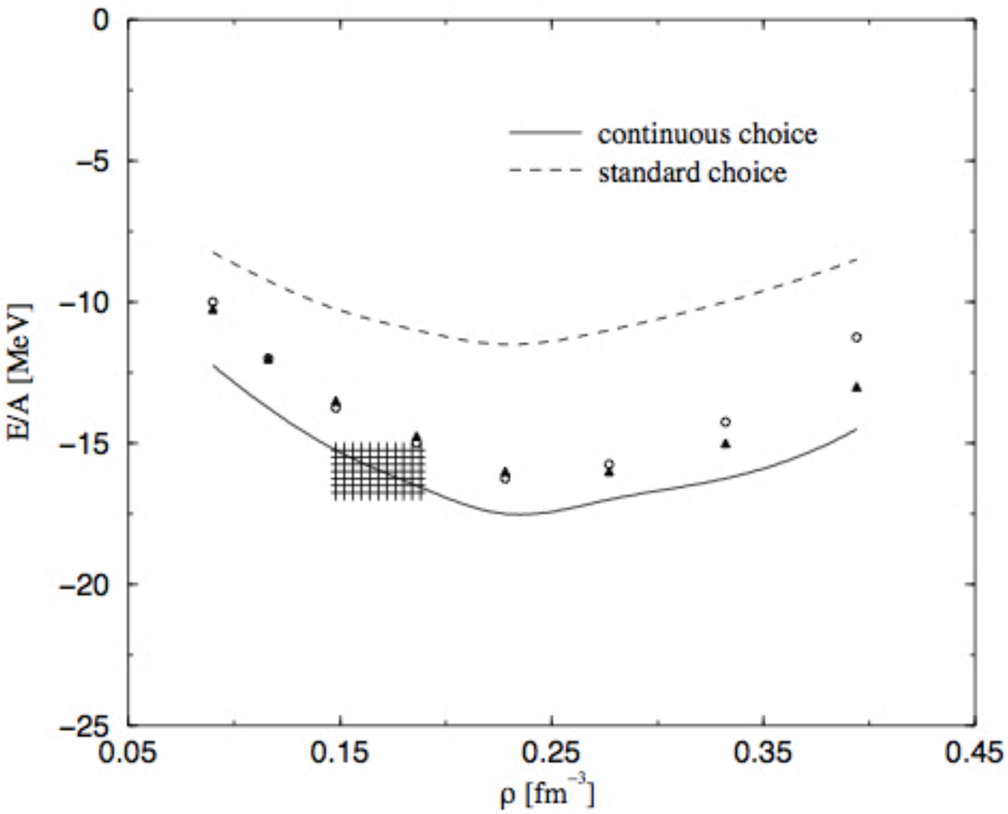

H. Q. Song et al.,, PRL 81, 1584 (1998)

- **Standard or Gap Choice**
  - $k < k_F$

$$U_B(k) = \sum_{B'} \sum_{k' \le k_{F_{B'}}} \left\langle \vec{k}\vec{k}' \middle| G\left(\omega = E_B(k) + E_{B'}(k')\right) \middle| \vec{k}\vec{k}' \right\rangle$$

  - $k > k_F$

$$U_B(k) = 0$$

- **Continuous Choice**

$$U_B(k) = \sum_{B'} \sum_{k' \le k_{F_{B'}}} \left\langle \vec{k}\vec{k}' \middle| G\left(\omega = E_B(k) + E_{B'}(k')\right) \middle| \vec{k}\vec{k}' \right\rangle$$

✧ Extended BHF approach: Hyperonic Matter

➢ Bethe-Goldstone equation (coupled channels)

- $$G(\omega)_{B_1B_2;B_3B_4} = V_{B_1B_2;B_3B_4} + \sum_{B_iB_j} V_{B_1B_2;B_jB_k} \frac{Q_{B_iB_j}}{\omega - E_{B_i} - E_{B_j} + i\eta} G(\omega)_{B_jB_k;B_3B_4}$$
- $$E_B(k) = \frac{\hbar^2 k^2}{2m_B} + \mathrm{Re}\left[U_B(k)\right] + m_B$$
- $$U_B(k) = \sum_{B'} \sum_{k' \le k_{F_{B'}}} \left\langle \vec{k}\vec{k}' \middle| G\left(\omega = E_B(k) + E_{B'}(k')\right) \middle| \vec{k}\vec{k}' \right\rangle$$

➢ Energy per particle

- $$\frac{E}{A}(\rho,\beta) = \frac{1}{A} \sum_B \sum_{k \le k_{F_B}} \left(\frac{\hbar^2 k^2}{2m_B} + \frac{1}{2} \mathrm{Re}\left[U_B(\vec{k})\right] + m_B \right)$$

Infinite sumation of two-hole line diagrams

✧ Coupled Channels

	S = 0	S = -1	S = -2	S = -3	S = -4
I = 0	$(NN \to NN)$		$\begin{pmatrix} \Lambda\Lambda \to \Lambda\Lambda & \Lambda\Lambda \to \Xi N & \Lambda\Lambda \to \Sigma\Sigma \\ \Xi N \to \Lambda\Lambda & \Xi N \to \Xi N & \Xi N \to \Sigma\Sigma \\ \Sigma\Sigma \to \Lambda\Lambda & \Sigma\Sigma \to \Xi N & \Sigma\Sigma \to \Sigma\Sigma \end{pmatrix}$		$(\Xi\Xi \to \Xi\Xi)$
I = 1/2		$\begin{pmatrix} \Lambda N \to \Lambda N & \Lambda N \to \Sigma N \\ \Sigma N \to \Lambda N & \Sigma N \to \Sigma N \end{pmatrix}$		$\begin{pmatrix} \Lambda\Xi \to \Lambda\Xi & \Lambda\Xi \to \Sigma\Xi \\ \Sigma\Xi \to \Lambda\Xi & \Sigma\Xi \to \Sigma\Xi \end{pmatrix}$	
I = 1	$(NN \to NN)$		$\begin{pmatrix} \Xi N \to \Xi N & \Xi N \to \Lambda\Sigma & \Xi N \to \Sigma\Sigma \\ \Lambda\Sigma \to \Xi N & \Lambda\Sigma \to \Lambda\Sigma & \Lambda\Sigma \to \Sigma\Sigma \\ \Sigma\Sigma \to \Xi N & \Sigma\Sigma \to \Lambda\Sigma & \Sigma\Sigma \to \Sigma\Sigma \end{pmatrix}$		$(\Xi\Xi \to \Xi\Xi)$
I = 3/2		$(\Sigma N \to \Sigma N)$		$(\Sigma\Xi \to \Sigma\Xi)$	
I = 2			$(\Sigma\Sigma \to \Sigma\Sigma)$		

Hyperons in Nuclear Matter

s.p. potentials

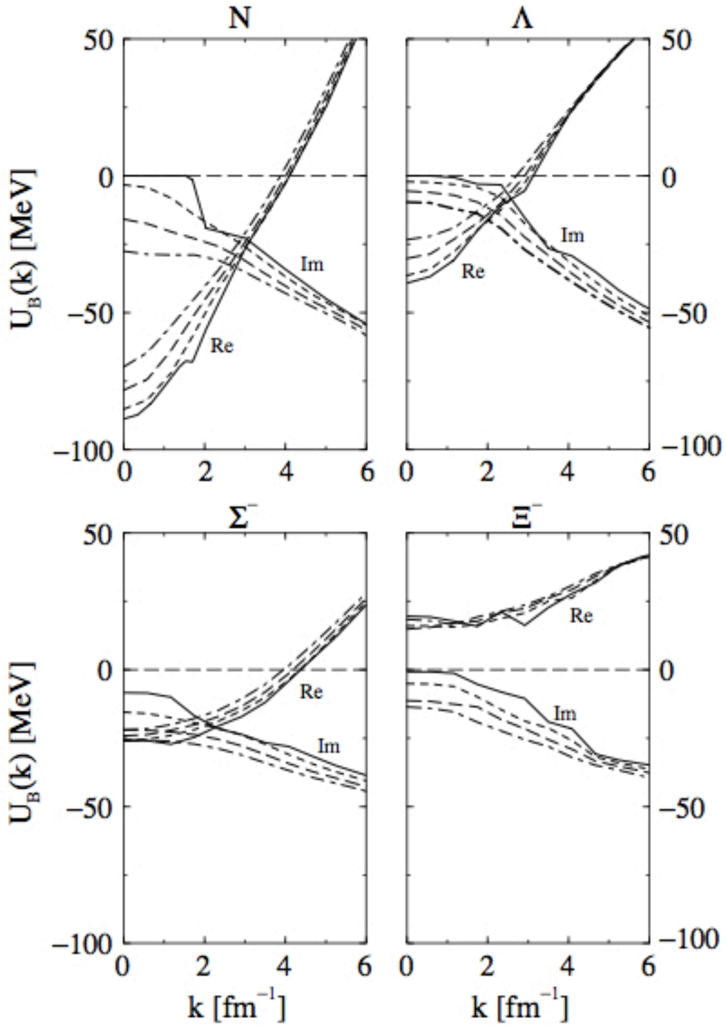

binding energy

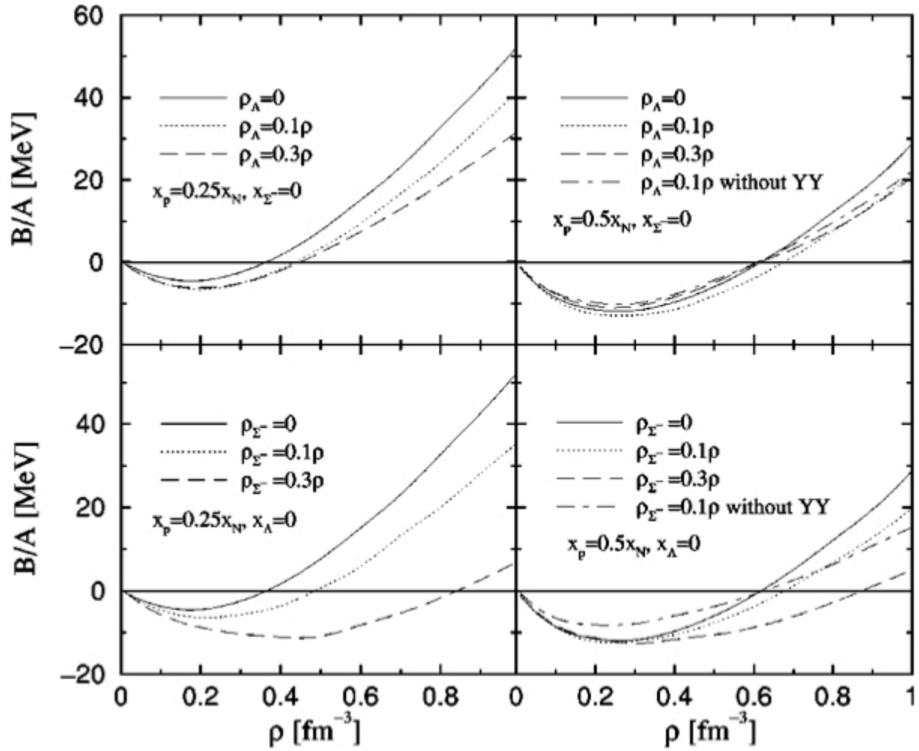

BHF calculation with NSC97

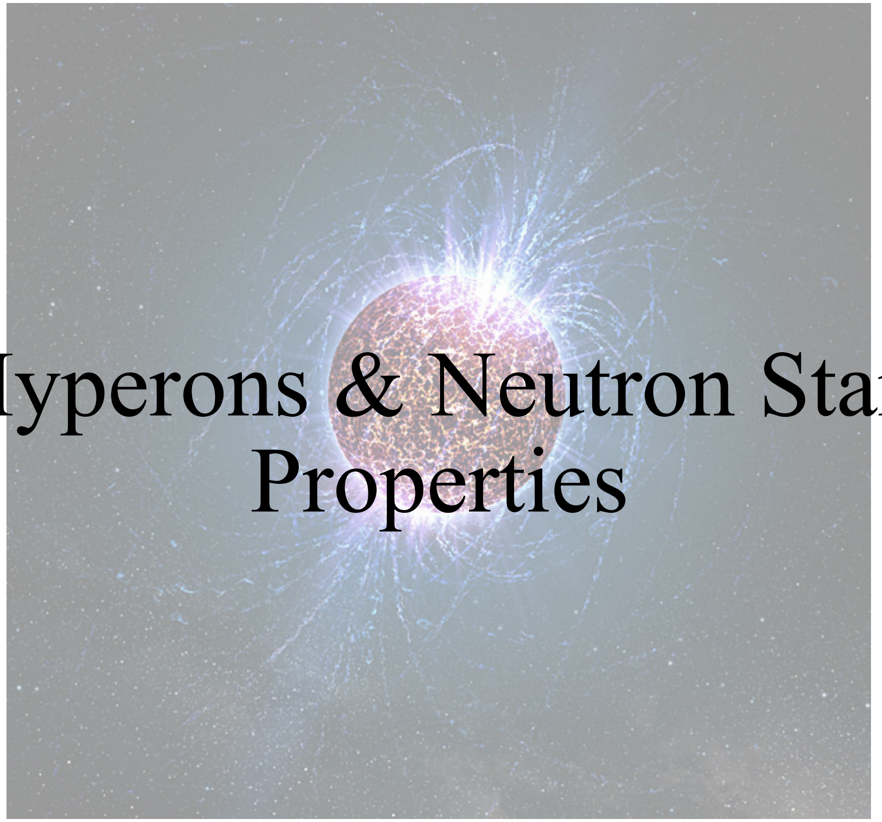

Hyperons & Neutron Star Properties

Some known facts about Neutron Stars

- Mass: $M \sim 1 - 2\ M_\odot$
- Radius: $R \sim\ 10 - 12$ km (or less ?)
- Density: $\rho \sim 10^{14} - 10^{15}\ g/cm^3$

$$\rho_{universe} \sim\ 10^{-30}\ g/cm^3$$
$$\rho_{sun} \sim\ 1.4\ \ g/cm^3$$
$$\rho_{earth} \sim\ 5.5\ \ g/cm^3$$

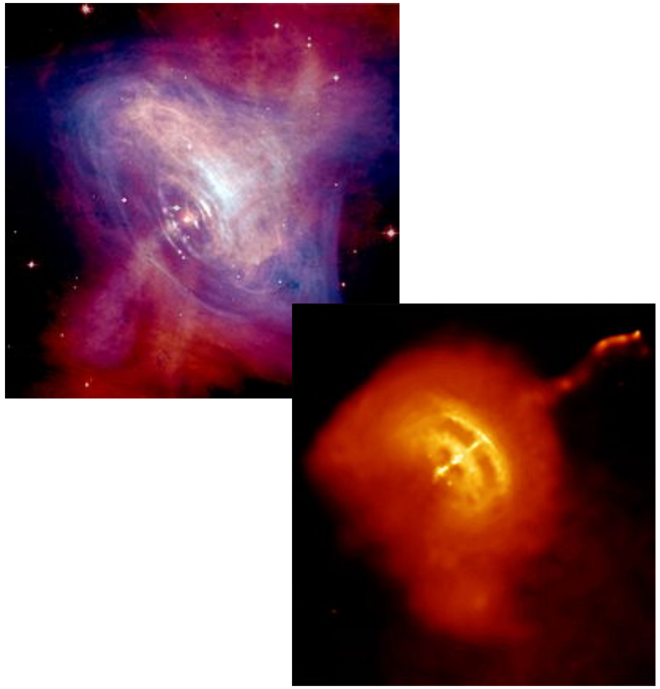

$$\pi R_{NS}^2 \sim 300\ \ km^2$$

- Firenze

$$M_{Firenze} \sim \left(3.65\times10^5\right)\times 75\ \ kg$$
$$\sim 1.37\times10^{-23} M_\odot$$
$$A_{Firenze} \sim 102\ \ km^2,\quad H_{Fiorentini} \sim 1.75m$$
$$\rho_{Fiorentini} \sim 1.55\times10^{-4}\ \ g/cm^3$$

- Baryonic number: $N_b \sim 10^{57}$ ("giant (hyper)nuclei")
- Magnetic field: $B \sim 10^{8\ldots16}$ G ($10^{4\ldots12}$ T)

$0.3-0.5G$	10^3-10^4G	10^5G	$4.5x10^5G$	$2.8x10^7G$
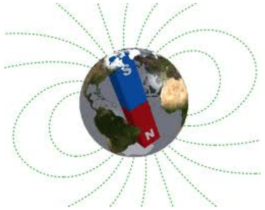		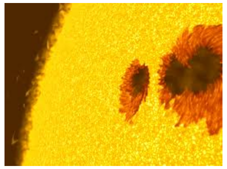	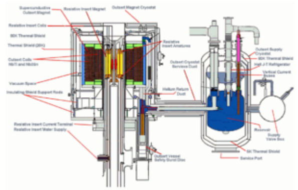	
Earth	Magnet	Sunspots	Largest continuous field in lab. (FSU, USA)	Largest magnetic pulse in lab. (Russia)

- Electric field: $E \sim 10^{18}$ V/cm
- Temperature: $T \sim 10^{6\ldots11}$ K
- Rotational period distribution
  ➔ two types of pulsars:
  - pulsars with P ~ s
  - pulsars with P ~ ms

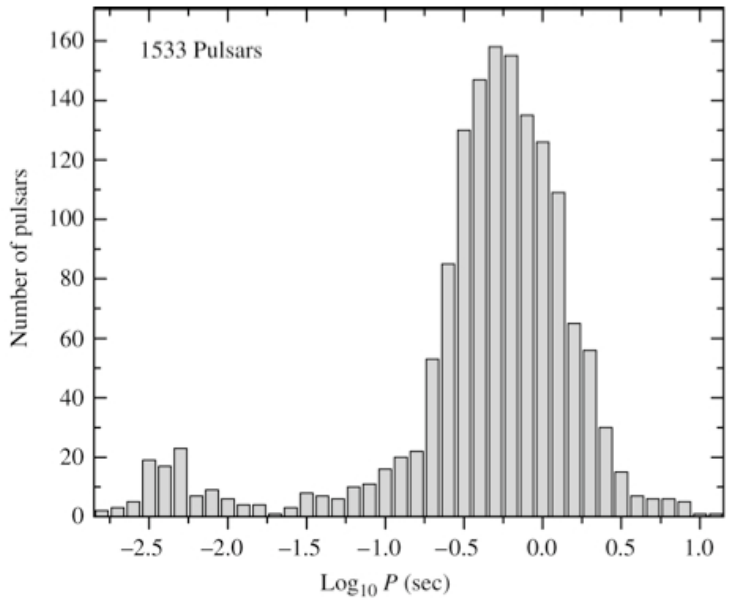

Shortest rotational period PSR in Terzan 5: $P_{J1748\text{-}2446ad} = 1.39$ ms

Most NS are observed as pulsars. Nowadays more than 2000 pulsars are known

Observables

- Period (P, dP/dt)
- Masses
- Luminosity
- Temperature
- Magnetic Field
- Gravitational Waves (future)

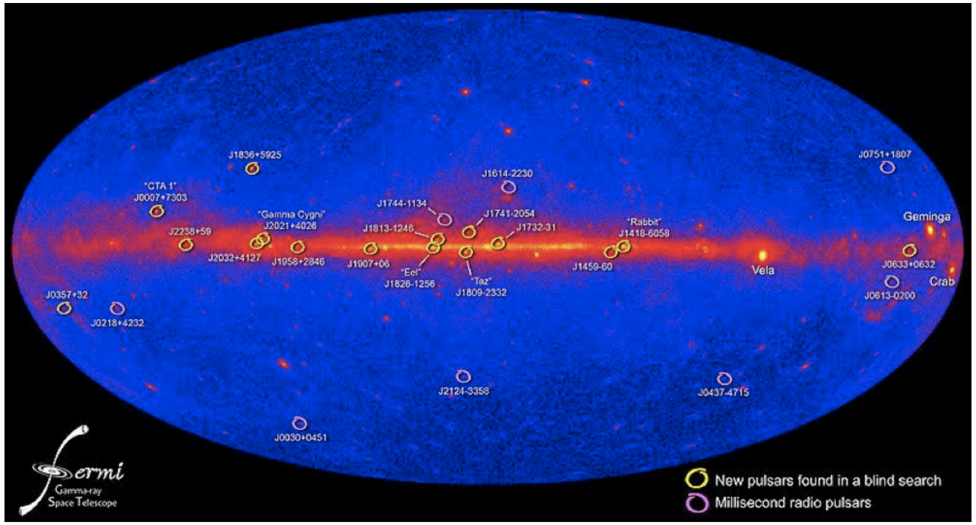

http://www.phys.ncku.edu.tw/~astrolab/mirrors/apod_e/ap090709.html

The 1001 Astrophysical Faces of Neutron Stars

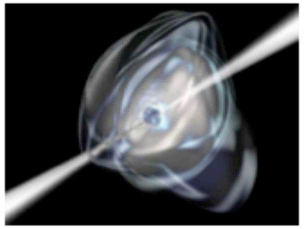

Anomalous X-ray Pulsars

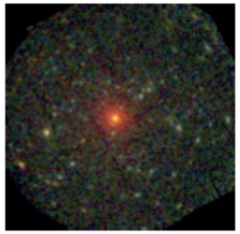

dim isolated neutron stars

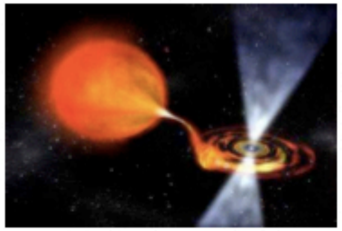

X-ray binaries

bursting pulsars

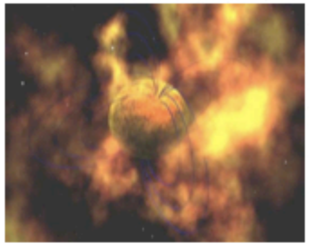

Soft Gamma Repeaters

pulsars

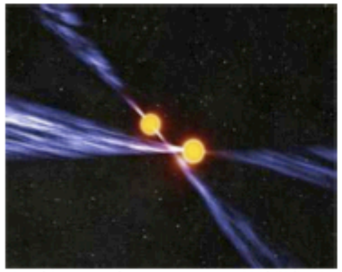

binary pulsars

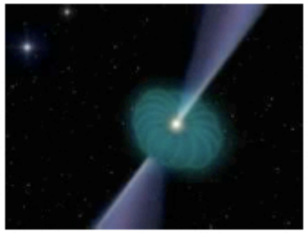

Rotating Radio Transients

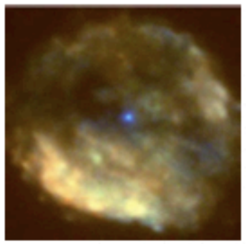

Compact Central Objects

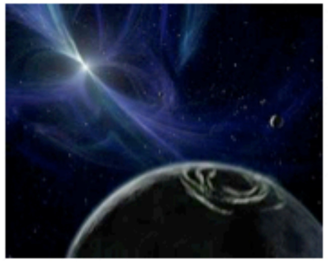

planets around pulsar

Observation of Neutron Stars

X- and γ-ray telescopes

Chandra

Fermi

Space telescopes

HST (Hubble)

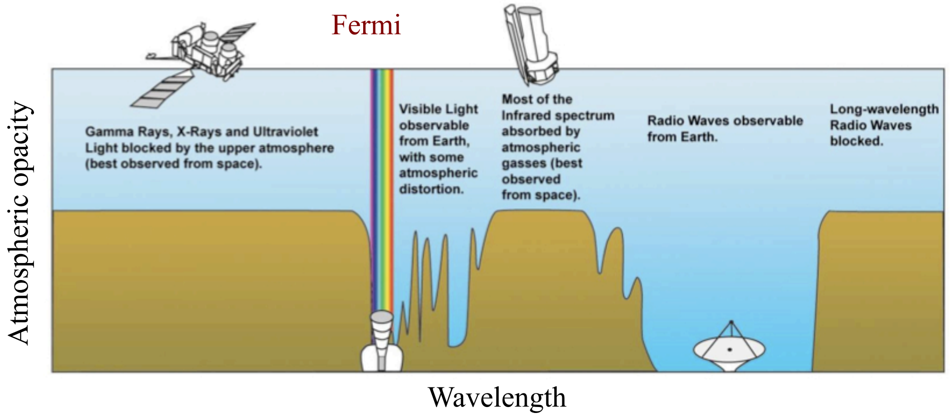

Optical telescopes

VLT (Atacama, Chile)

Radio telescopes

Arecibo (Puerto Rico): 305 m

Green Banks (USA): 100 m

Nançay (France): 94 m

How to Measure Neutron Star Masses

Use Doppler variations in spin period to measure orbital velocity changes along the line-of-sight

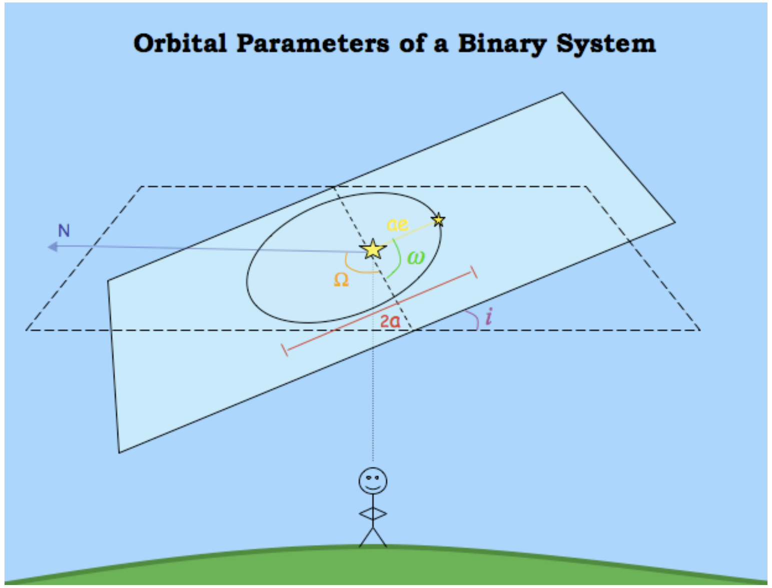

- 5 Keplerian parameters can normally be determined:

  P, a sin i, ε, T_0 & ω

- 3 unknowns: M_1, M_2, i

Kepler's 3rd law

$$\frac{G(M_1+M_2)}{a^3}=\left(\frac{2\pi}{P}\right)^2 \rightarrow f(M_1,M_2,i)\equiv\frac{(M_2\sin i)^3}{(M_1+M_2)^2}=\frac{Pv^3}{2\pi G}$$

mass function

In few cases small deviations from Keplerian orbit due to GR effects can be detected

Measure of at least 2 post-Keplerian parameters $\rightarrow$ High precision NS mass determination

$$\dot{\omega} = 3T_{\otimes}^{2/3}\left(\frac{P_b}{2\pi}\right)^{-5/3}\frac{1}{1-\varepsilon}\left(M_p + M_c\right)^{2/3} \longrightarrow$$ Periastron precession

$$\gamma = T_{\otimes}^{2/3}\left(\frac{P_b}{2\pi}\right)^{1/3}\varepsilon\frac{M_c\left(M_p + 2M_c\right)}{\left(M_p + M_c\right)^{4/3}} \longrightarrow$$ Time dilation and grav. redshift

$$r = T_{\otimes}M_c \longrightarrow$$ Shapiro delay “range”

$$s = \sin i = T_{\otimes}^{-1/3}\left(\frac{P_b}{2\pi}\right)^{-2/3}x\frac{\left(M_p + M_c\right)^{2/3}}{M_c} \longrightarrow$$ Shapiro delay “shape”

$$\dot{P}_b = -\frac{192\pi}{5}T_{\otimes}^{5/3}\left(\frac{P_b}{2\pi}\right)^{-5/3}f(\varepsilon)\frac{M_p M_c}{\left(M_p + M_c\right)^{1/3}} \longrightarrow$$ Orbit decay due to GW emission

An example: the mass of the Hulse-Taylor pulsar (PSR J1913+16)

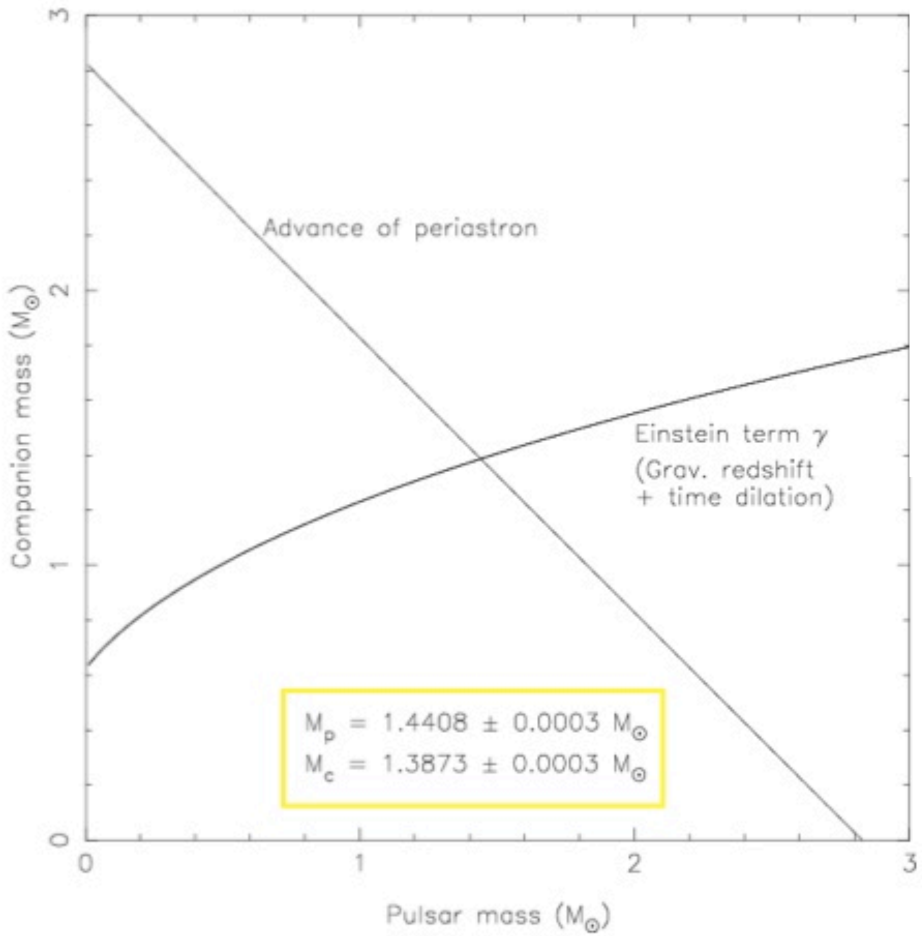

Parameter	Value
Orbital period P_b (d)	0.322997462727(5)
Projected semi-major axis x (s)	2.341774(1)
Eccentricity e	0.6171338(4)
Longitude of periastron ω (deg)	226.57518(4)
Epoch of periastron T_0 (MJD)	46443.99588317(3)
Advance of periastron $\dot{\omega}$ (deg yr^{-1})	4.226607(7)
Gravitational redshift γ (ms)	4.294(1)
Orbital period derivative $(\dot{P}_b)^{\mathrm{obs}}$ (10^{-12})	−2.4211(14)

Neutron Star Radii Measurements

Not much to say after the excellent seminar by Sebastien Guillot yesterday ….

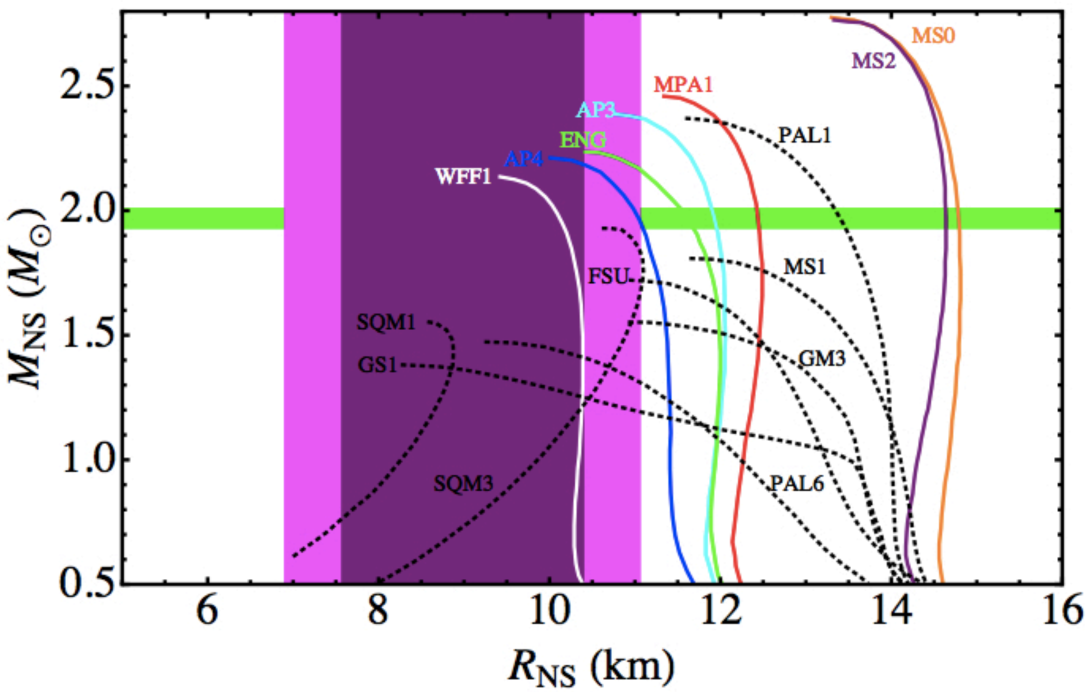

Guillot et al., 2013:

Analysis of thermal spectrum of 5quiescent LMXB in globular clusters, assuming that all NS have the same radius

$$R = 9.1^{+1..3}_{-1.5}\, km$$

Anatomy of a Neutron Star

Equilibrium composition determined by

✓ Charge neutrality

$$\sum_i q_i \rho_i = 0$$

✓ Equilibrium with respect to weak interacting processes

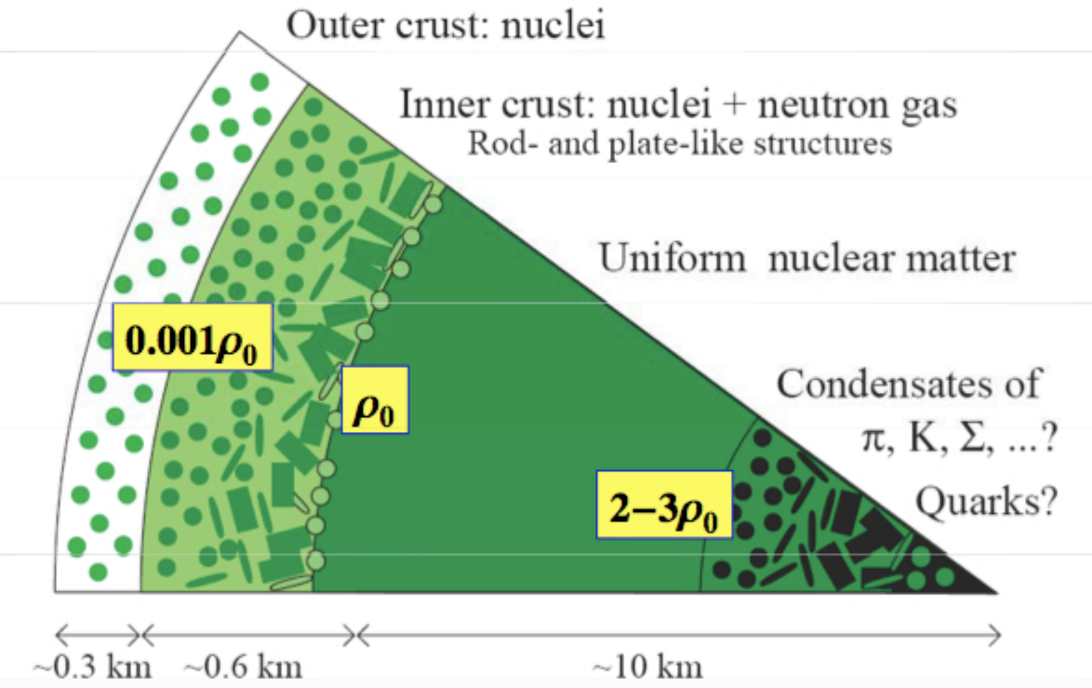

$$b_1 \to b_2 + l + \bar{\nu}_l \qquad b_2 + l \to b_1 + \nu_l \quad \longrightarrow \quad \mu_i = b_i \mu_n - q_i\left(\mu_e - \mu_{\nu_e}\right), \quad \mu_i = \frac{\partial \varepsilon}{\partial \rho_i}$$

Hyperons in Neutron Stars

Hyperons in NS considered by many authors since the pioneering work of Ambartsumyan & Saakyan (1960)

Phenomenological approaches

- ✧ Relativistic Mean Field Models: Glendenning 1985; Knorren et al. 1995; Shaffner-Bielich & Mishustin 1996, Bonano & Sedrakian 2012, …
- ✧ Non-realtivistic potential model: Balberg & Gal 1997
- ✧ Quark-meson coupling model: Pal et al. 1999, …
- ✧ Chiral Effective Lagrangians: Hanauske et al., 2000
- ✧ Density dependent hadron field models: Hofmann, Keil & Lenske 2001

Microscopic approaches

- ✧ Brueckner-Hartree-Fock theory: Baldo et al. 2000; I. V. et al. 2000, Schulze et al. 2006, I.V. et al. 2011, Burgio et al. 2011, Schulze & Rijken 2011
- ✧ $V_{\text{low k}}$: Djapo, Schaefer & Wambach, 2010

Sorry if I missed somebody

Hyperons are expected to appear in the core of neutron stars at $\rho \sim (2\text{-}3)\rho_0$ when μ_N is large enough to make the conversion of N into Y energetically favorable.

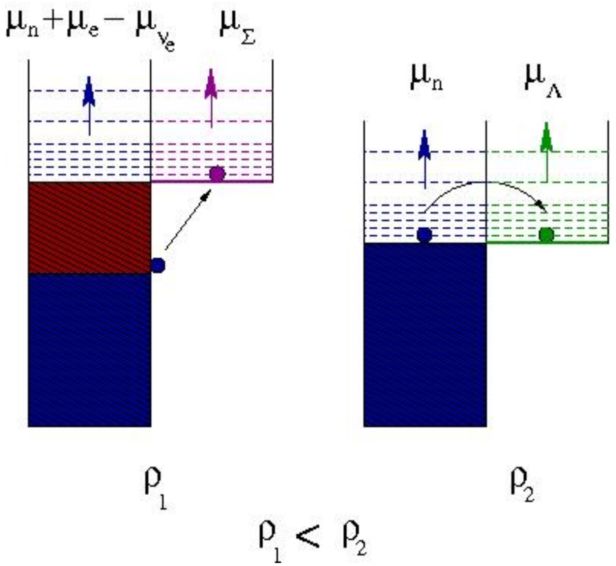

$$\mu_{\Sigma^-} = \mu_n + \mu_{e^-} - \mu_{\nu_{e^-}}$$

$$\mu_\Lambda = \mu_n$$

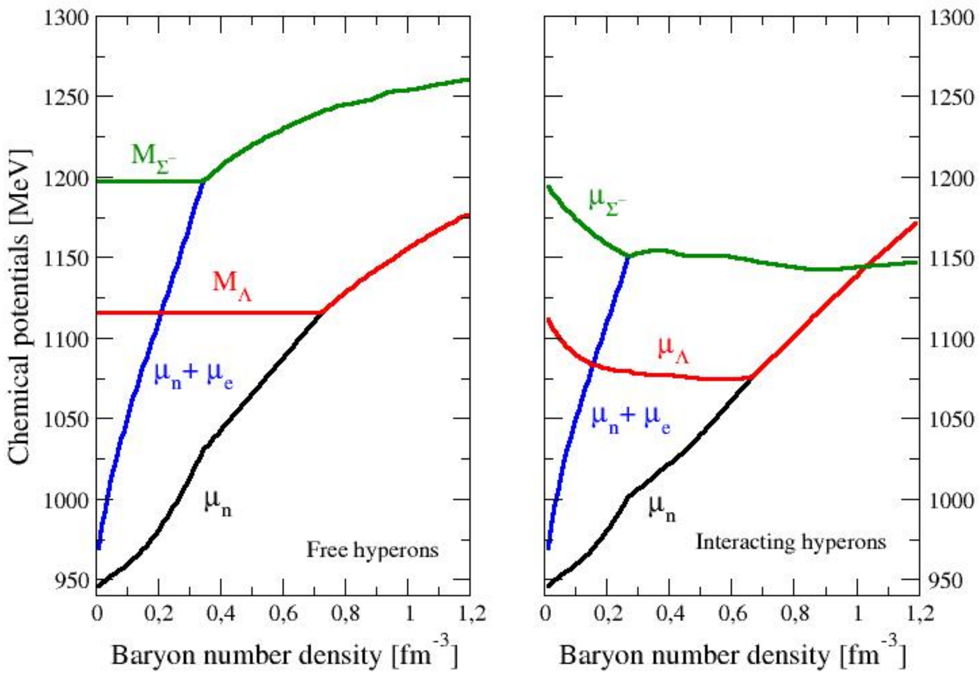

$$n + n \rightarrow n + \Lambda$$

$$p + e^- \rightarrow \Lambda + \nu_{e^-}$$

$$n + n \rightarrow p + \Sigma^-$$

$$n + e^- \rightarrow \Sigma^- + \nu_{e^-}$$

Neutron Star Matter Composition

RMFT

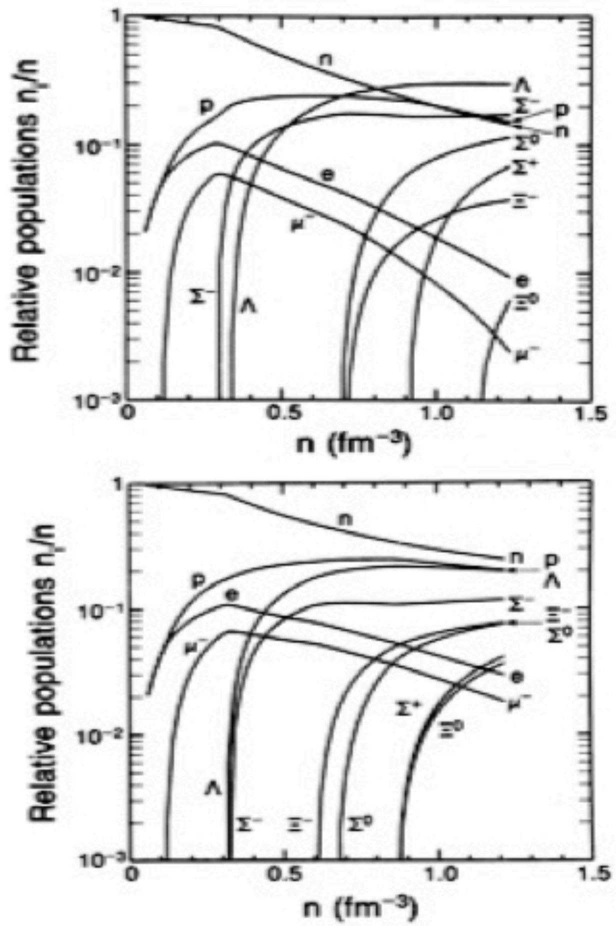

N. K. Glendenning, APJ 293, 470 (1985)

BHF

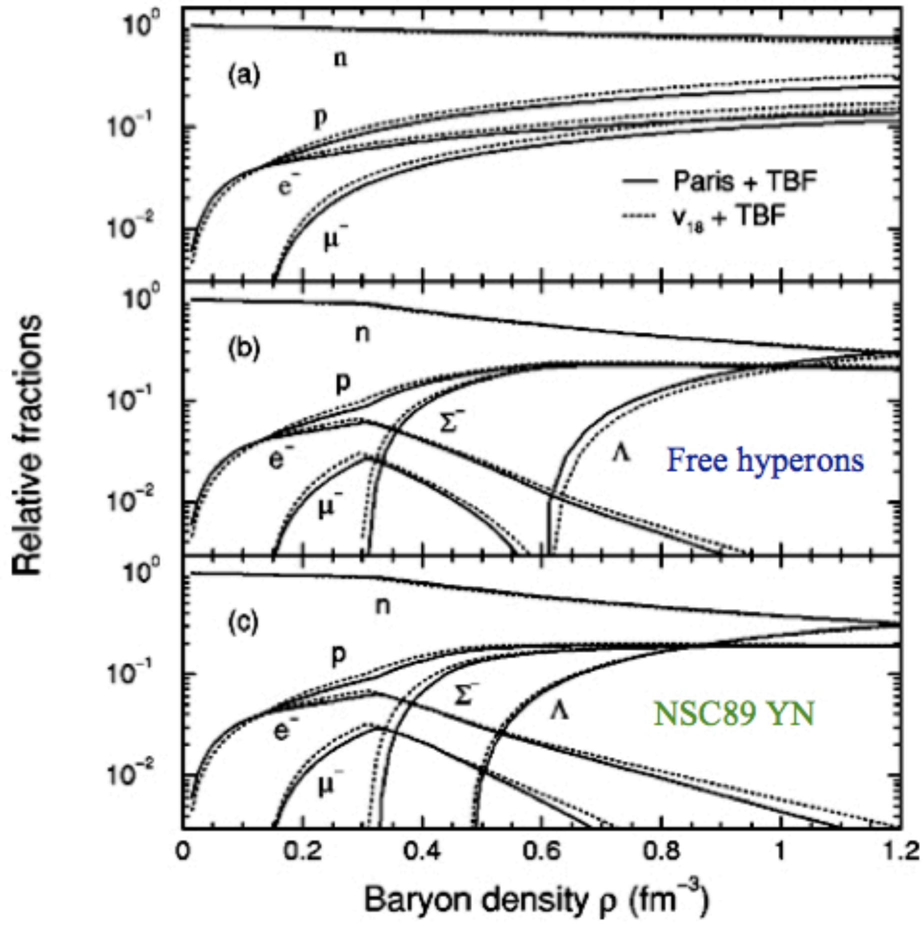

M. Baldo et al.,, PRC 61, 055801 (2000)

Effect of Hyperons in the EoS and Mass of Neutron Stars

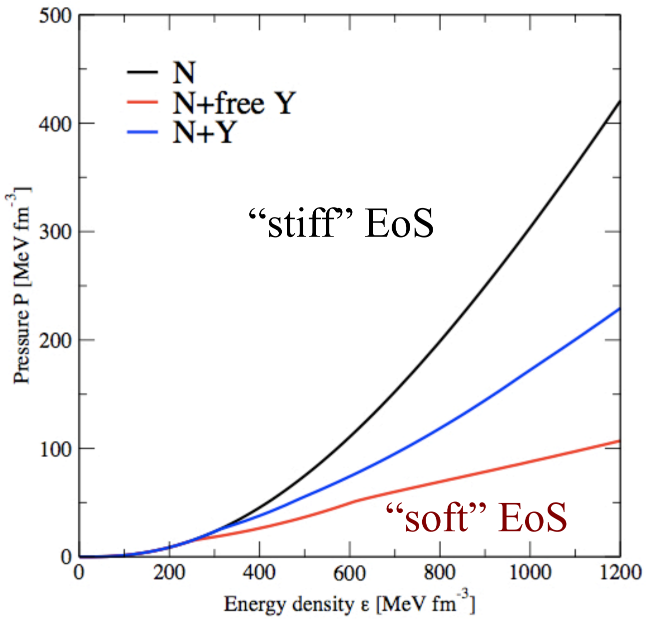

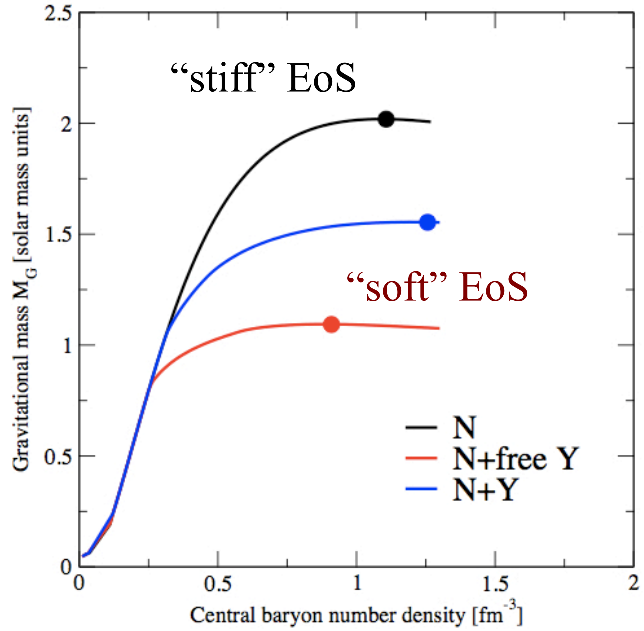

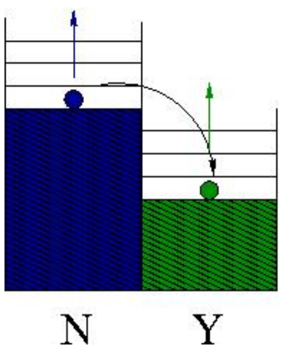

Relieve of Fermi pressure due to the appearance of hyperons ➔

EoS softer ➔ reduction of the mass

Measured Neutron Star Masses (up to ~ 2006-2008)

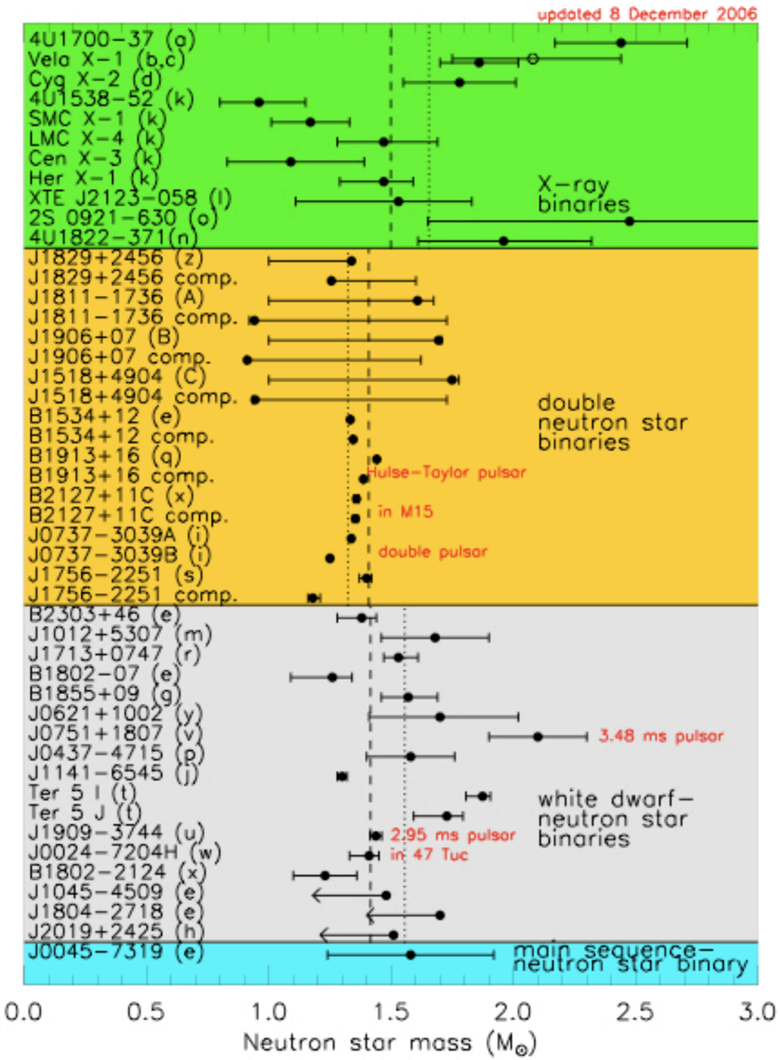

(Lattimer & Prakash 2007)

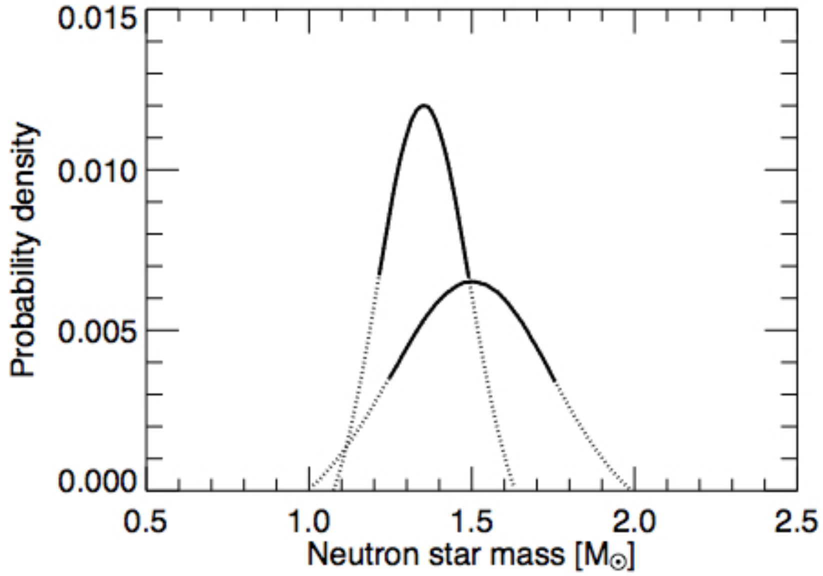

up to ~ 2006-2008 any valid EoS should predict

$$M_{\max}[EoS] > 1.4 - 1.5 M_\odot$$

Hyperons in NS
(up to ~ 2006-2008)

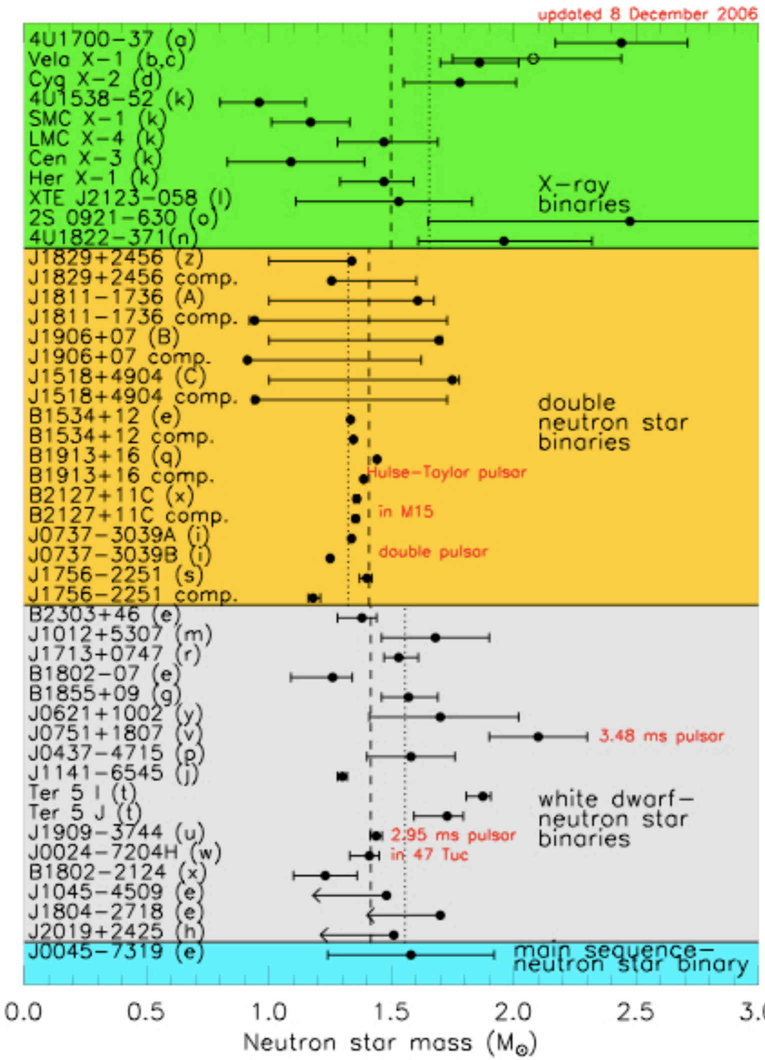

(Lattimer & Prakash 2007)

Phenomenological: M_{max} compatible with 1.4-1.5 $M_\odot$

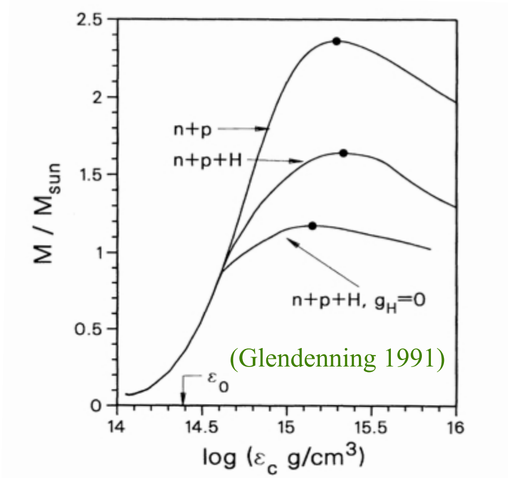

(Glendenning 1991)

Microscopic : M_{max} < 1.4-1.5 $M_\odot$

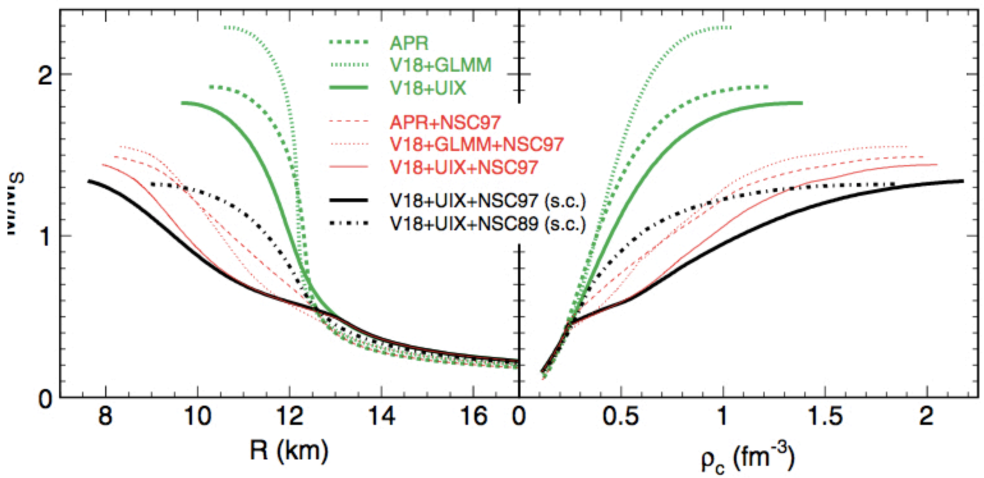

(Schulze, Polls, Ramos & IV 2006)

Recent measurements of high masses $\longrightarrow$ life of hyperons more difficult

Eccentric Binary Millisecond Pulsars

Paulo C. C. Freire

Arecibo Observatory, HC 3 Box 53995, Arecibo PR 00612, USA
West Virginia University, PO Box 6315, Morgantown WV 26505, USA

Abstract. In this paper we review recent discovery of millisecond pulsars (MSPs) in eccentric binary systems. Timing these MSPs we were able to estimate (and in one case precisely measure) their masses. These results suggest that, as a class, MSPs have a much wider range of masses (1.3 to $> 2M_{\odot}$) than the normal and mildly recycled pulsars found in double neutron star (DNS) systems ($1.25 < M_p < 1.44 M_{\odot}$). This is very likely to be due to the prolonged accretion episode that is thought to be required to form a MSP. The likely existence of massive MSPs makes them a powerful probe for understanding the behavior of matter at densities larger than that of the atomic nucleus; in particular, the precise measurement of the mass of PSR J1903+0327 ($1.67 \pm 0.01 M_{\odot}$) excludes several "soft" equations of state for dense matter.

Keywords: Neutron Stars, Pulsars, Binary Pulsars, General Relativity, Nuclear Equation of State
PACS: 97.60.Gb; 97.60.Jd; 97.80.Fk; 95.30.Sf; 26.60; 91.60.Fe

The precise measurement of the mass of PSR J1903+0328 (1.67 +/- 0.01 M_{sun}) excludes several "soft" EoS for dense matter

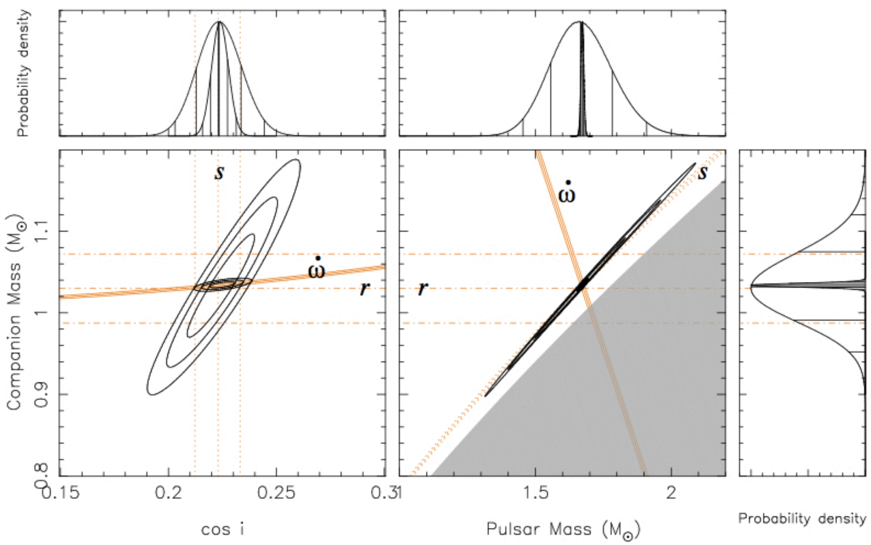

- ✓ binary sytem (P=95.17 d)
- ✓ high eccentricity (ε=0.437)
- ✓ companion mass: $\sim 1 M_{\odot}$
- ✓ pulsar mass: $M = 1.67 \pm 0.11 M_{\odot}$

Two-solar mass neutron star measured

Nature 464, 1081 (2010)

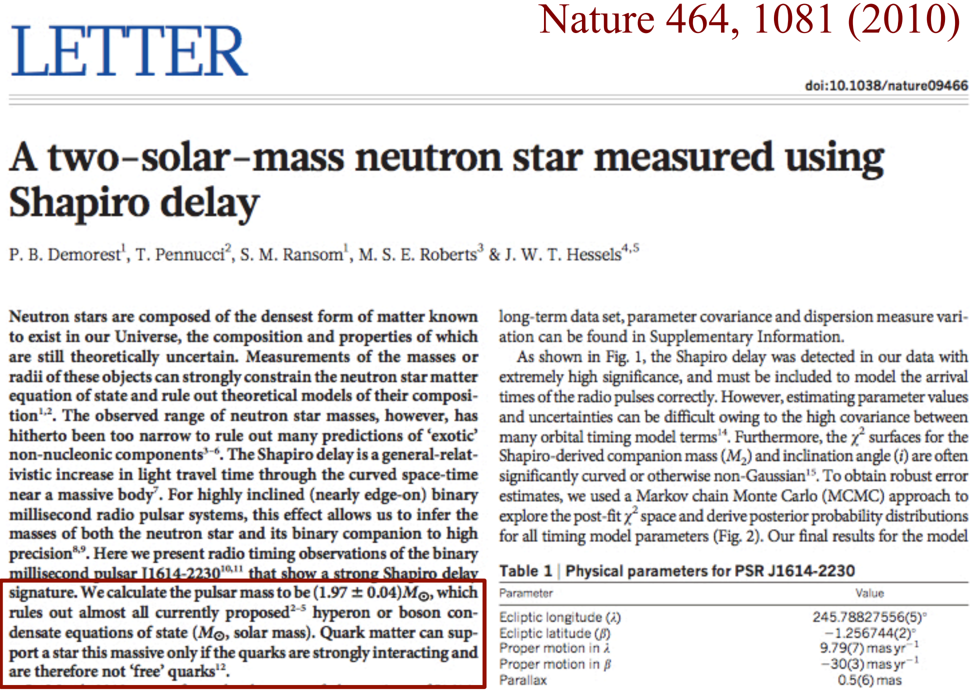

LETTER

doi:10.1038/nature09466

A two-solar-mass neutron star measured using Shapiro delay

P. B. Demorest[1], T. Pennucci[2], S. M. Ransom[1], M. S. E. Roberts[3] & J. W. T. Hessels[4,5]

Neutron stars are composed of the densest form of matter known to exist in our Universe, the composition and properties of which are still theoretically uncertain. Measurements of the masses or radii of these objects can strongly constrain the neutron star matter equation of state and rule out theoretical models of their composition[1,2]. The observed range of neutron star masses, however, has hitherto been too narrow to rule out many predictions of 'exotic' non-nucleonic components[3–6]. The Shapiro delay is a general-relativistic increase in light travel time through the curved space-time near a massive body[7]. For highly inclined (nearly edge-on) binary millisecond radio pulsar systems, this effect allows us to infer the masses of both the neutron star and its binary companion to high precision[8,9]. Here we present radio timing observations of the binary millisecond pulsar J1614-2230[10,11] that show a strong Shapiro delay signature. We calculate the pulsar mass to be $(1.97 \pm 0.04)M_\odot$, which rules out almost all currently proposed[2–5] hyperon or boson condensate equations of state ($M_\odot$, solar mass). Quark matter can support a star this massive only if the quarks are strongly interacting and are therefore not 'free' quarks[12].

long-term data set, parameter covariance and dispersion measure variation can be found in Supplementary Information.

As shown in Fig. 1, the Shapiro delay was detected in our data with extremely high significance, and must be included to model the arrival times of the radio pulses correctly. However, estimating parameter values and uncertainties can be difficult owing to the high covariance between many orbital timing model terms[14]. Furthermore, the χ^2 surfaces for the Shapiro-derived companion mass (M_2) and inclination angle (i) are often significantly curved or otherwise non-Gaussian[15]. To obtain robust error estimates, we used a Markov chain Monte Carlo (MCMC) approach to explore the post-fit χ^2 space and derive posterior probability distributions for all timing model parameters (Fig. 2). Our final results for the model

Table 1 | Physical parameters for PSR J1614-2230

Parameter	Value
Ecliptic longitude (λ)	245.78827556(5)°
Ecliptic latitude (β)	−1.256744(2)°
Proper motion in λ	9.79(7) mas yr^{-1}
Proper motion in β	−30(3) mas yr^{-1}
Parallax	0.5(6) mas

The mass 1.97 +/- 0.04 M_{sun} of the pulsar PSR J1614+2230 rules out almost all currently proposed hyperon or boson condensate EoS. Quark matter can support such a massive star only if quarks are strongly interacting (not "free quarks")

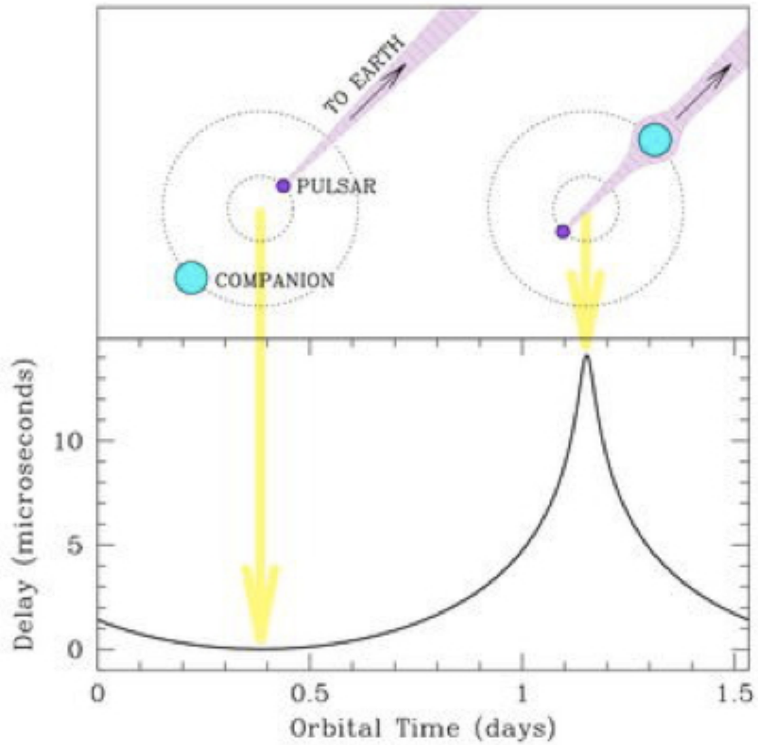

Binary millisecond pulsar PSR J1614+2230
Shapiro delay signature

$$\Delta t = -\frac{2GM}{c^3}\log\left(1-\vec{R}\cdot\vec{R}'\right)$$

On April 26th 2013 the discovery of the most massive (up to now) pulsar (PSR J0348+0432) was made public

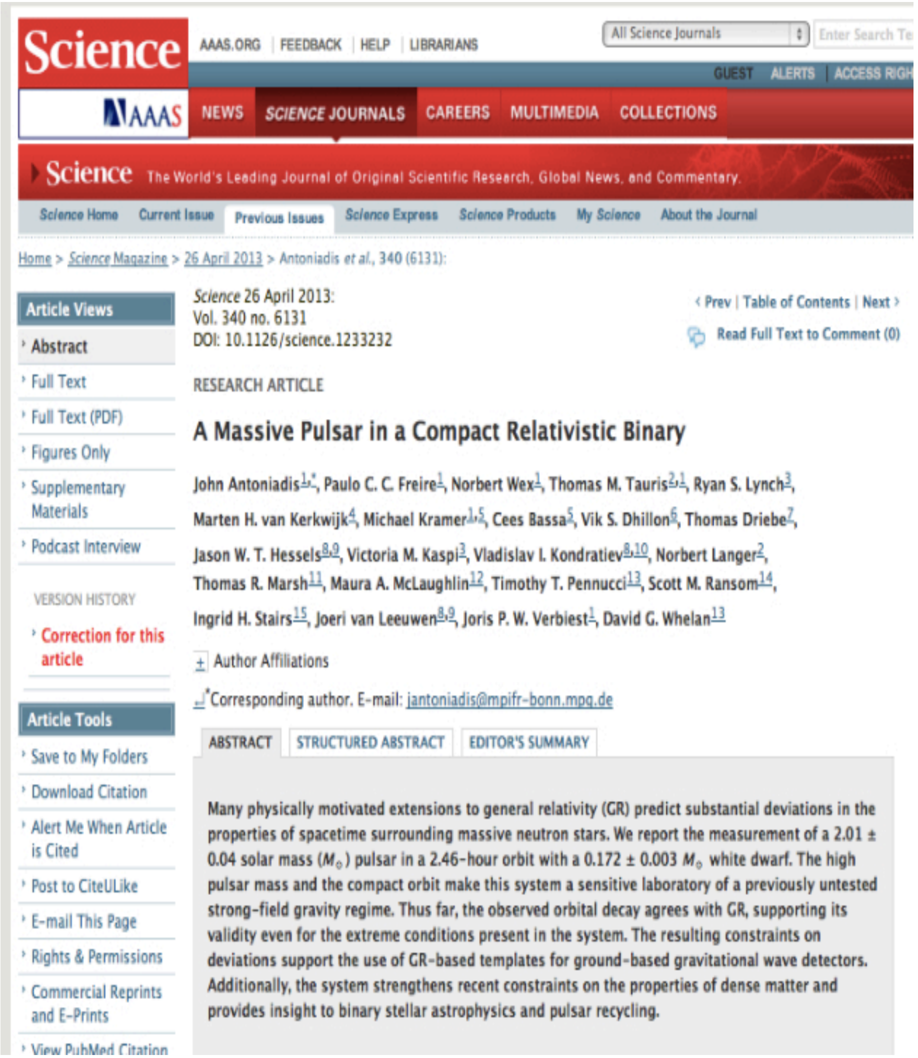

Science | AAAS.ORG | FEEDBACK | HELP | LIBRARIANS | All Science Journals | Enter Search Te

GUEST | ALERTS | ACCESS RIGH

AAAS | NEWS | SCIENCE JOURNALS | CAREERS | MULTIMEDIA | COLLECTIONS

Science The World's Leading Journal of Original Scientific Research, Global News, and Commentary.

Science Home | Current Issue | Previous Issues | Science Express | Science Products | My Science | About the Journal

Home > Science Magazine > 26 April 2013 > Antoniadis et al., 340 (6131):

Article Views
- Abstract
- Full Text
- Full Text (PDF)
- Figures Only
- Supplementary Materials
- Podcast Interview

VERSION HISTORY
- Correction for this article

Article Tools
- Save to My Folders
- Download Citation
- Alert Me When Article is Cited
- Post to CiteULike
- E-mail This Page
- Rights & Permissions
- Commercial Reprints and E-Prints
- View PubMed Citation

Science 26 April 2013:
Vol. 340 no. 6131
DOI: 10.1126/science.1233232

‹ Prev | Table of Contents | Next ›

Read Full Text to Comment (0)

RESEARCH ARTICLE

A Massive Pulsar in a Compact Relativistic Binary

John Antoniadis[1,*], Paulo C. C. Freire[1], Norbert Wex[1], Thomas M. Tauris[2,1], Ryan S. Lynch[3], Marten H. van Kerkwijk[4], Michael Kramer[1,5], Cees Bassa[5], Vik S. Dhillon[6], Thomas Driebe[7], Jason W. T. Hessels[8,9], Victoria M. Kaspi[3], Vladislav I. Kondratiev[8,10], Norbert Langer[2], Thomas R. Marsh[11], Maura A. McLaughlin[12], Timothy T. Pennucci[13], Scott M. Ransom[14], Ingrid H. Stairs[15], Joeri van Leeuwen[8,9], Joris P. W. Verbiest[1], David G. Whelan[13]

+ Author Affiliations

*Corresponding author. E-mail: jantoniadis@mpifr-bonn.mpg.de

ABSTRACT | STRUCTURED ABSTRACT | EDITOR'S SUMMARY

Many physically motivated extensions to general relativity (GR) predict substantial deviations in the properties of spacetime surrounding massive neutron stars. We report the measurement of a 2.01 ± 0.04 solar mass ($M_\odot$) pulsar in a 2.46-hour orbit with a 0.172 ± 0.003 $M_\odot$ white dwarf. The high pulsar mass and the compact orbit make this system a sensitive laboratory of a previously untested strong-field gravity regime. Thus far, the observed orbital decay agrees with GR, supporting its validity even for the extreme conditions present in the system. The resulting constraints on deviations support the use of GR-based templates for ground-based gravitational wave detectors. Additionally, the system strengthens recent constraints on the properties of dense matter and provides insight to binary stellar astrophysics and pulsar recycling.

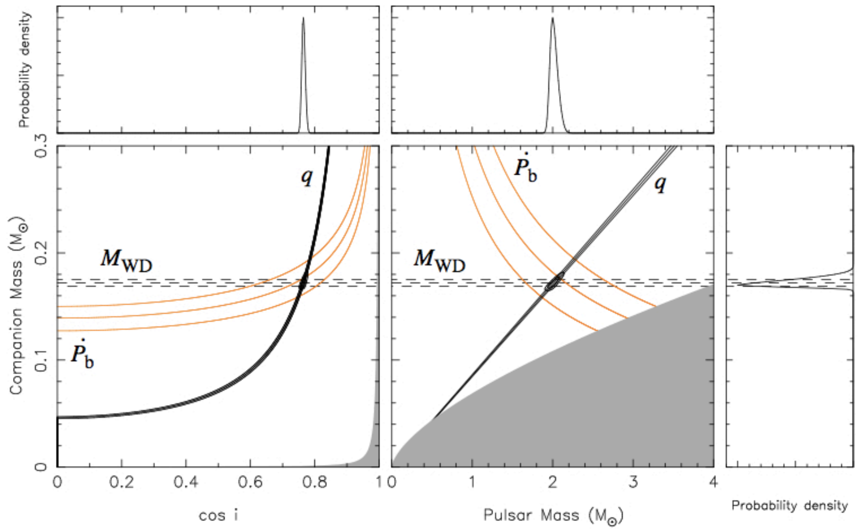

- ✓ binary system (P=2.46 h)
- ✓ very low eccentricity
- ✓ companion mass: $0.172 \pm 0.003 M_\odot$
- ✓ pulsar mass: $M = 2.01 \pm 0.04 M_\odot$

Measured Neutron Star Masses (2014)

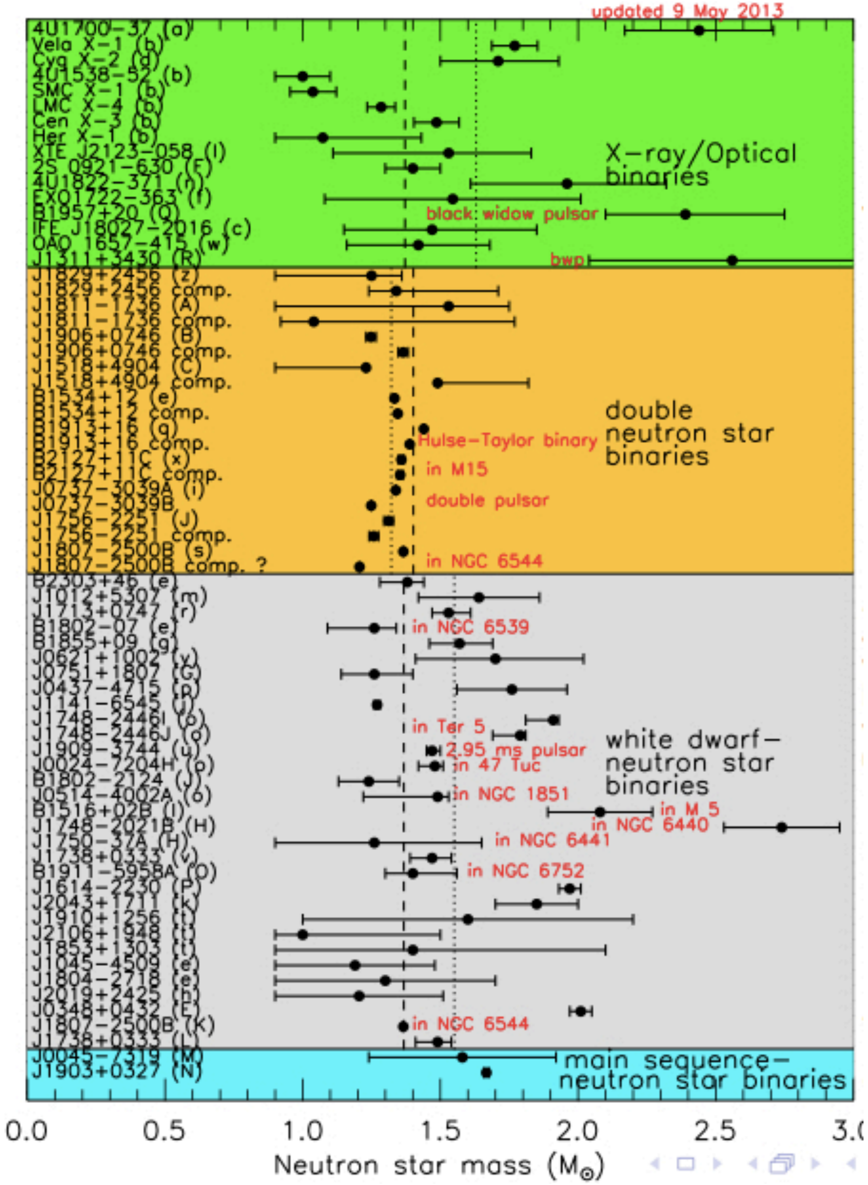

updated from Lattimer 2013

Observation of ~ 2 M_{sun} neutron stars

↓

Dense matter EoS stiff enough is required such that

$$M_{\max}\left[EoS\right] > 2M_{\odot}$$

Can strangeness (hyperons, kaons, quarks) still be present in the interior of neutron stars in view of this constraint ?

The Hyperon Puzzle

"Hyperons → "soft (or too soft) EoS" not compatible (mainly in microscopic approaches) with measured (high) masses. However, the presence of hyperons in the NS interior seems to be unavoidable."

- ✓ can YN & YY interactions still solve it ?
- ✓ or perhaps hyperonic three-body forces ?
- ✓ what about quark matter ?

Solution I: Hyperonic Three Body Forces

Natural solution based on: Importance of NNN force in Nuclear Physics
(Considered by several authors: Chalk, Gal, Usmani, Bodmer, Takatsuka, Loiseau, Nogami, Bahaduri, IV)

NNN Force

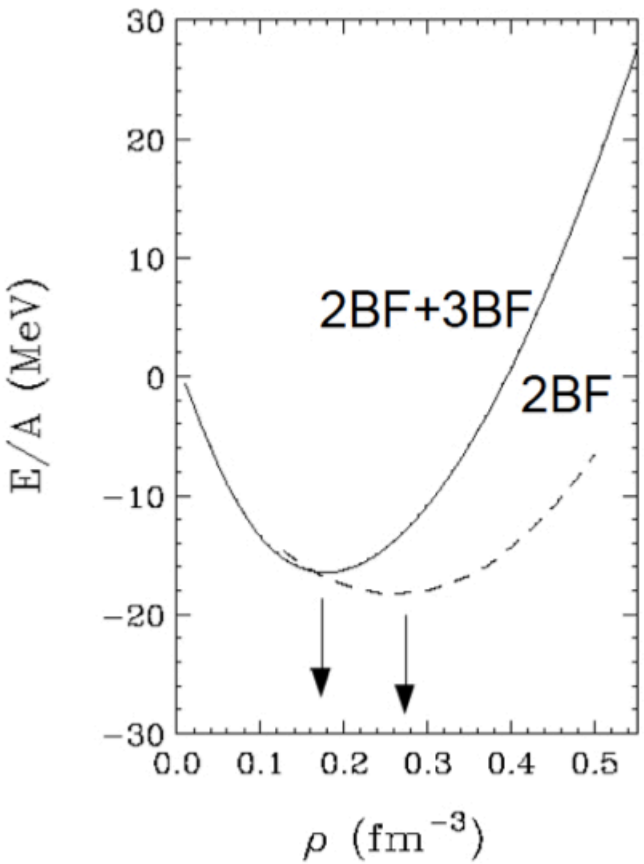

NNY, NYY & YYY Forces

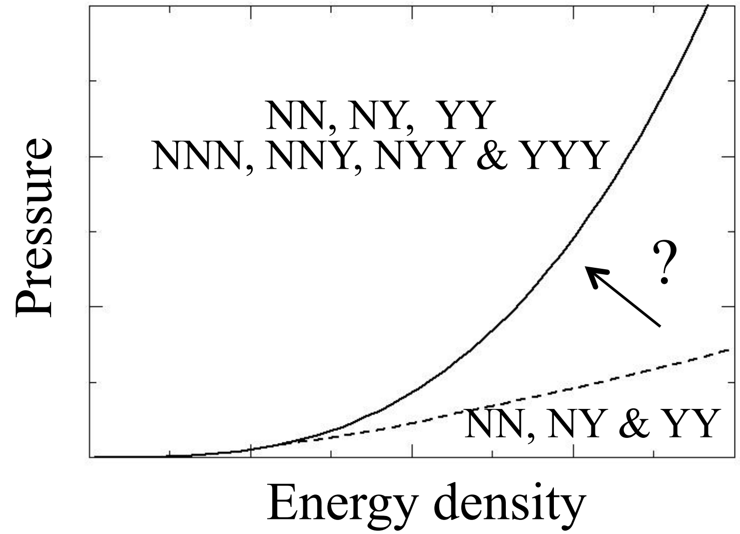

Can hyperonic TBF provide enough repulsion at high densities to reach $2M_\odot$?

Two-meson exchange Hyperonic TBF

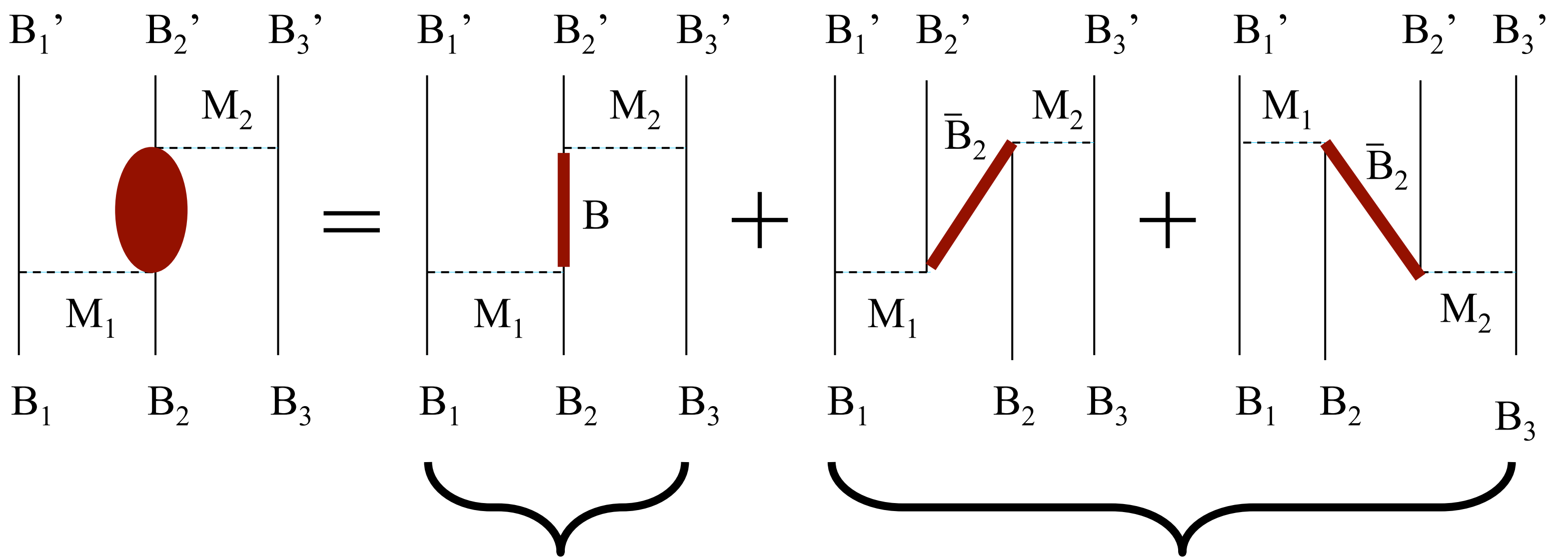

B - excitation

Z – diagram

B_i B_i': N, Λ, Σ

M_i: π, K, ρ, K^*, σ, ω

B: N, Λ, Σ, Δ, N*, Σ*

$\bar{B}_2$: $\bar{N}$, $\bar{\Lambda}$, $\bar{\Sigma}$

Vertices: consistent with YN and YY

Repulsion at high densities due to Z-diagram as in NNN

D. Logoteta, Ph.D. Thesis (2013)

Example: the NNΛ force

- ππ contribution

$$V_{NN\Lambda}^{\Sigma,\Sigma^*}(\vec{r}_{N_1\Lambda},\vec{r}_{N_2\Lambda}) = -C_{NN\Lambda}^{\Sigma,\Sigma^*}\left\{X_{N_1\Lambda}(\vec{r}_{N_1\Lambda}), X_{N_2\Lambda}(\vec{r}_{N_2\Lambda})\right\}\vec{\tau}_{N_1}\cdot\vec{\tau}_{N_2}$$

with

$$X_{ij}(\vec{x}) = \vec{\sigma}_i\cdot\vec{\sigma}_j Y(x) + S_{ij}(\hat{x})T(x)$$

$$Y(x) = \frac{\partial^2 Z}{\partial x^2} + \frac{2}{x}\frac{\partial Z}{\partial x}$$

$$T(x) = \frac{\partial^2 Z}{\partial x^2} - \frac{1}{x}\frac{\partial Z}{\partial x}$$

$$Z(x) = \frac{4}{m_\pi}\int\frac{d\vec{k}}{(2\pi)^3}\frac{e^{-i\vec{k}\cdot\vec{x}}}{k^2+m_\pi^2}F_{NN\pi}(k^2)F_{\Lambda(\Sigma,\Sigma^*)\pi}(k^2)$$

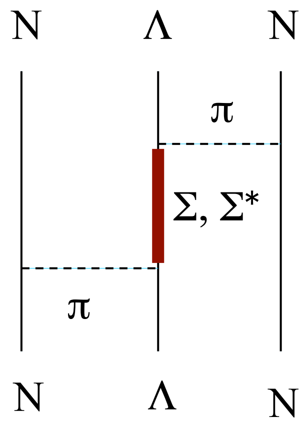

$$C_{NN\Lambda}^{\Sigma} = -\frac{1}{9}\frac{g_{NN\pi}^2 g_{\Lambda\Sigma\pi}^2}{16\pi^2}\frac{m_\pi^2}{m_\Sigma - m_\Lambda}$$

$$C_{NN\Lambda}^{\Sigma^*} = \frac{2}{27}\frac{g_{NN\pi}^2 f_{\Lambda\Sigma^*\pi}^2}{16\pi^2}\frac{m_\pi^2}{m_{\Sigma^*} - m_\Lambda}$$

$$\left(C_{NNN}^{\Delta} = \frac{2}{81}\frac{g_{NN\pi}^2 f_{N\Delta\pi}^2}{16\pi^2}\frac{m_\pi^2}{m_\Delta - m_\Lambda}, \frac{C_{NN\Lambda}^{\Sigma^*}}{C_{NNN}^{\Delta}} \sim 0.185\right)$$

D. Logoteta, Ph.D. Thesis (2013)

- <u>KK contribution</u>

$$V^{\Lambda}_{NN\Lambda}(\vec{r}_{N_1\Lambda},\vec{r}_{N_2\Lambda}) = -C^{\Lambda}_{NN\Lambda}\left\{X_{N_1\Lambda}(\vec{r}_{N_1\Lambda}),X_{N_2\Lambda}(\vec{r}_{N_2\Lambda})\right\}$$

$$V^{\Sigma}_{NN\Lambda}(\vec{r}_{N_1\Lambda},\vec{r}_{N_2\Lambda}) = -C^{\Sigma}_{NN\Lambda}\Big(\left\{\vec{\rho}_{\Lambda_1}\cdot\vec{\tau}_{N_2},\vec{\tau}_{N_2}\cdot\vec{\rho}_{\Lambda_2}\right\}$$

$$+\quad\left[\vec{\rho}_{\Lambda_1}\cdot\vec{\tau}_{N_2},\vec{\tau}_{N_2}\cdot\vec{\rho}_{\Lambda_2}\right]\Big)\ \left\{X_{N_1\Lambda}(\vec{r}_{N_1\Lambda}),X_{N_2\Lambda}(\vec{r}_{N_2\Lambda})\right\}$$

$$V^{\Sigma^*}_{NN\Lambda}(\vec{r}_{N_1\Lambda},\vec{r}_{N_2\Lambda}) = -C^{\Sigma^*}_{NN\Lambda}\Big(\left\{\vec{\rho}_{\Lambda_1}\cdot\vec{\tau}_{N_2},\vec{\tau}_{N_2}\cdot\vec{\rho}_{\Lambda_2}\right\}$$

$$+\quad\frac{1}{2}\left[\vec{\rho}_{\Lambda_1}\cdot\vec{\tau}_{N_2},\vec{\tau}_{N_2}\cdot\vec{\rho}_{\Lambda_2}\right]\Big)\ \left\{X_{N_1\Lambda}(\vec{r}_{N_1\Lambda}),X_{N_2\Lambda}(\vec{r}_{N_2\Lambda})\right\}$$

with

$$Z(x) = \frac{4}{m_K}\int\frac{d\vec{k}}{(2\pi)^3}\frac{e^{-i\vec{k}\cdot\vec{x}}}{k^2+m_K^2}F_{N\Lambda K}(k^2)F_{N(\Sigma,\Sigma^*)K}(k^2)$$

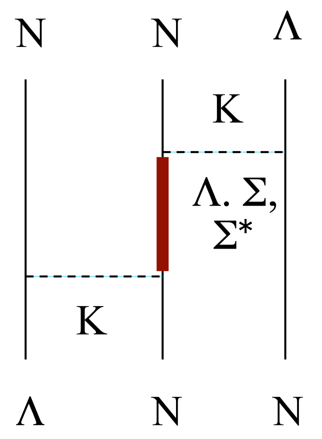

$$C^{\Lambda}_{NN\Lambda} = -\frac{1}{9}\frac{g^4_{N\Lambda K}}{16\pi^2}\frac{m_\pi^2}{m_\Lambda - m_N}\left(\frac{m_K}{m_\pi}\right)^4$$

$$C^{\Sigma}_{NN\Lambda} = -\frac{1}{18}\frac{g^2_{N\Lambda K}g^2_{N\Sigma K}}{16\pi^2}\frac{m_\pi^2}{m_\Sigma - m_N}\left(\frac{m_K}{m_\pi}\right)^4$$

$$C^{\Sigma^*}_{NN\Lambda} = \frac{1}{27}\frac{g^2_{N\Lambda K}f^2_{N\Sigma^* K}}{16\pi^2}\frac{m_\pi^2}{m_{\Sigma^*} - m_N}\left(\frac{m_K}{m_\pi}\right)^4$$

D. Logoteta, Ph.D. Thesis (2013)

$\sigma\sigma$, $\omega\omega$ and $\sigma\omega$ contributions

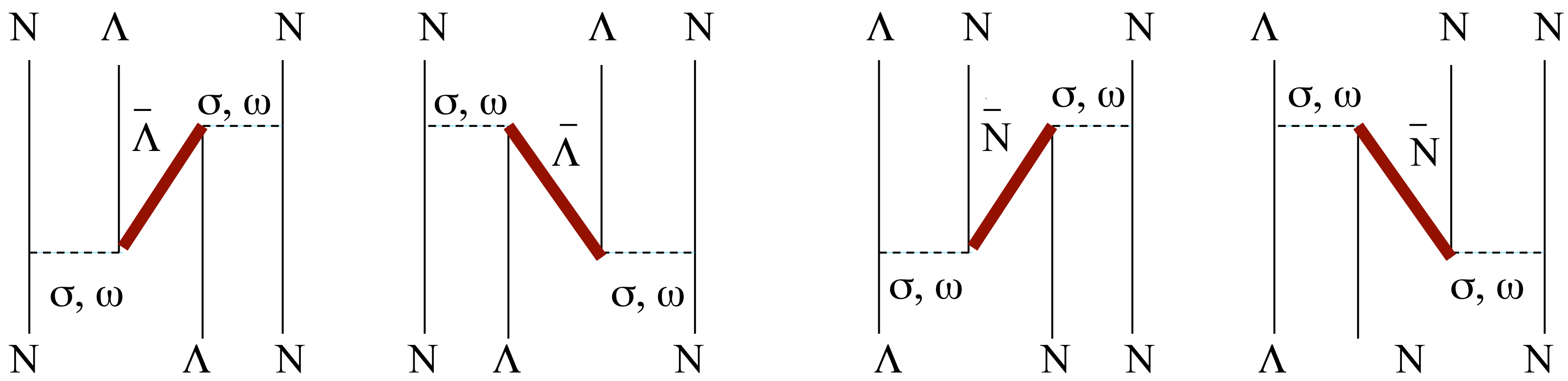

For instance $\sigma\sigma$ looks like:

$$
\begin{aligned}
V^{\bar{\Lambda}}_{N\Lambda N} = C^{\bar{\Lambda}}_{N\Lambda N}\ & \delta(\boldsymbol{r}'_1-\boldsymbol{r}_1)\,\delta(\boldsymbol{r}'_2-\boldsymbol{r}_2) \\
& \{-4Z(r_{13})Z(r_{32})\ \nabla^2_{\boldsymbol{r}'_3} - 4Z'(r_{13})Z(r_{32})\ \hat{\boldsymbol{r}}_{13}\cdot\nabla_{\boldsymbol{r}'_3} - 4Z(r_{13})Z'(r_{32})\ \hat{\boldsymbol{r}}_{32}\cdot\nabla_{\boldsymbol{r}'_3} \\
& -[Y(r_{13})Z(r_{32})+Z(r_{13})Y(r_{32})] - \hat{\boldsymbol{r}}_{13}\cdot\hat{\boldsymbol{r}}_{32}\ Z'(r_{13})Z'(r_{32}) \\
& -2i[Z'(r_{13})Z(r_{32})\ \boldsymbol{\sigma}_3\cdot\hat{\boldsymbol{r}}_{13}\wedge\nabla_{\boldsymbol{r}'_3} + Z'(r_{32})Z(r_{13})\ \boldsymbol{\sigma}_3\cdot\hat{\boldsymbol{r}}_{32}\wedge\nabla_{\boldsymbol{r}'_3}]\}\ \delta(\boldsymbol{r}'_3-\boldsymbol{r}_3)
\end{aligned}
$$

$$
\begin{aligned}
V^{\bar{N}}_{\Lambda NN} = C^{\bar{N}}_{\Lambda NN}\ & \delta(\boldsymbol{r}'_1-\boldsymbol{r}_1)\,\delta(\boldsymbol{r}'_2-\boldsymbol{r}_2) \\
& \{-4Z_1(r_{13})Z_2(r_{32})\ \nabla^2_{\boldsymbol{r}'_3} - 4Z'_1(r_{13})Z_2(r_{32})\ \hat{\boldsymbol{r}}_{13}\cdot\nabla_{\boldsymbol{r}'_3} - 4Z_1(r_{13})Z'_2(r_{32})\ \hat{\boldsymbol{r}}_{32}\cdot\nabla_{\boldsymbol{r}'_3} \\
& -[Y_1(r_{13})Z_2(r_{32})+Z_1(r_{13})Y_2(r_{32})] - \hat{\boldsymbol{r}}_{13}\cdot\hat{\boldsymbol{r}}_{32}\ Z'_1(r_{13})Z'_2(r_{32}) \\
& -2i[Z'_1(r_{13})Z_2(r_{32})\ \boldsymbol{\sigma}_3\cdot\hat{\boldsymbol{r}}_{13}\wedge\nabla_{\boldsymbol{r}'_3} + Z'_2(r_{32})Z_1(r_{13})\ \boldsymbol{\sigma}_3\cdot\hat{\boldsymbol{r}}_{32}\wedge\nabla_{\boldsymbol{r}'_3}]\}\ \delta(\boldsymbol{r}'_3-\boldsymbol{r}_3)\ ,
\end{aligned}
$$

D. Logoteta, Ph.D. Thesis (2013)

But that's only the beginning of the story

there are

MANY MANY MANY more forces & contributions

....

Three-Body Forces within the BHF approach

TBF can be introduced in our BHF approach by adding effective density-dependent two body forces to the baryon-baryon interactions V when solving the Bethe-Goldstone equation

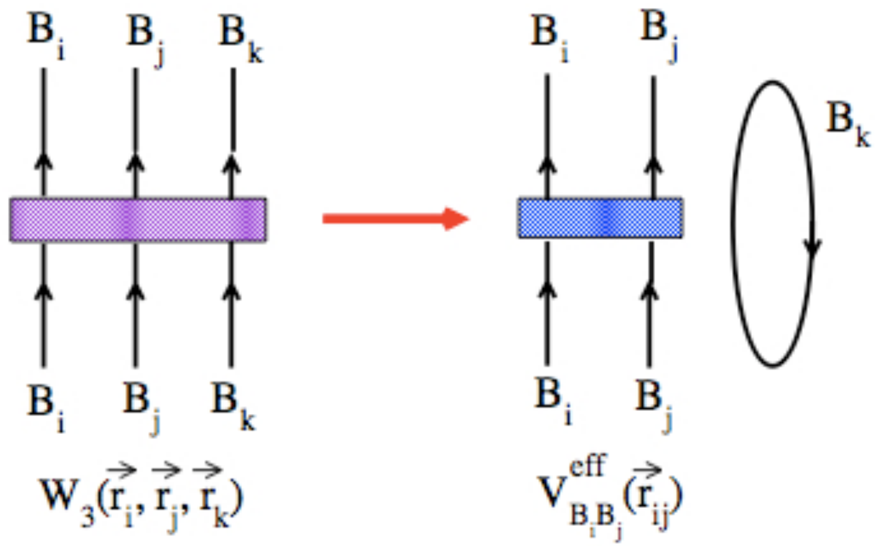

$$W_{B_iB_j}\left(\vec{r}_{ij}\right) = \int W_3\left(\vec{r}_i,\vec{r}_j,\vec{r}_k\right) n\left(\vec{r}_i,\vec{r}_j,\vec{r}_k\right) d^3\vec{r}_k$$

$W_3\left(\vec{r}_i,\vec{r}_j,\vec{r}_k\right)$: genuine TBF

$n\left(\vec{r}_i,\vec{r}_j,\vec{r}_k\right)$: three-body correlation function

From the genuine NNN,NNY, NYY and YYY TBF …

NNN ➔ NN

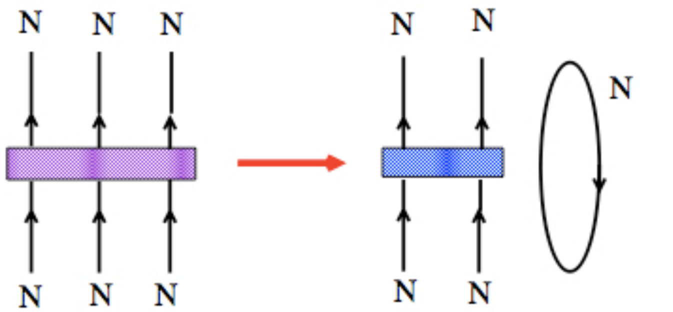

NNY ➔ NN, NY

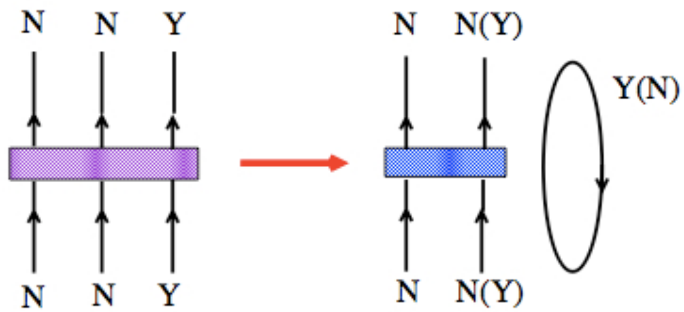

NYY ➔ NY, YY

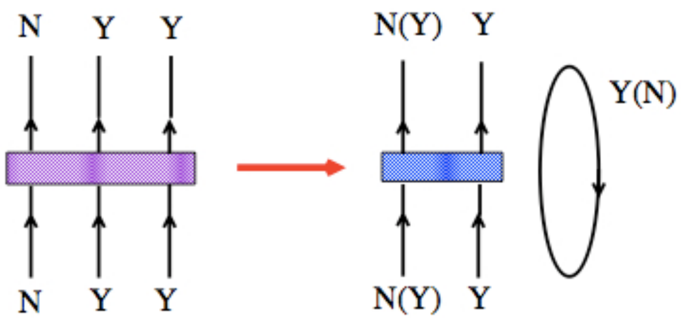

YYY ➔ YY

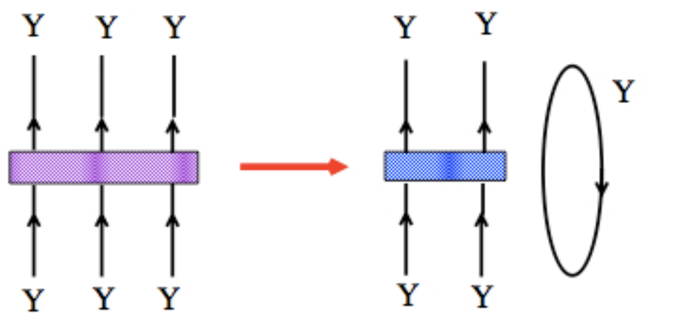

Effective density-dependent 2BF from NNY

- ππ contribution

$$W_{NN}^{B}\left(\vec{r}\right) = -C_{NNY}^{B}\rho_{Y}\left[V_{\sigma}^{\pi\pi}\left(\vec{r}\right)\vec{\sigma}_{1}\cdot\vec{\sigma}_{2} + V_{T}^{\pi\pi}\left(\vec{r}\right)S_{12}\left(\hat{r}\right)\right]\vec{\tau}_{1}\cdot\vec{\tau}_{2}$$

(B=Λ, Σ, Σ* Y=Λ,Σ)

$$W_{N\Sigma}^{\Delta}\left(\vec{r}\right) = -C_{NN\Sigma}^{\Delta}\rho_{N}\left[V_{\sigma}^{\pi\pi}\left(\vec{r}\right)\vec{\sigma}_{1}\cdot\vec{\sigma}_{2} + V_{T}^{\pi\pi}\left(\vec{r}\right)S_{12}\left(\hat{r}\right)\right]\vec{\tau}_{1}\cdot\vec{I}_{2}$$

$$W_{N\Sigma\to N\Lambda}^{\Delta}\left(\vec{r}\right) = -C_{NN\Sigma\to NN\Lambda}^{\Delta}\rho_{N}\left[V_{\sigma}^{\pi\pi}\left(\vec{r}\right)\vec{\sigma}_{1}\cdot\vec{\sigma}_{2} + V_{T}^{\pi\pi}\left(\vec{r}\right)S_{12}\left(\hat{r}\right)\right]\vec{\tau}_{1}\cdot\vec{\rho}_{2}$$

D. Logoteta, Ph.D. Thesis (2013)

- KK contribution

$$W_{N\Lambda}^{\Lambda}(\vec{r}) = -C_{NN\Lambda}^{\Lambda}\rho_N\left[V_\sigma^{KK}(\vec{r})\vec{\sigma}_1\cdot\vec{\sigma}_2 + V_T^{KK}(\vec{r})S_{12}(\hat{r})\right]$$

$$W_{N\Lambda}^{\Sigma,\Sigma^*}(\vec{r}) = -C_{NN\Lambda}^{\Sigma,\Sigma^*}\rho_N\left[V_\sigma^{KK}(\vec{r})\vec{\sigma}_1\cdot\vec{\sigma}_2 + V_T^{KK}(\vec{r})S_{12}(\hat{r})\right]\vec{\tau}_1\cdot\vec{\rho}_2$$

$$W_{N\Sigma}^{\Lambda,\Sigma}(\vec{r}) = -C_{NN\Sigma}^{\Lambda,\Sigma}\rho_N\left[V_\sigma^{KK}(\vec{r})\vec{\sigma}_1\cdot\vec{\sigma}_2 + V_T^{KK}(\vec{r})S_{12}(\hat{r})\right]\vec{\tau}_1\cdot\vec{\tau}_2$$

$$W_{N\Sigma}^{\Sigma^*}(\vec{r}) = -C_{NN\Sigma}^{\Sigma^*}\rho_N\left[V_\sigma^{KK}(\vec{r})\vec{\sigma}_1\cdot\vec{\sigma}_2 + V_T^{KK}(\vec{r})S_{12}(\hat{r})\right]\vec{\tau}_1\cdot\vec{\rho}_2$$

$$W_{N\Sigma\to N\Lambda}^{\Lambda,\Sigma,\Sigma^*}(\vec{r}) = -C_{NN\Sigma\to NN\Lambda}^{\Lambda,\Sigma,\Sigma^*}\rho_N\left[V_\sigma^{KK}(\vec{r})\vec{\sigma}_1\cdot\vec{\sigma}_2 + V_T^{KK}(\vec{r})S_{12}(\hat{r})\right]\vec{\tau}_1\cdot\vec{\rho}_2$$

D. Logoteta, Ph.D. Thesis (2013)

- σσ contribution

$$W_{NN}^{\bar{\Lambda}}(\vec{r}) = C_{NN\Lambda}^{\bar{\Lambda}}\left[\rho_N V_{c_1}^{\sigma\sigma}(\vec{r}) + \rho_N^{5/3} V_{c_2}^{\sigma\sigma}(\vec{r})\right]$$

$$W_{N\Lambda}^{\bar{N}}(\vec{r}) = C_{NN\Lambda}^{\bar{N}}\left[\rho_\Lambda V_{c_1}^{\sigma\sigma}(\vec{r}) + \rho_\Lambda^{5/3} V_{c_2}^{\sigma\sigma}(\vec{r})\right]$$

$$W_{N\Sigma}^{\bar{N}}(\vec{r}) = C_{NN\Sigma}^{\bar{N}}\left[\rho_\Sigma V_{c_1}^{\sigma\sigma}(\vec{r}) + \rho_\Sigma^{5/3} V_{c_2}^{\sigma\sigma}(\vec{r})\right]$$

- ωω contribution

$$W_{NN}^{\bar{\Lambda}}(\vec{r}) = C_{NN\Lambda}^{\bar{\Lambda}}\rho_\Lambda\left[V_c^{\omega\omega}(\vec{r}) + V_\sigma^{\omega\omega}(\vec{r})\vec{\sigma}_1\cdot\vec{\sigma}_2 + V_T^{\omega\omega}(\vec{r})S_{12}(\hat{r})\right]$$

$$W_{N\Lambda}^{\bar{N}}(\vec{r}) = C_{NN\Lambda}^{\bar{N}}\rho_N\left[V_c^{\omega\omega}(\vec{r}) + V_\sigma^{\omega\omega}(\vec{r})\vec{\sigma}_1\cdot\vec{\sigma}_2 + V_T^{\omega\omega}(\vec{r})S_{12}(\hat{r})\right]$$

$$W_{N\Lambda}^{\bar{N}}(\vec{r}) = C_{NN\Lambda}^{\bar{N}}\rho_N\left[V_c^{\omega\omega}(\vec{r}) + V_\sigma^{\omega\omega}(\vec{r})\vec{\sigma}_1\cdot\vec{\sigma}_2 + V_T^{\omega\omega}(\vec{r})S_{12}(\hat{r})\right]$$

D. Logoteta, Ph.D. Thesis (2013)

- σω contribution

$$W_{NN}^{\bar{\Lambda}}\left(\vec{r}\right) = C_{NN\Lambda}^{\bar{\Lambda}}\rho_N V_c^{\sigma\omega}\left(\vec{r}\right)$$

$$W_{N\Lambda}^{\bar{N}}\left(\vec{r}\right) = C_{NN\Lambda}^{\bar{N}}\rho_\Lambda V_c^{\sigma\omega}\left(\vec{r}\right)$$

$$W_{N\Sigma}^{\bar{N}}\left(\vec{r}\right) = C_{NN\Sigma}^{\bar{N}}\rho_\Sigma V_c^{\sigma\sigma}\left(\vec{r}\right)$$

and so on and so forth ….

D. Logoteta, Ph.D. Thesis (2013)

- $W_{NN}^{\Lambda}(r)$

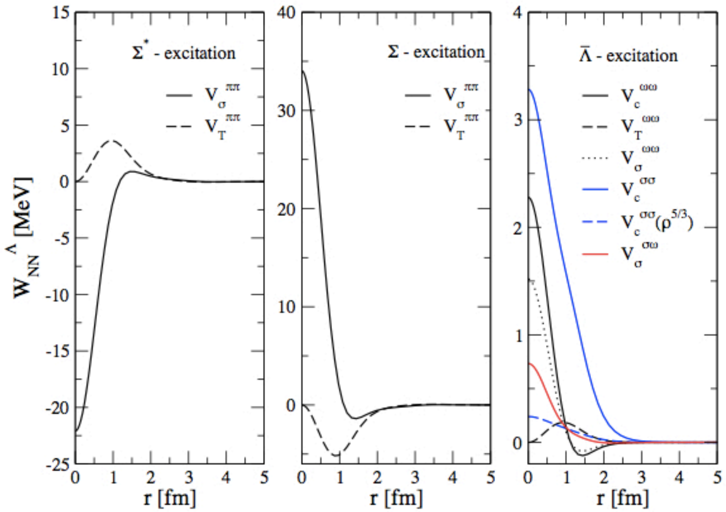

- $W_{\Lambda N}^{N}(r)$

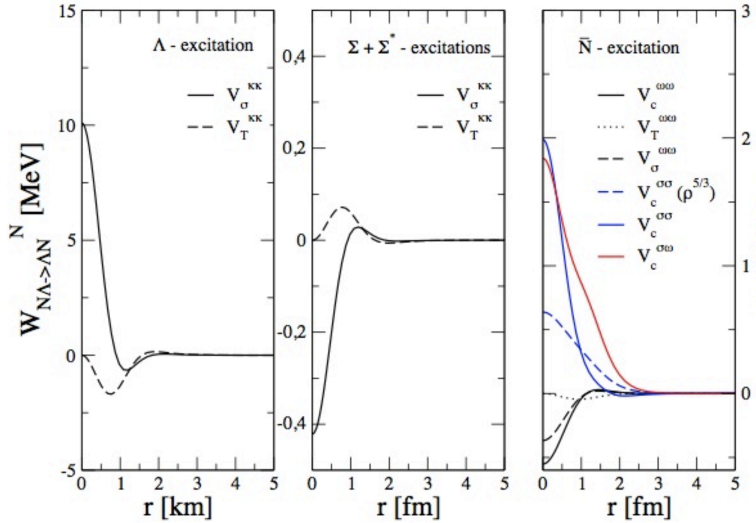

- $W_{NN}^{\Sigma}(r)$

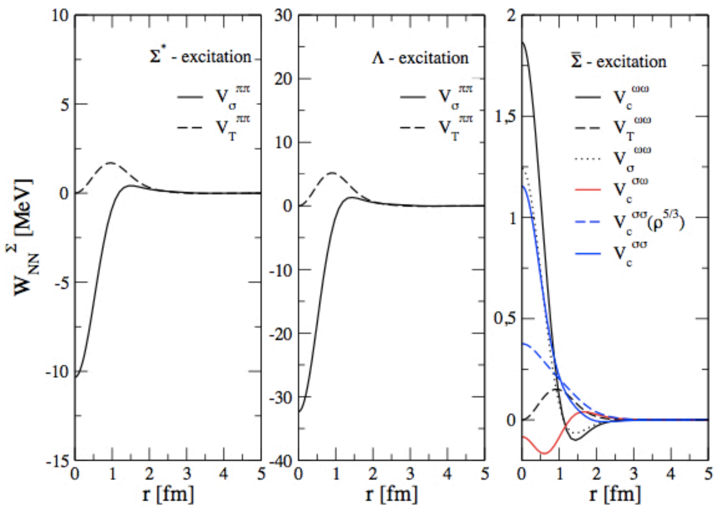

- $W_{\Sigma N}^{N}(r)$

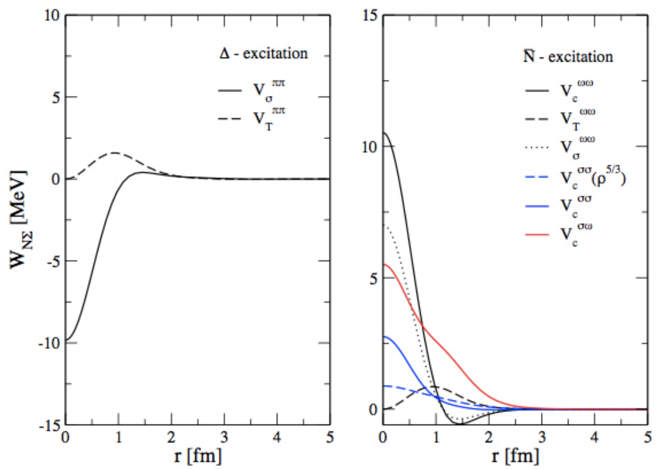

D. Logoteta, Ph.D. Thesis (2013)

Effect of TBF on Mean Field & E/A

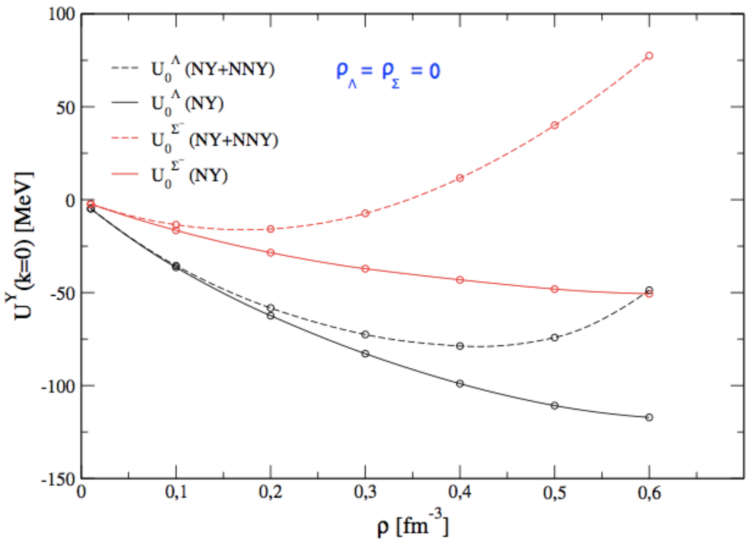

- ✓ Only NNY considered (preliminar)
- ✓ Repulsion at high densities due to Z-diagram contribution as in NNN

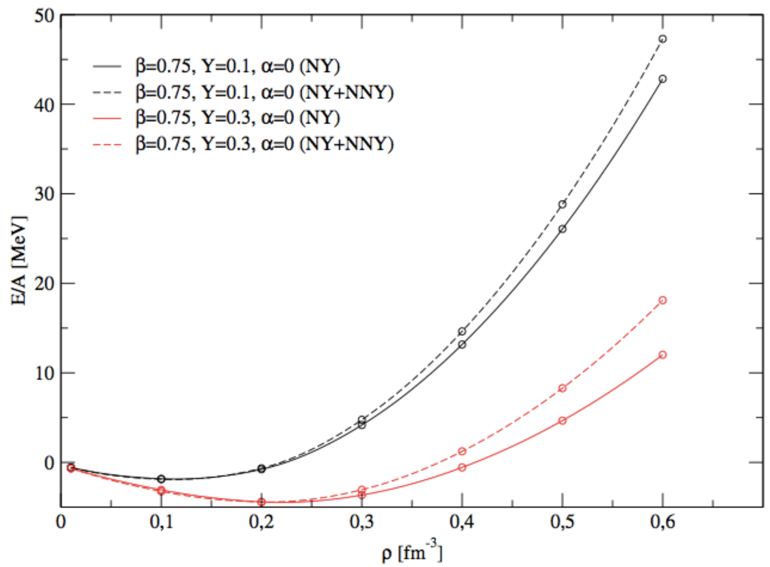

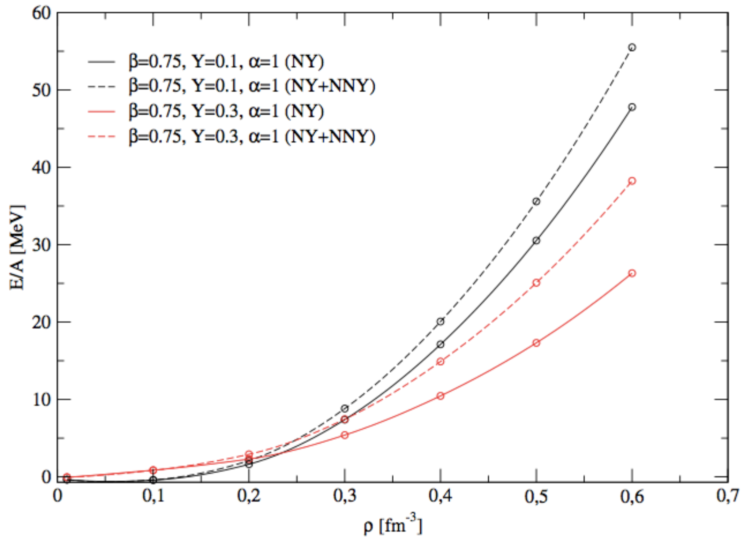

D. Logoteta, Ph.D. Thesis (2013)

Work is in progress, but we can still estimate the effect of hyperonicTBF in NS

1-. Construct the hyperonic matter EoS within the BHF at 2 body level (Av18 NN + NSC89 YN)

2-. Add simple phenomenological density-dependent contact terms that mimic the effect of TBF.

Density-dependent contact terms: (Balberg & Gal 1997)

Potential of a baryon B_y in a sea of baryons B_x of density ρ_x

$$V_y(\rho_x) = a_{xy}\rho_x + b_{xy}\rho_x^{\gamma_{xy}}$$

attraction repulsion larger than 1

Folding $V_y(\rho_x)$ with ρ_x, $V_x(\rho_y)$ with ρ_y and combining with weight factors ρ_x/ρ and ρ_y/ρ

$$\varepsilon_{xy}(\rho_x,\rho_y) = a_{xy}\rho_x\rho_y + b_{xy}\rho_x\rho_y\left(\frac{\rho_x^{\gamma_{xy}} + \rho_y^{\gamma_{xy}}}{\rho_x + \rho_y}\right)$$

Then, we have …

$$\varepsilon_{CT} = a_{NN}\rho_N^2 + b_{NN}\rho_N^{\gamma_{NN}}$$

$$+a_{\Lambda N}\rho_\Lambda\rho_N + b_{\Lambda N}\rho_\Lambda\rho_N\left(\frac{\rho_\Lambda^{\gamma_{\Lambda N}} + \rho_N^{\gamma_{\Lambda N}}}{\rho_\Lambda + \rho_N}\right)$$

$$+a_{\Sigma N}\rho_\Sigma\rho_N + b_{\Sigma N}\rho_\Sigma\rho_N\left(\frac{\rho_\Sigma^{\gamma_{\Sigma N}} + \rho_N^{\gamma_{\Sigma N}}}{\rho_\Sigma + \rho_N}\right)$$

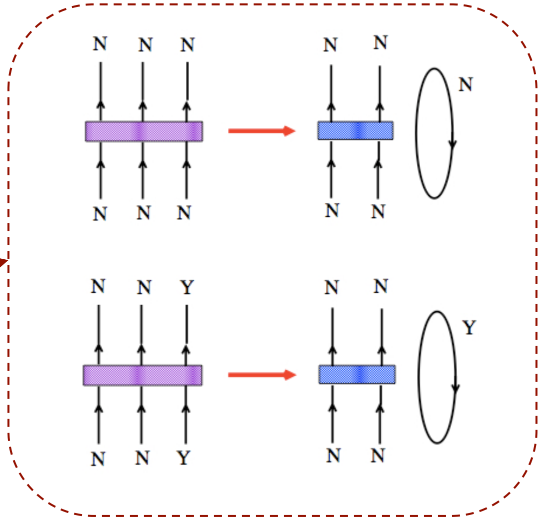

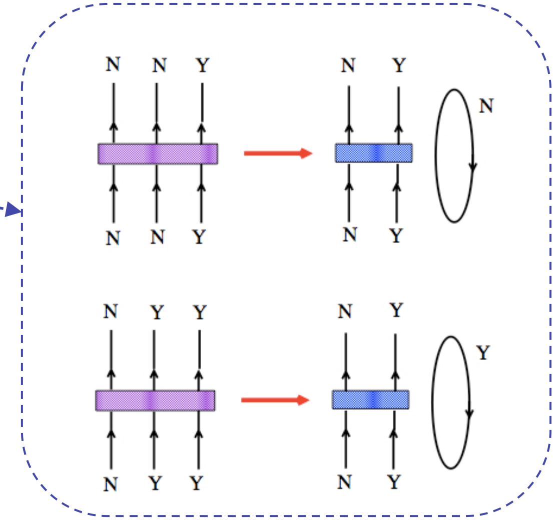

$$\rho_N = \rho_n + \rho_p\,, \quad \rho_\Sigma = \rho_{\Sigma^-} + \rho_{\Sigma^0} + \rho_{\Sigma^+}$$

NYY ➔ YY and YYY ➔ YY
not included for consistency

The parameters a_{NN}, b_{NN} and γ_{NN} fitted to reproduce ρ_0=0.16 fm^{-3}, E/A=-16 MeV and K =211-285 MeV

γ_{NN}	a_{NN} [MeV fm^3]	b_{NN} [MeV fm$^{3\gamma_{NN}}$]	K_∞ [MeV]
2	−33.44	213.02	211
2.5	−22.08	355.03	236
3	−16.40	665.68	260
3.5	−12.99	1331.36	285

For simplicity, we take $a_{\Lambda N}=a_{\Sigma N}$, $b_{\Lambda N}=b_{\Sigma N}$ and $\gamma_{\Lambda N}=\gamma_{\Sigma N}$ with

$$a_{\Lambda N} = x a_{NN}\,, \quad b_{\Lambda N} = x b_{NN}\,, \quad x = 0, \frac{1}{3}, \frac{2}{3}, 1$$

to explore different strength of the hyperonic TBF

$\gamma_{\Lambda N}$ is obtained using the value of -28 MeV for the binding energy of a Λ in nuclear matter

$$\left(\frac{B}{A}\right)_\Lambda = 28 MeV = -U_\Lambda(k=0) - a_{YN}\rho_0 - b_{YN}\rho_0^{\gamma_{YN}}$$

$$U_\Lambda(k=0) = -30.8 MeV$$

Effect of hyperonic TBF on M_{max}

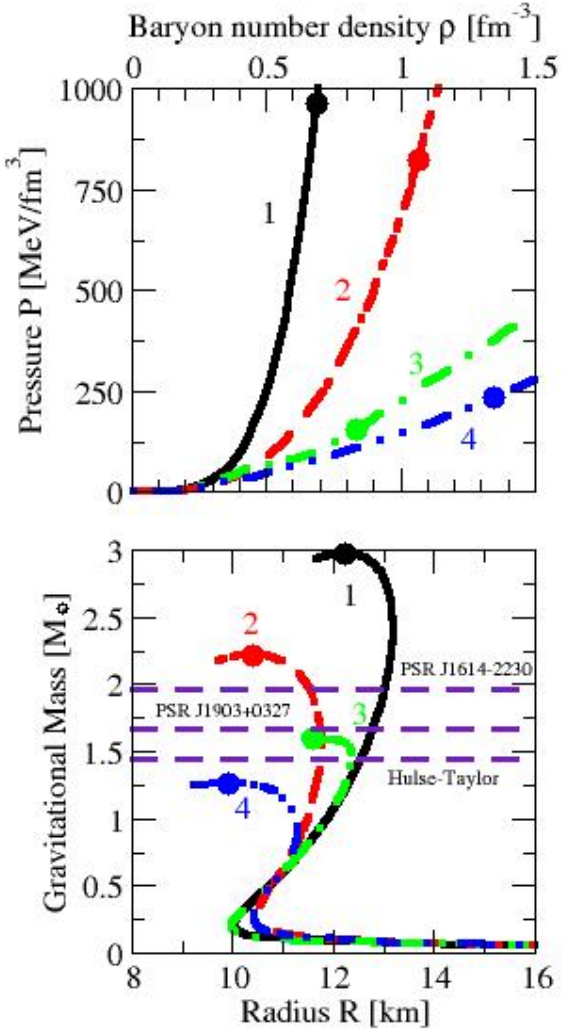

γ_{NN}	x	γ_{YN}	Maximum Mass
	0	-	1.27 (2.22)
	1/3	1.49	1.33
2	2/3	1.69	1.38
	1	1.77	1.41
	0	-	1.29 (2.46)
	1/3	1.84	1.38
2.5	2/3	2.08	1.44
	1	2.19	1.48
	0	-	1.34 (2.72)
	1/3	2.23	1.45
3	2/3	2.49	1.50
	1	2.62	1.54
	0	-	1.38 (2.97)
	1/3	2.63	1.51
3.5	2/3	2.91	1.56
	1	3.05	1.60

Hyperonic TBFs seem not to be the full solution of the "Hyperon Puzzle", although they probably contribute to its solution

$$1.27 < M_{max} < 1.6 M_{\odot}$$

IV, Logoteta, et al., (2011)

Solution II: YY vector meson repulsion

(explored in the context of RMF models)

General Feature:

Exchange of scalar mesons generates attraction (softening), but the exchange of vector mesons generates repulsion (stiffening)

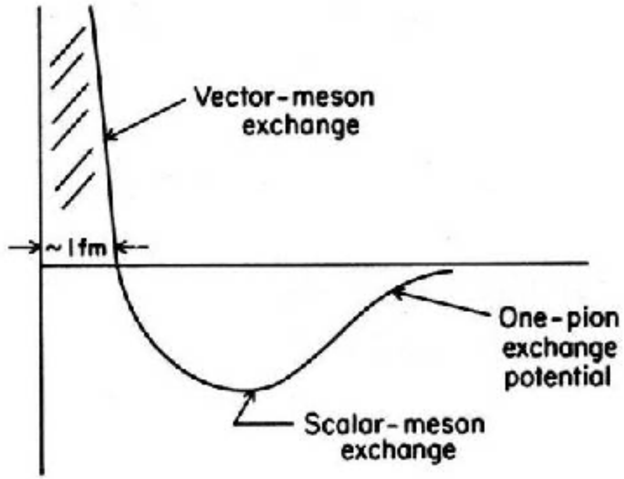

Add vector mesons with hidden strangeness (ϕ) coupled to hyperons yielding a strong repulsive contribution at high densities

$M_{max} > 2M_\odot$, but smaller population of hyperons

Dexhamer & Schramm (2008), Bednarek et al, (2012), Weissenborn et al., (2012)

- Non-linear RMF

- ✓ σ^2, σ^3, σ^4 terms
- ✓ ρ^2, ρ^4, ω^2, ω^4 terms
- ✓ "hidden strangeness" mesons: σ^*, ϕ (σ^{*2}, ϕ^2, ϕ^4)
- ✓ cross terms: $\omega^2\rho^2$, $\phi^2\omega^2$, $\phi^2\rho^2$
- ✓ g_{YV} couplings fixed by SU(6)
- ✓ g_{YS} couplings adjusted by fitting $U_B^{(B)}$

($U_\Lambda^{(N)}$=-28, $U_\Sigma^{(N)}$=+30, $U_\Xi^{(N)}$=-18 MeV)

($U_\Xi^{(\Xi)}=U_\Lambda^{(\Xi)}=2U_\Lambda^{(\Lambda)}$, $U_\Lambda^{(\Lambda)}$=-5 MeV)

- Hyperonic EoS stiffer than the nucleonic one at $\rho>5\rho_0$ due to the quartic terms involving ϕ meson

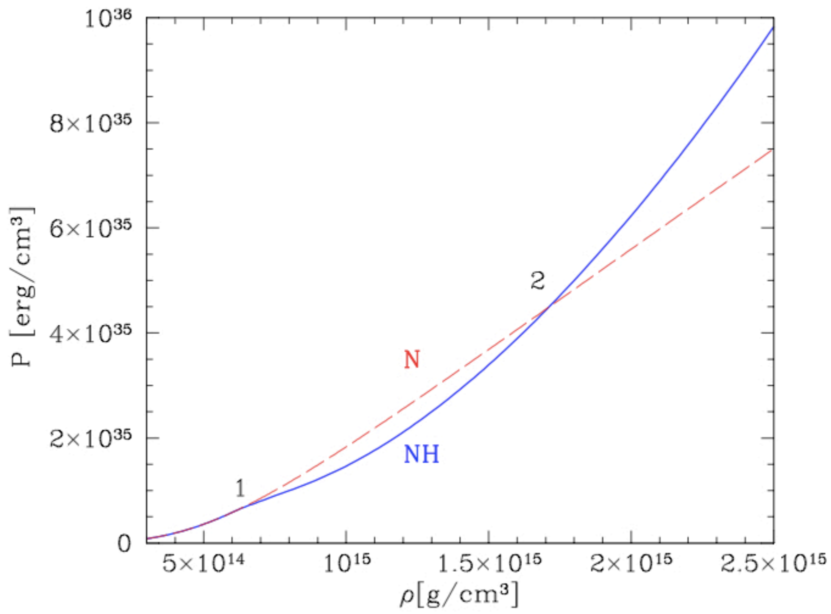

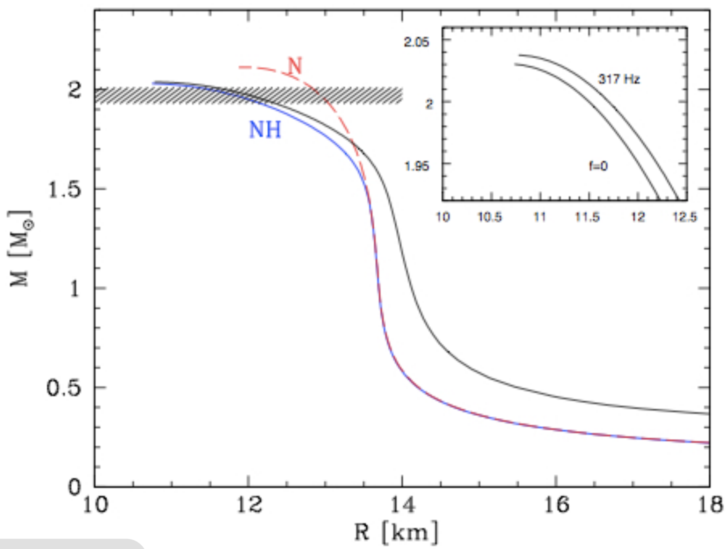

$M_{\max} > 2M_\odot$ but if $E^{NY}(n_b) > E^N(n_b) \Rightarrow instability$

Bednarek et al., (2012)

- **Non-linear RMF**

  - ✓ σ^2, σ^3, σ^4 terms
  - ✓ ρ^2, ω^2, ω^4 terms
  - ✓ "hidden strangeness" mesons: σ^*, ϕ (σ^{*2}, ϕ^2)
  - ✓ g_{YV} couplings: from SU(6) to SU(3)

    vary $z=g_8/g_1$ & $\alpha=F/(F+D)$
  - ✓ g_{YS} couplings adjusted by fitting $U_B^{(N)}$

    ($U_\Lambda^{(N)}=-30$, $U_\Sigma^{(N)}=+30$, $U_\Xi^{(N)}=-28$ MeV)

- **Stiffest EoS when including ϕ & σ^* is ommited for $z=0$ & $\alpha=0$**

$M_{\max} > 2M_\odot$ but $z=0 \Rightarrow g_{N\rho}=0$

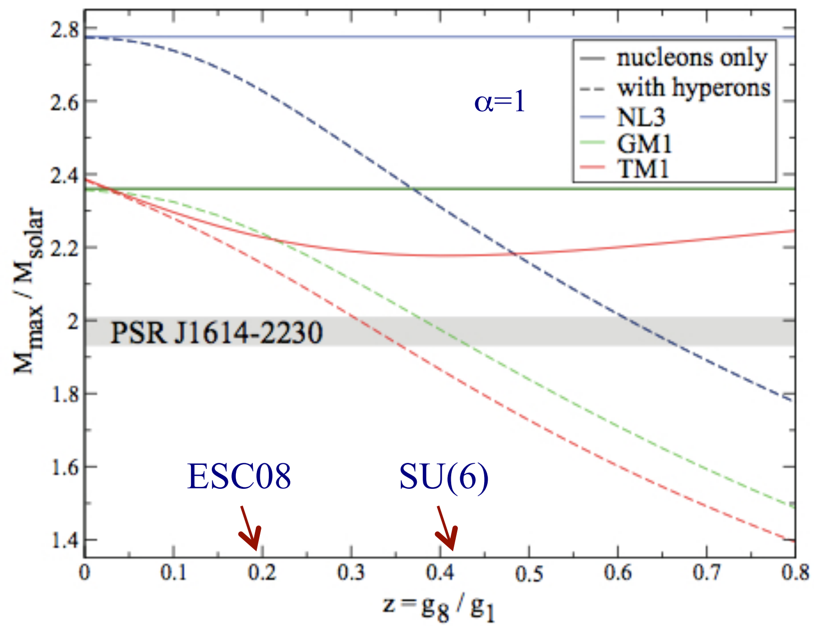

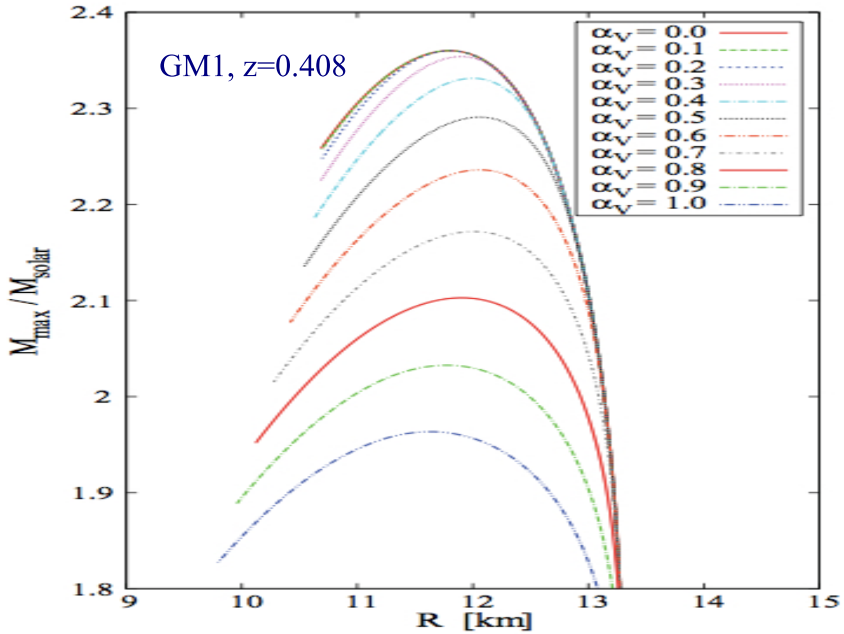

Weissenborn et al., (2012)

Particle Cocktail

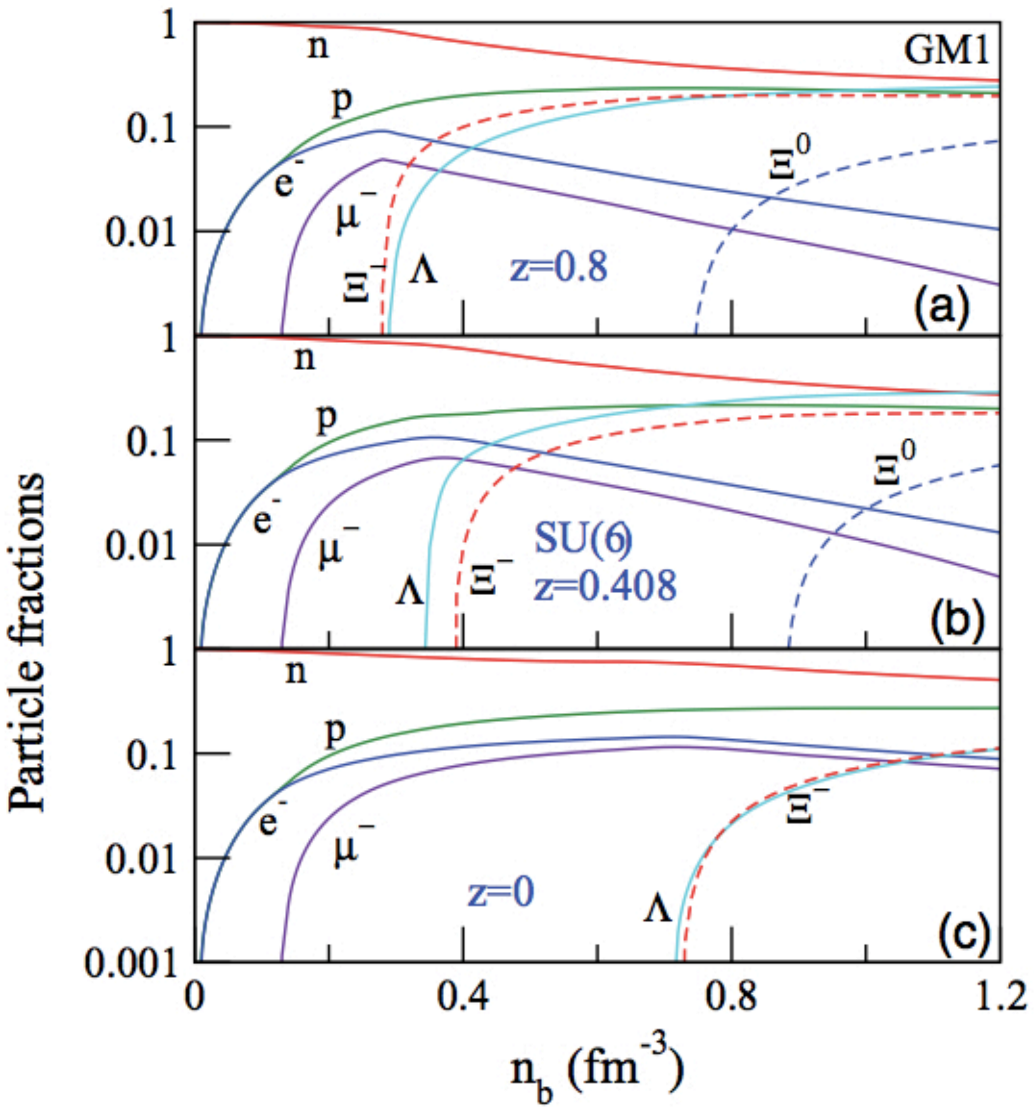

Moving from SU(6) to SU(3):

- Hyperon thresholds moved to very high densities
- Small hyperon fraction

The problem seems to be solved (?) because there is not much strangeness

Weissenborn et al., (2012)

Solution III: Quark Matter Core

General Feature:

Some authors have suggested that the hyperon core in neutron stars could be replaced by a cores of uds quark mater. Massive neutron stars could actually be hybrid stars with a stiff quark matter core

To yield $M_{\max} > 2M_{\odot}$ Quark Matter should have:

- significant overall quark repulsion $\longrightarrow$ stiff EoS
- strong attraction in a channel $\longrightarrow$ strong color superconductivity

Ozel et al., (2010), Weissenborn et al., (2011), Klaehn et al., (2011), Bonano & Sedrakian (2012), Lastowiecki et al., (2012), Zdunik & Haensel (2012)

Recent General Analysis by Zdunik & Haensel

Based on:

Simple linear EoS is a rather precise analytic representation of modern quark EoS in a phase 2SC, CFL.

$$P(\varepsilon) = a\left(\varepsilon - \varepsilon^*\right), \quad \mu(P) = \frac{\varepsilon^*}{n^*}\left(1 + \frac{1+a}{a}\frac{P}{\varepsilon^*}\right)^{\frac{a}{1+a}}$$

$$n(P) = n^*\left(1 + \frac{1+a}{a}\frac{P}{\varepsilon^*}\right)^{\frac{1}{1+a}}$$

3 parameters:

- a: squared of v_{sound}
- ε^*: energ. dens. at P=0
- n^*: num. dens. at P=0

Zdnunik & Haensel (2012)

Fitting 2SC & CLF quark matter EoS

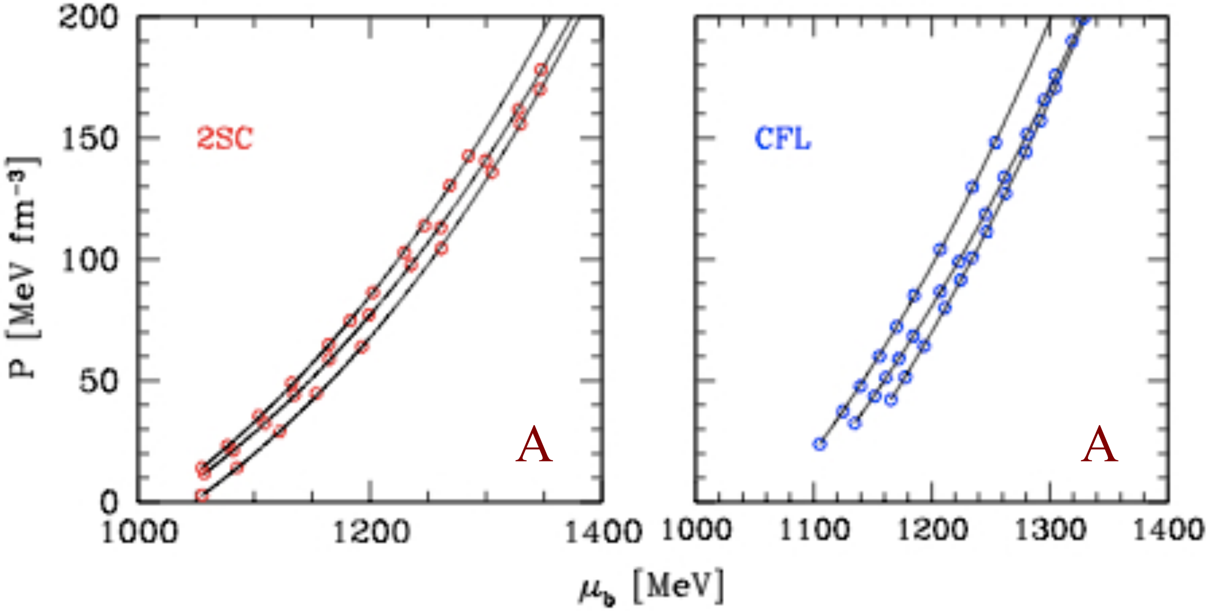

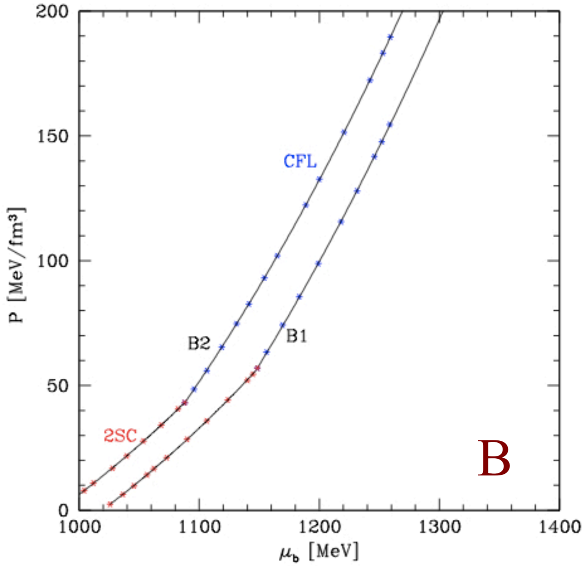

Numerical calculations based on:
Nambu-Jona-Lasinio+Color Superconductivity

A. Agrawal (2010)
B. Blaschke et al., (2010)

Zdnunik & Haensel (2012)

From Hadrons to Quarks

match to a soft hadron EoS

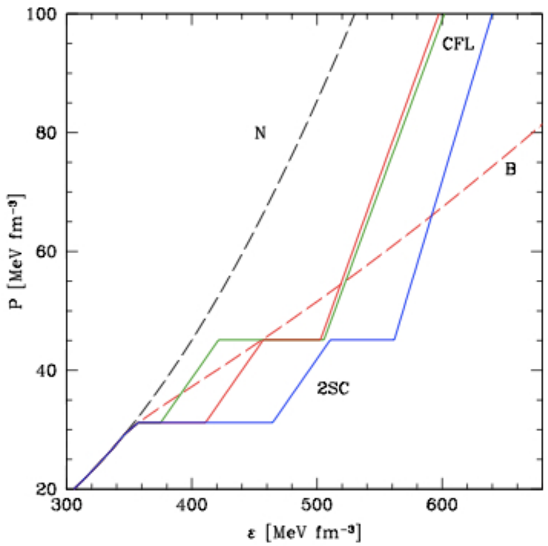

match to a stiff hadron EoS

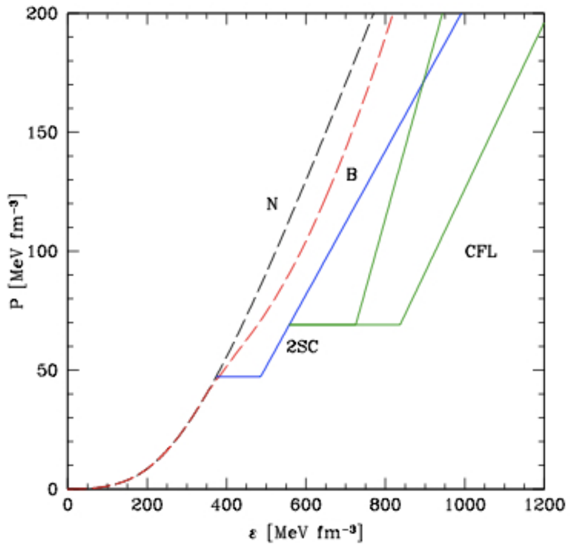

They simulate the sequence:

Hadron phase $\longrightarrow$ 2SC phase $\longrightarrow$ CFL phase

$$P_i = P^{(B)}(\varepsilon_1^i) = P^{(Q)}\left(\varepsilon_2^i\right), \quad \mu^{(B)}\left(P_i\right) = \mu^{(Q)}\left(P_i\right), \quad \lambda_i = \frac{\varepsilon_2^i}{\varepsilon_1^i} > 1$$

Zdnunik & Haensel (2012)

Stability of QM core and M_{max}

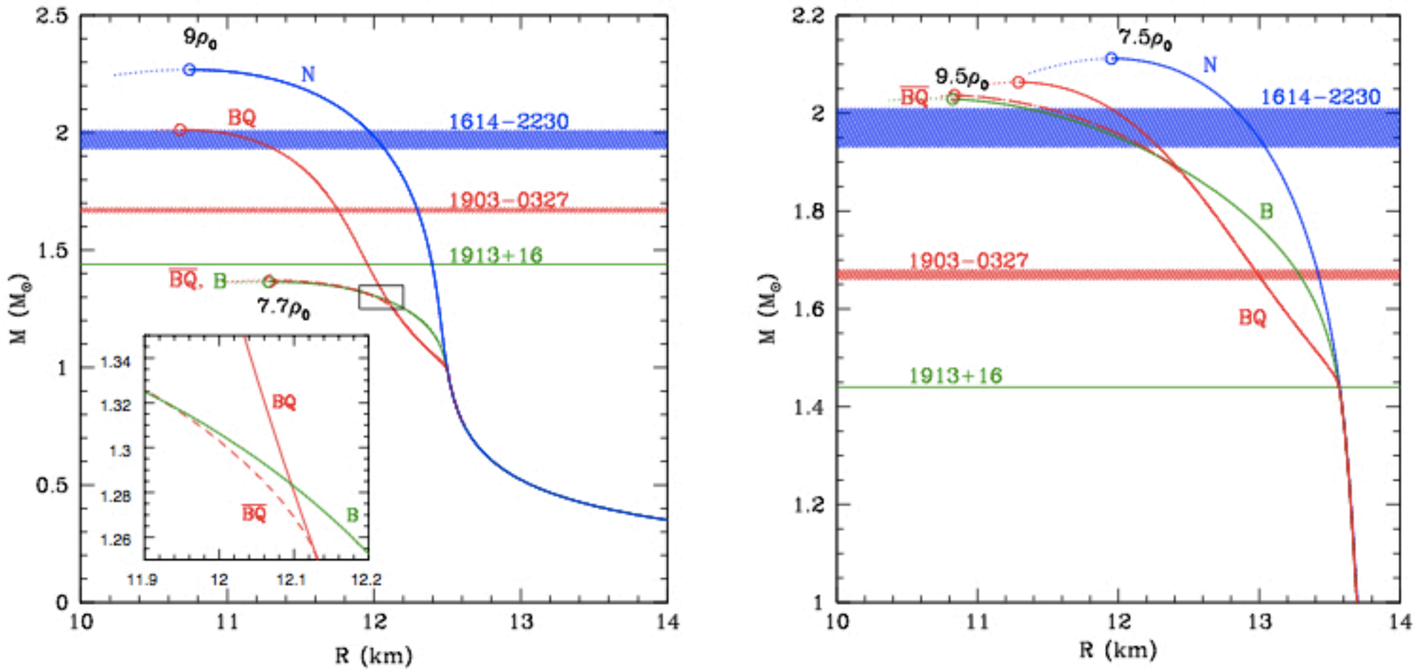

$M_{\max} > 2M_{\odot}$ requires:

- BQ transition must be rather low ~ $2\rho_0$-$3\rho_0$
- Density jumps λ_i should not bee too large (< 1.2)
- v_{sound} ~ 0.8-0.9 if $2.2 - 2.4 M_{\odot}$ is observed
- Stiffening EoS $\longrightarrow$ μ_b increases
- If $\mu_b^Q(P) > \mu_b^H(P) \longrightarrow$ instability (reconfinement)

Zdnunik & Haensel (2012)

Question is so open that …


EMMI Rapid Reaction Task Force
Quark Matter in Compact Stars
7-10 October 2013 FIAS
Frankfurt, Germany
Chairs: J. Schaffner-Bielich & S. Schramm

Hyperon Stars at Birth

Proto-Neutron Stars

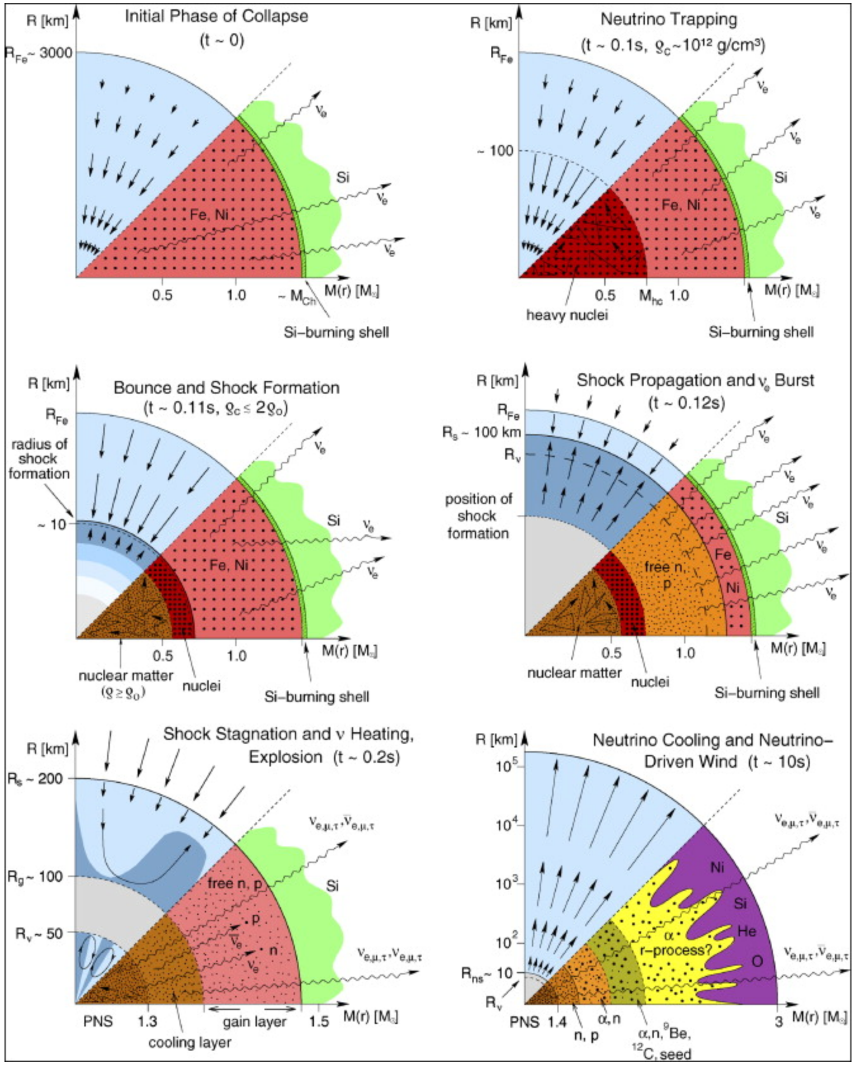

(Janka, Langanke, Marek, Martinez-Pinedo & Muller 2006)

New effects on PNS matter:

- Thermal effects

$$T \cong 30 - 40 \quad MeV$$
$$S / A \cong 1 - 2$$

- Neutrino trapping

$$\mu_\nu \neq 0$$
$$Y_e = \frac{\rho_e + \rho_{\nu_e}}{\rho_B} \approx 0.4$$
$$Y_\mu = \frac{\rho_\mu + \rho_{\nu_\mu}}{\rho_B} \approx 0$$

Proto-Neutron Stars: Composition

- Neutrino free $\mu_\nu = 0$

(Burgio & Schulze 2011)

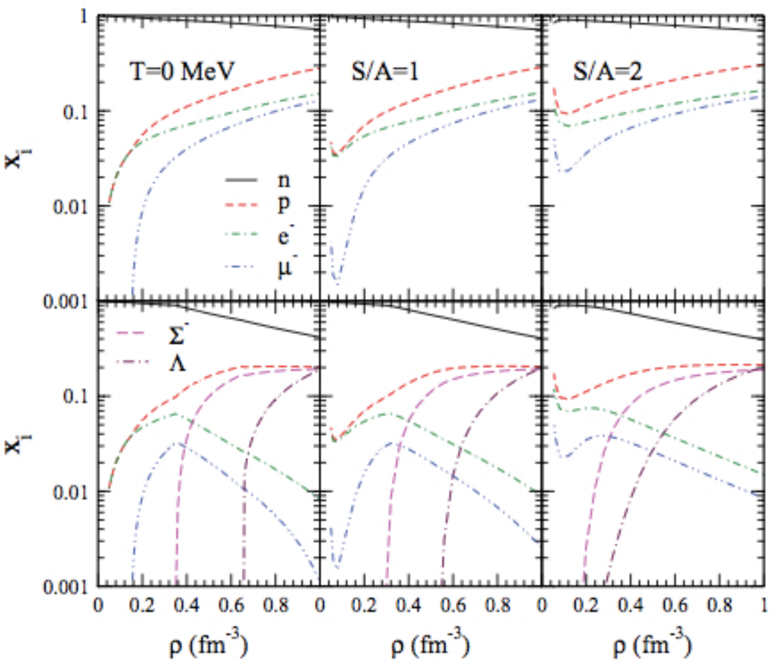

- Neutrino trapped $\mu_\nu \neq 0$

(Burgio & Schulze 2011)

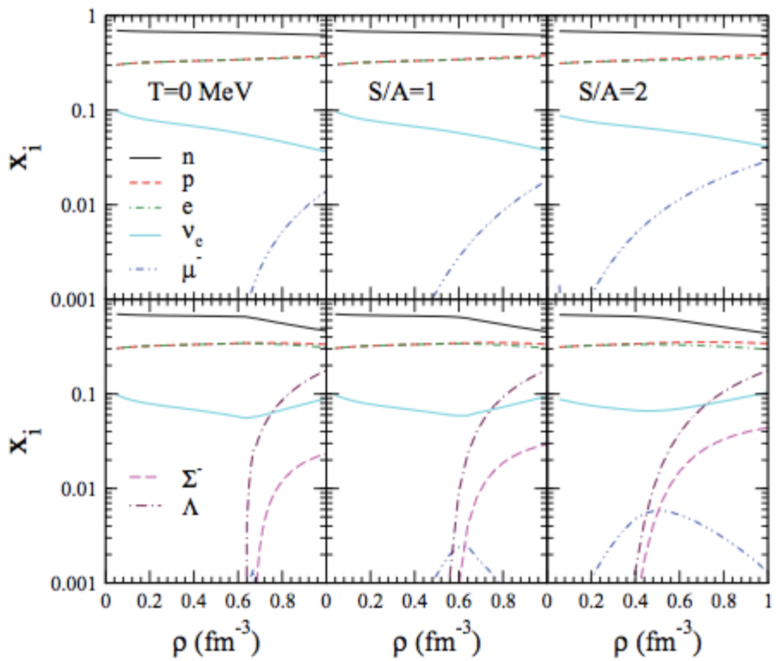

Neutrino trapped

- ✓ Large proton fraction
- ✓ Small number of muons
- ✓ Onset of $\Sigma^-(\Lambda)$ shifted to higher (lower) density
- ✓ Hyperon fraction lower in n-trapped matter

Proto-Neutron Stars: EoS

(Burgio & Schulze 2011)

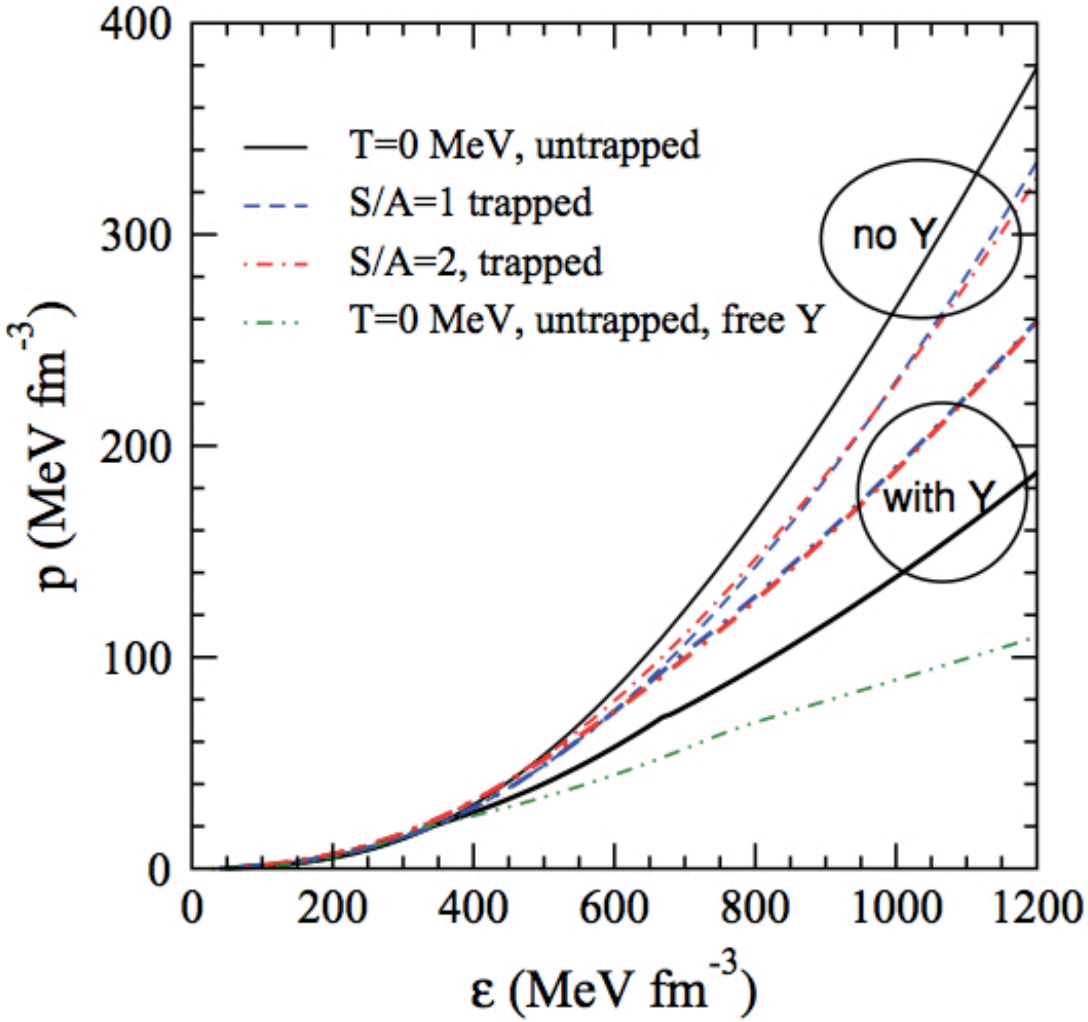

- Nucleonic matter

✧ ν-trapping + temperature → softer EoS

- Hyperonic matter

✧ ν-trapping + temperature → stiffer EoS

✧ More hyperon softening in ν-untrapped matter (larger hyperon fraction)

Proto-Neutron Stars: Structure

(Burgio & Schulze 2011)

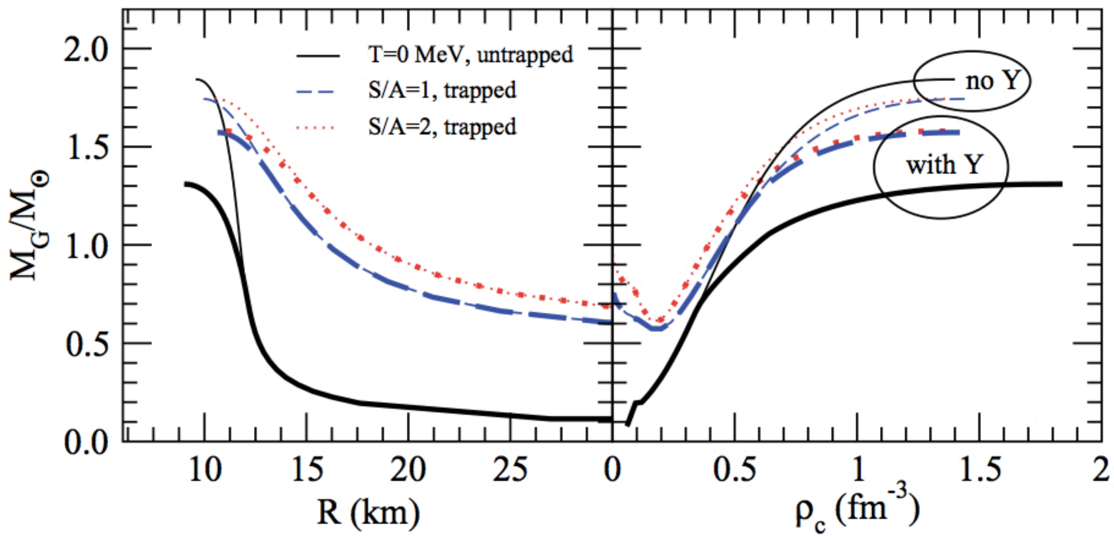

- Nucleonic matter

  ν-trapping + T:
  reduction of M_{max}

(IV et al. 2003)

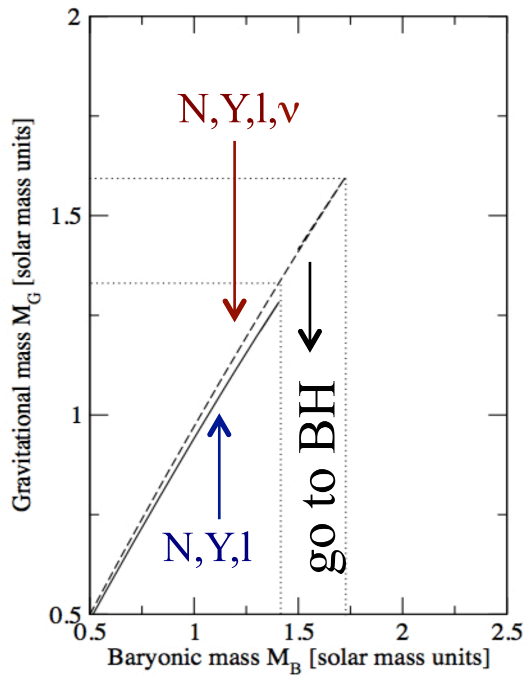

- Hyperonic matter

  ν-trapping + T:
  increase of M_{max} → delayed formation of a low mass BH

Hyperons & Neutron Star Cooling

Neutron Star Cooling in a Nutshell

Two cooling regimes

Slow	Fast
Low NS mass	High NS mass

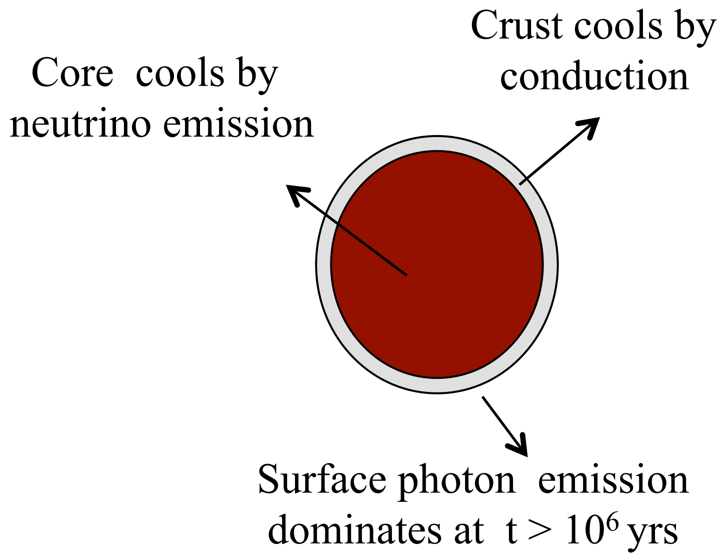

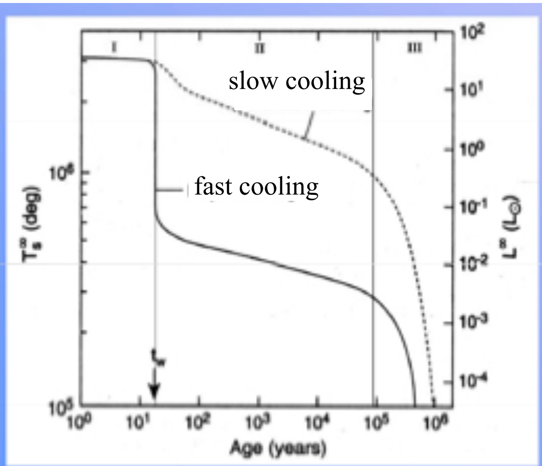

I. Core relaxation epoch
II. Neutrino cooling epoch
III. Photon cooling epoch

$$\frac{dE_{th}}{dt} = C_v \frac{dT}{dt} = -L_\gamma - L_\nu + H$$

- ✓ C_v: specific heat
- ✓ L_γ: photon luminosity
- ✓ L_ν: neutrino luminosity
- ✓ H: “heating”

Neutrino Emission

Name	Process	Emissivity	
Direct URCA	$n \rightarrow p + l + \bar{\nu}_l$ $p + l \rightarrow n + \nu_l$	$\sim T^6$	Fast
Modified URCA	$N + n \rightarrow N + p + l + \bar{\nu}_l$ $N + p + l \rightarrow N + n + \nu_l$	$\sim T^8$	Slow
Bremsstrahlung	$N + N \rightarrow N + N + \nu + \bar{\nu}$	$\sim T^8$	Slow
Cooper pair formation	$n + n \rightarrow [nn] + \nu + \bar{\nu}$ $p + p \rightarrow [pp] + \nu + \bar{\nu}$	$\sim T^7$	Medium

Hyperonic DURCA processes possible as soon as hyperons appear (nucleonic DURCA requires $x_p > 11\text{-}15\ \%$) ➔ Additional Fast Cooling Processes

Process	R
$\Lambda \rightarrow p + l + \bar{\nu}_l$	0.0394
$\Sigma^- \rightarrow n + l + \bar{\nu}_l$	0.0125
$\Sigma^- \rightarrow \Lambda + l + \bar{\nu}_l$	0.2055
$\Sigma^- \rightarrow \Sigma^0 + l + \bar{\nu}_l$	0.6052
$\Xi^- \rightarrow \Lambda + l + \bar{\nu}_l$	0.0175
$\Xi^- \rightarrow \Sigma^0 + l + \bar{\nu}_l$	0.0282
$\Xi^0 \rightarrow \Sigma^+ + l + \bar{\nu}_l$	0.0564
$\Xi^- \rightarrow \Xi^0 + l + \bar{\nu}_l$	0.2218

+ partner reactions generating neutrinos, Hyperonic MURCA, …

(Schaab, Shaffner-Bielich & Balberg 1998)

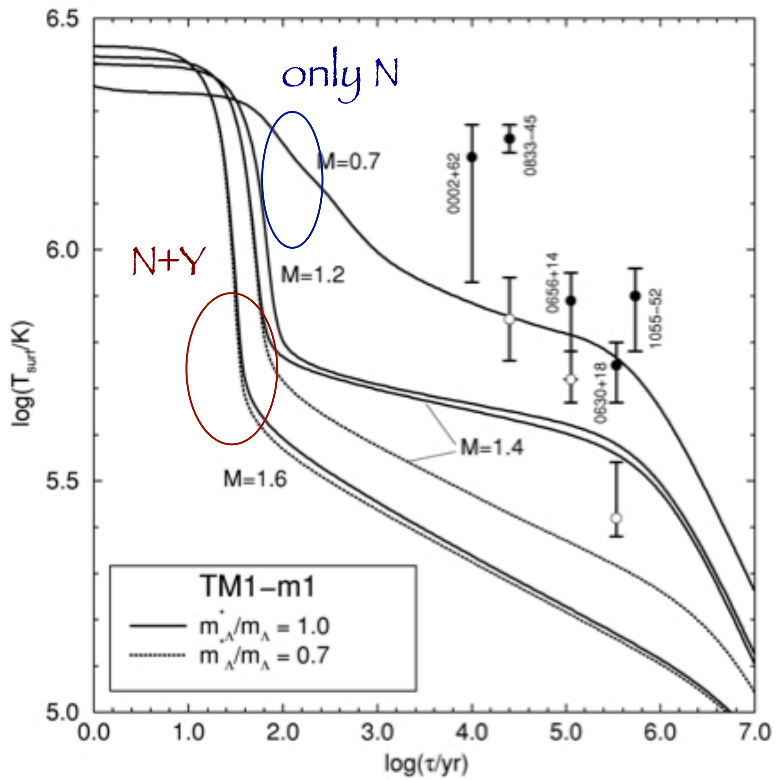

R: relative emissitivy w.r.t. nucleonic DURCA

Pairing Gap $\longrightarrow$ suppression of C_v & ε by $\sim e^{(-\Delta/k_B T)}$

- $^1S_0$, $^3SD_1$ ΣN & $^1S_0$ ΛN gap

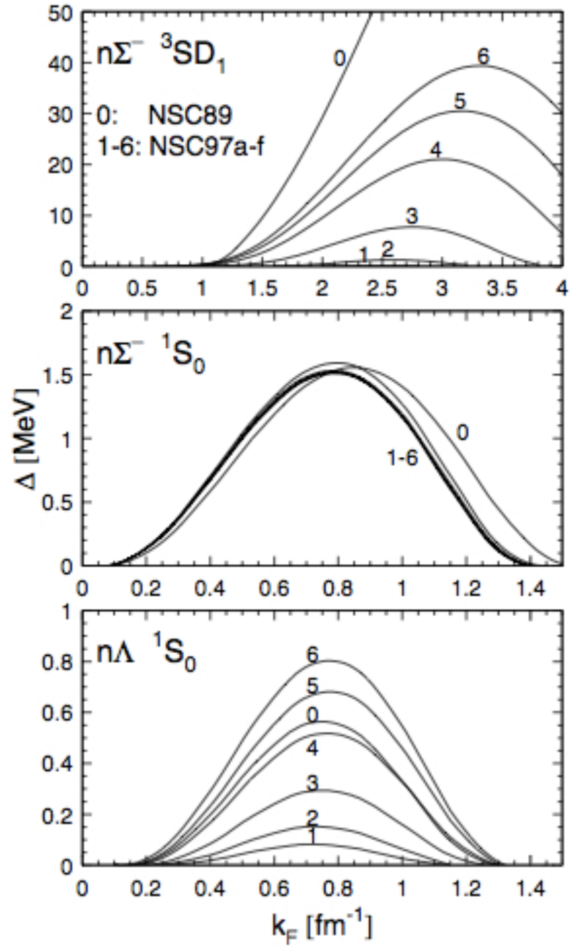

(Zhou, Schulze, Pan & Draayer 2005)

- $^1S_0$ $\Lambda\Lambda$ gap

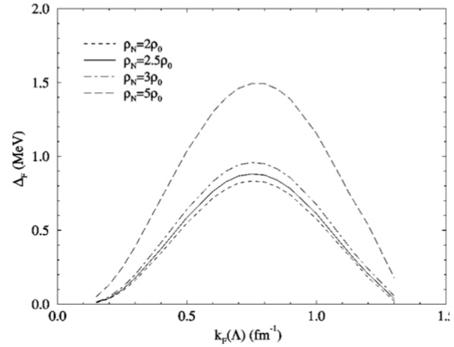

(Balberg & Barnea 1998)

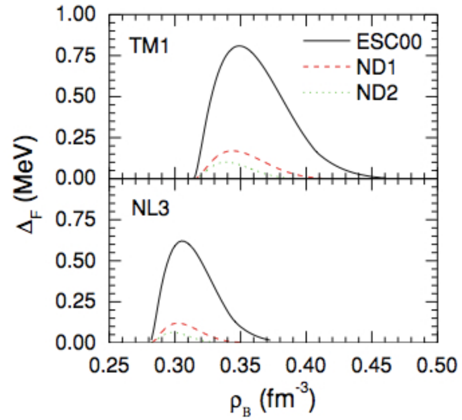

(Wang & Shen 2010)

- $^1S_0$ $\Sigma\Sigma$ gap

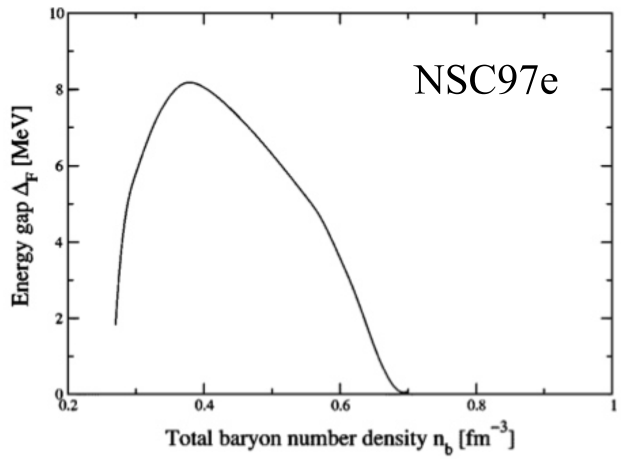

(IV & Tolós 2004)

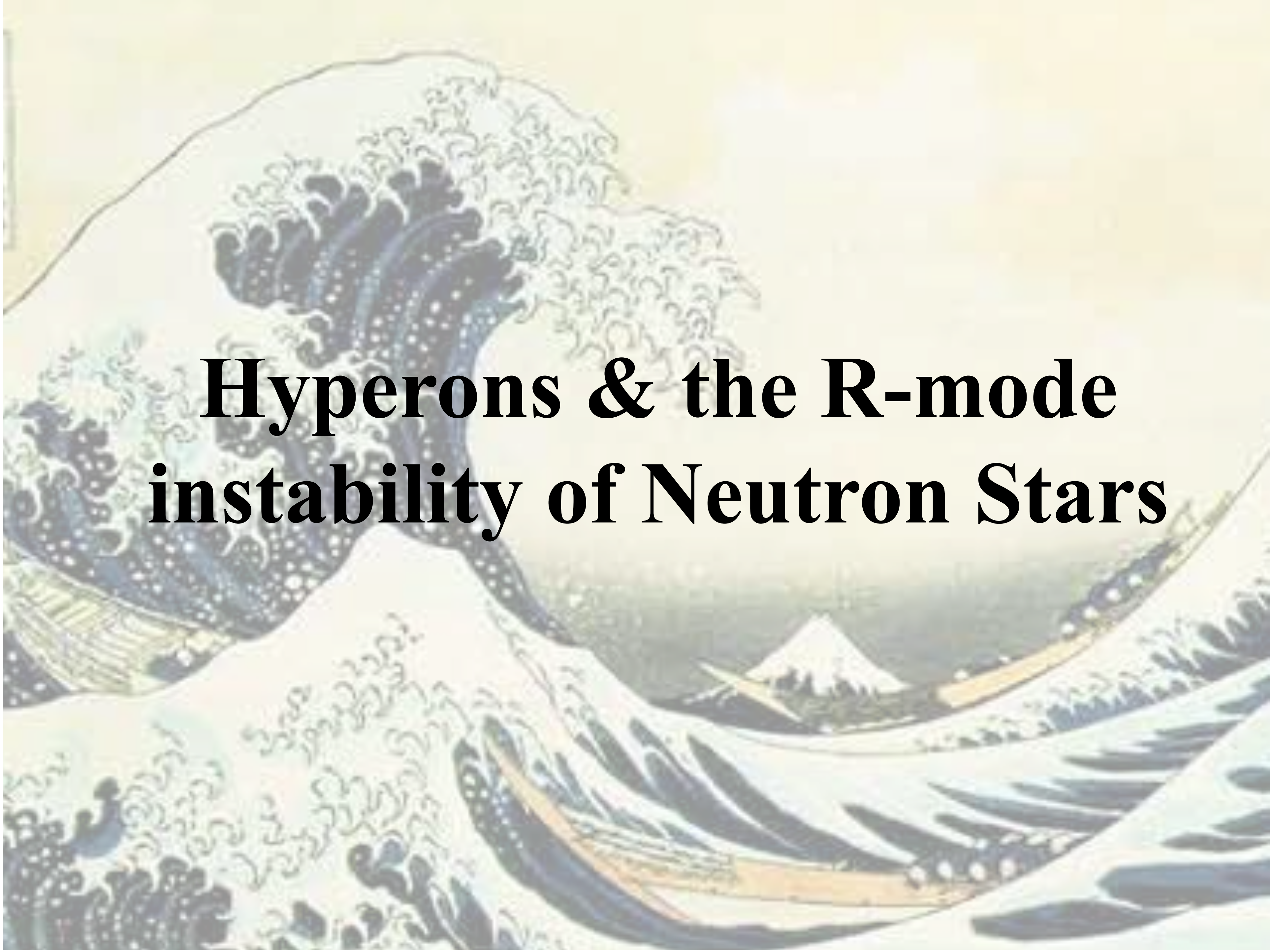

Hyperons & the R-mode instability of Neutron Stars

The R-mode Instability

Ω_{Kepler} : Absolute Upper Limit of Rot. Freq.

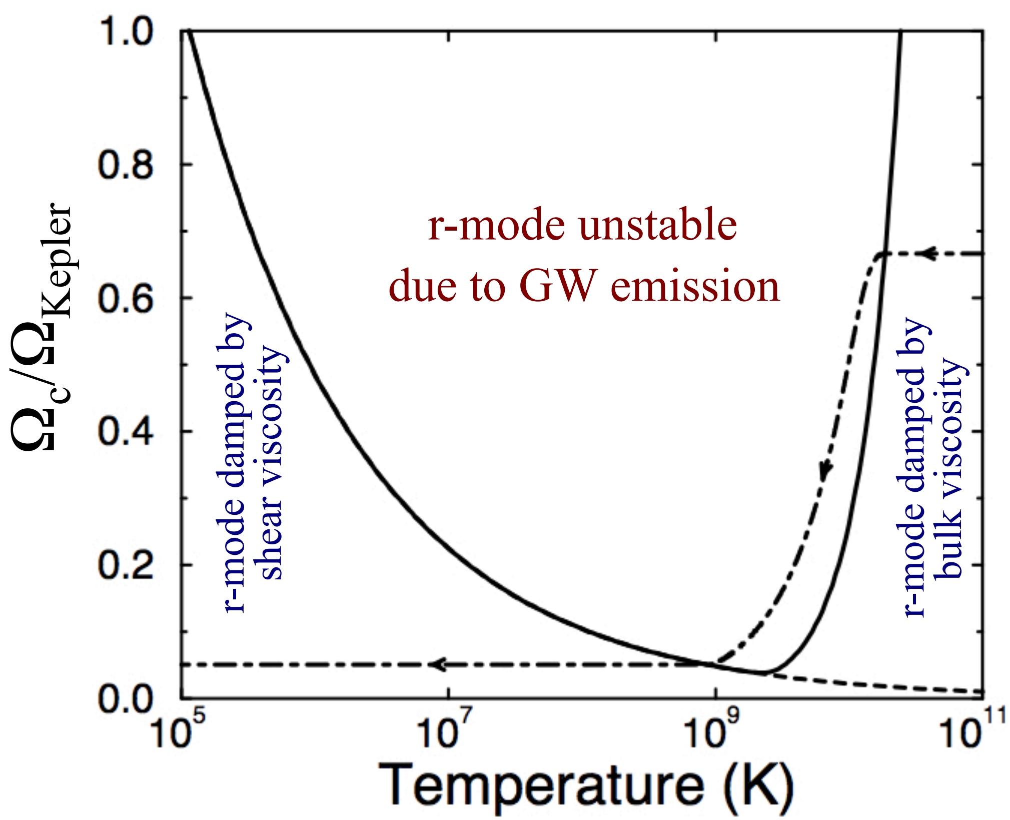

Instabilities prevent NS to reach Ω_{Kepler}

R-mode Instability : toroidal mode of oscillation

✓ restoring force: Coriolis

✓ emission of GW in hot & rapidly rotating NS (CFS mechanism)

- GW makes the mode unstable
- Viscosity stabilizes the mode

$$A \propto A_0 e^{-i\omega(\Omega) - t/\tau(\Omega,T)}$$

$$\frac{1}{\tau(\Omega,T)} = -\frac{1}{\tau_{GW}(\Omega)} + \frac{1}{\tau_{Viscosity}(\Omega,T)}$$

Hyperon Bulk Viscosity ξ_Y

(Lindblom et al. 2002, Haensel et al 2002, van Dalen et al. 2002, Chatterjee et al. 2008, Gusakov et al. 2008, Shina et al. 2009, Jha et al. 2010,…)

Sources of ξ_Y:

non-leptonic weak reactions	$N + N \leftrightarrow N + Y$ $N + Y \leftrightarrow Y + Y$
Direct & Modified URCA	$Y \to B + l + \bar{\nu}_l$ $B' + Y \to B' + B + l + \bar{\nu}_l$
strong reactions	$N + Y \leftrightarrow N + Y$ $N + \Xi \leftrightarrow Y + Y$ $Y + Y \leftrightarrow Y + Y$

(Haensel, Levenfish & Yakovlev 2002)

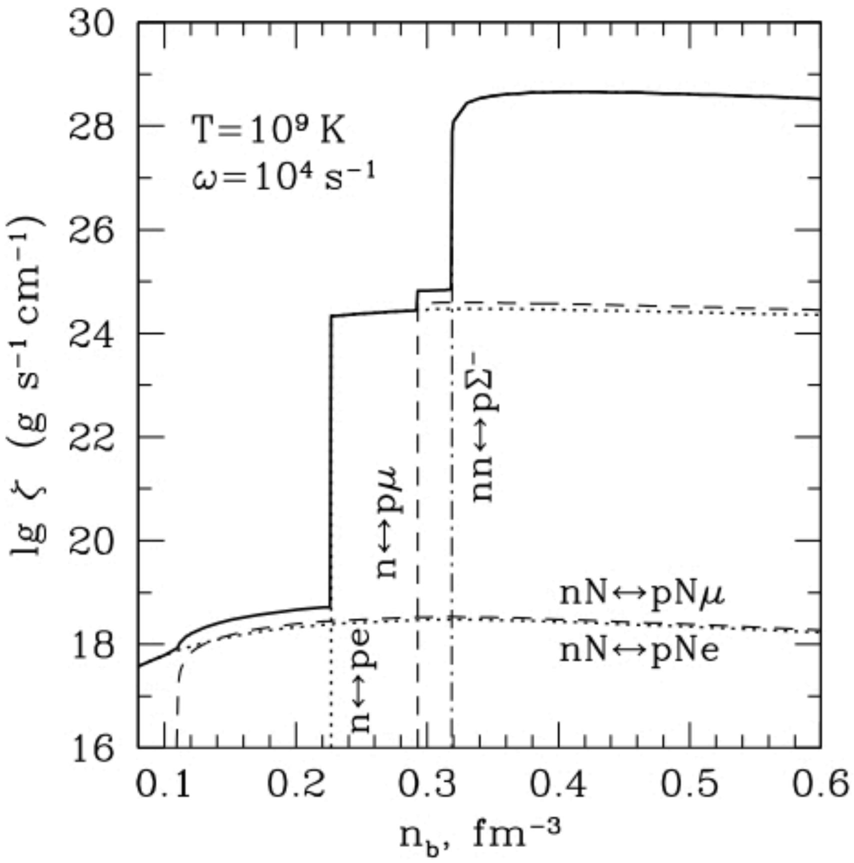

Reaction Rates & ξ_Y reduced by Hyperon Superfluidity

Critical Angular Velocity of Neutron Stars

- r-mode amplitude: $A \propto A_o e^{-i\omega(\Omega)t - t/\tau(\Omega)}$

$$\frac{1}{\tau(\Omega,T)} = -\frac{1}{\tau_{GW}(\Omega)} + \frac{1}{\tau_{\xi}(\Omega,T)} + \frac{1}{\tau_{\eta}(T)}$$

➔ $\frac{1}{\tau(\Omega_c,T)} = 0$ r-mode instability region

$\Omega < \Omega_c$ stable

$\Omega > \Omega_c$ unstable

As expected:
smaller r-mode instability region
due to hyperons

(I.V. & C. Albertus in preparation)

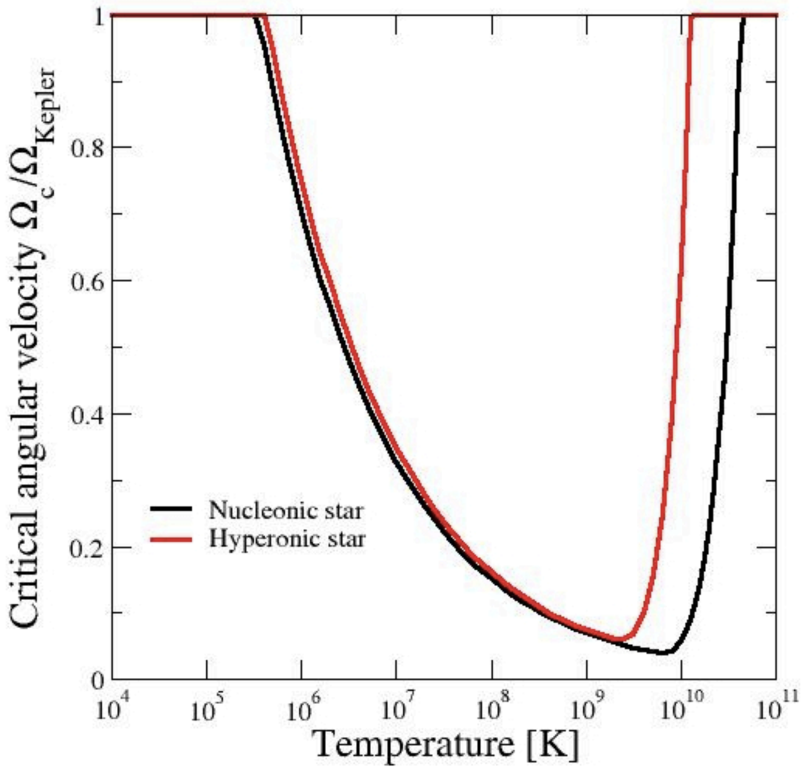

BHF: NN (Av18)+NY (NSC89)
(M=1.27$M_\odot$)

Take away message

Strangeness adds a new dimension to nuclear physics & astrophysics which gives us the oportunity to study fundamental interactions from an enlarge perpective

- You for your time & attention

- The organizers for their invitation

- The sponsors for their support

COMPETE
PROGRAMA OPERACIONAL FACTORES DE COMPETITIVIDADE

comp star